Context-Dependent Interaction of the Androgen Receptor with Oncogenic Pathways Common to Prostate Cancer

by

Jacob Emerson Higgins

A dissertation submitted in partial fulfillment
of the requirements for the degree of
Doctor of Philosophy
(Human Genetics)
in the University of Michigan
2015

Doctoral Committee:

Professor Diane M. Robins, Chair
Associate Professor Anthony Antonellis
Associate Professor Jun Li
Professor Andrew P. Lieberman
Assistant Professor Scott A. Tomlins

For Alicia

Acknowledgements

First of all I must thank my advisor, Didi Robins, for her support throughout this project. Didi encouraged me to think beyond whatever problem I was struggling with that week, to look at things from an alternative perspective and to keep in mind the broader biological significance of the experimental questions. I was privileged to have a thoughtful and involved thesis committee: Scott Tomlins, Andy Lieberman, Tony Antonellis and Jun Li. Their feedback during meetings as well as "offline" was very helpful and facilitated productive collaborations. The project would not have been possible without their assistance.

I am grateful to many members of the Robins lab, past and present, for their support. Michele Brogley maintained the mouse colony, took care of day-to-day issues and had a hand in many of the experiments described in this thesis. Chris Krebs provided helpful and insightful advice at quite a few points along the way, in particular the early chromatin immunoprecipitation runs. Allison Fullenkamp and Pia Bagamasbad were always willing to discuss questions or ideas, take turns feeding cells when someone was out of town, and were just positive and supportive in general. Sravanthi Gutta and Megan Hull provided valuable assistance with tissue culture, qPCR and other experiments.

Many thanks are owed to the additional labs and individuals who facilitated this work. The Moran, Camper, Li and Meisler labs allowed me to frequently use their equipment. Arul Chinnaiyan and his lab members generously shared reagents and advice, in particular Mohan

Table of Contents

List of Tables

List of Figures

Abstract

Androgen receptor (AR) is a hormone-responsive transcription factor central to prostate cancer (PCa) onset and progression. Therapies targeting AR signaling are initially successful, yet acquired resistance is a major problem. This thesis examines how AR cooperates with common pathways of oncogene activation and tumor suppressor loss in PCa.

Recurrent genomic rearrangements in PCa fuse the coding region of ETS family transcription factors with androgen-responsive regulatory elements, driving high expression in half of all tumors. Oncogenic ETS proteins promote early neoplasia and invasion in model systems, yet their prognostic value is unclear. Loss of the tumor suppressor PTEN occurs frequently in PCa, is associated with poor prognosis and treatment resistance, and causes neoplasia in model systems.

To probe the interaction of the androgen axis with oncogenic ETS expression and PTEN loss, mice expressing a stronger or weaker humanized *AR* allele were crossed with mice overexpressing the less-studied ETS factor ETV1 or lacking one *Pten* allele. While AR strength did not affect ETV1-driven neoplasia, global gene expression analysis by RNA-seq revealed that ETV1 strongly antagonized AR transcriptional activity. Repressed targets included tumor suppressors and prostate differentiation genes such as *Nkx3-1* and *Hoxb13*. This suggests that the ETV1 oncogenic program primes the prostate for disease progression following additional genetic lesions. Indeed, the combination of ETV1 overexpression and *Pten* reduction promoted

progression of disease, and this was more frequent with a stronger *AR* allele. RNA-seq showed that ETV1 antagonism of AR was abrogated in neoplasia with reduced *Pten*, but in tumors AR was again repressed. Comparison to patient data revealed known and novel PCa-associated genes with potential ETV1 regulation.

Benign human prostate cells, as well as PCa cells harboring ETV1 overexpression with or without PTEN loss, were used to model PCa progression *in vitro*. In malignant cells ETV1 consistently antagonized the same key AR targets as in mouse tissue, but in benign cells cooperation as well as repression was shown. These experiments highlight the interdependent relationships of the androgen axis, oncogene activation and tumor suppressor loss in PCa, revealing multiple pathways that should be considered simultaneously in future research and therapy.

Chapter 1

Introduction

Prostate cancer (PCa) is one of the most common cancers in Western countries, leading

to the deaths of 27,000 men per year in the United States. The prostate is a hormone-responsive

tissue, and prostate differentiation and PCa progression are driven by the androgen receptor (AR)

(Heinlein and Chang, 2004). Thus, standard therapeutic strategies for metastatic PCa include

targeting AR via ablation of circulating androgens or directly with AR inhibitors

(antiandrogens). Unfortunately, despite initial positive response, metastatic PCa evades current

AR-targeted therapies and often recurs as fatal castration-resistant prostate cancer (CRPC). In

this state, the tumor is still dependent on AR despite ongoing androgen ablation. AR overcomes

therapeutic inhibition by a variety of means including gene mutation, amplification and cofactor

dysregulation, allowing a hypersensitive response to low androgen levels so that AR signaling

persists in CRPC (Feldman and Feldman, 2001). This thesis probes the interaction between AR

and the molecular pathways most commonly disrupted in PCa progression.

A significant difficulty in clinical management of PCa is accurately identifying the subset

of early-stage patients who will develop metastatic disease. The majority of primary prostate

tumors occur late in life, are slow growing, and will not present substantial health problems

during the patient's lifetime (Waterbor and Bueschen, 1995). While radiation or prostatectomy

can cure localized disease, improved biomarkers could supplement clinicopathological

parameters to best identify the patients who will benefit from these interventions. For patients whose tumors do metastasize, novel therapeutic strategies are needed to combat resistance. Alternative targets or more individually stratified treatments would help to achieve maximum therapeutic benefit.

AR signaling is central to prostate differentiation and PCa progression, and must be considered when asking how additional disruptions promote oncogenesis. AR transcriptional strength varies inversely with the length of an N-terminal polyglutamine tract (Q-tract) whose length is polymorphic in the population. While not a risk factor for PCa by itself, varying AR strength has previously been shown to affect male physiology in humans and mice, as well as PCa initiation, progression and treatment response in a transgenic mouse model (Robins, 2011). In this thesis, AR variation will be incorporated into *in vivo* models of common somatic alterations in PCa to explore the impact of subtle differences in the AR axis.

Recurrent oncogene activation and/or tumor suppressor loss occur in the majority of PCa patients. Genomic rearrangements that fuse coding regions of members of the ETS family of cell cycle transcription factors to androgen-responsive regulatory regions, driving ETS gene overexpression, are seen in over half of prostate tumors in PSA-screened Caucasian cohorts (Rubin et al., 2011; Tomlins et al., 2005). These gene fusions occur early in patients, and in model systems ETS overexpression induces invasion, early neoplasia and altered AR signaling. Partial or complete loss of the tumor suppressor PTEN occurs in greater than 50% of PCa as well. PTEN loss promotes PCa in animal models in a dose-dependent manner and is associated with altered AR activity and progression to CRPC (Shen and Abate-Shen, 2010).

The aim of this thesis is to develop a more complete scientific understanding of the interaction of three commonly disrupted pathways described above: AR variation, ETS gene

fusion and PTEN loss. This understanding may inform patient stratification and help distinguish indolent from lethal tumors. Furthermore, examination of the molecular outcomes via downstream gene expression patterns may suggest potential biomarkers or new therapeutic targets.

Androgens and the Androgen Receptor

The prostate is a hormone-responsive tissue. Prostate tumors and metastases continue to be hormone dependent throughout most stages of progression, specifically requiring androgens acting via the AR. AR is a steroid hormone-responsive transcription factor in the nuclear receptor superfamily. The 110 kDa AR protein consists of an N-terminal transactivation domain (NTD), a DNA binding domain (DBD) consisting of two zinc fingers, a hinge region and a C-terminal ligand binding domain (LBD) that also has transactivation and coregulator recruitment functions, similar to other nuclear receptors (Figure 1.1) (Robins, 2005, 2011).

Testosterone can bind and activate AR, but it is not the usual or most potent ligand (Grino et al., 1990). After circulating testosterone enters an androgen-responsive cell, it is converted to the more potent ligand dihydrotestosterone (DHT) by the 5α-reductase enzyme (SRD5A2). DHT then binds the LBD of AR, inducing a conformational change. This conformational change releases AR from its cytoplasmic chaperone heat-shock protein 90 (HSP90), which holds AR in a ligand-receptive conformation as well as sequestering it in the cytoplasm in the absence of ligand (Fang et al., 1996). AR has a nuclear localization signal (NLS) in the hinge region beyond the DBD, and a cytoplasmic localization signal (CLS) in the LBD. Together, these motifs promote nuclear translocation of ligand-bound AR and cytoplasmic translocation of unliganded AR (Jenster et al., 1993; Saporita et al., 2003).

The repositioning of helices 3, 4 and 12 within the LBD creates a surface recognized by transcriptional coactivators (Moras and Gronemeyer, 1998). This activation function domain (AF-2) of the liganded LBD physically interacts with steroid receptor coactivator 1 (SRC1) and other members of the p160 family (He et al., 1999). The NTD contains AF-1 and AF-5 domains, which recruit transcriptional coactivators in a ligand-independent manner (Shen and Coetzee, 2005). Additionally, the NTD contains WxxLF and FxxLF motifs that facilitate interaction between the NTD and AF-2 in liganded AR, which can promote or compete with cofactor binding (Figure 1.1) (He et al., 1999; He et al., 2000).

Ligand-bound AR can translocate to the nucleus, undergo additional post-translational modifications, dimerize and bind at androgen-responsive elements (AREs) in the genome (Feldman and Feldman, 2001). Once bound in the genome, AR recruits coregulators to induce or repress transcription of target genes. Coactivators include histone acetylases that function to open chromatin and facilitate transcription. On the other hand, corepressors such as nuclear receptor corepressor 1 (NCoR1) are histone deacetylases that close chromatin and inhibit transcription. Expression studies have shown that AR activates or represses a comparable number of targets (DePrimo et al., 2002; Jones et al., 2005).

The consensus ARE is an inverted repeat of sequence 5'-GG(A/T)ACAnnnTGTTCT-3' (Beato, 1989; Roche et al., 1992). However, similar to other transcription factors, only a minority of individual AR binding sites are a perfect match to the consensus. The inverted repeat is also the consensus sequence for other steroid hormone receptors including glucocorticoid, progesterone and mineralocorticoid receptors. AR can also bind more selectively to elements that resemble direct repeats but are actually single half-sites or non-consensus sites (Sahu et al., 2014; Tewari et al., 2012).

AR often binds at distal enhancer regions in addition to proximal promoters. Some of the most well-characterized enhancers are up to several dozen kilobases (kb) upstream of the target gene's transcription start site (TSS), e.g. the *KLK3* (-4 kb) and *TMPRSS2* (-13 kb) enhancers. However, enhancers can be upstream or downstream of the associated gene, and can be hundreds of kb away. Chromatin immunoprecipitation-microarray (ChIP-chip) and more recent ChIP-sequencing (ChIP-seq) studies reveal up to tens of thousands of AR binding sites in the genome (Chen et al., 2013; Sahu et al., 2014; Yu et al., 2010). Genes may be regulated by multiple AR binding sites. Additionally, many AR binding sites are in gene deserts and therefore their function is unknown. ChIP-seq studies have also identified the FOXA1 consensus sequence as the top motif aside from the ARE sequence at AR-bound sites in prostate cells. Further experiments demonstrate that FOXA1 acts as a "pioneer factor" for AR, binding to many genomic sites first and facilitating subsequent binding of liganded AR (Lupien and Brown, 2009).

Through activation and repression of AR target genes, androgen signaling can produce physiological outcomes such as cell proliferation, differentiation, development or survival. These effects depend on tissue type and developmental stage. In the adult prostate, AR drives a gene expression program that is both pro-survival and pro-differentiation. During early tumorigenesis AR signaling is dysregulated, tipping the balance for later proliferation and invasion. In castration-resistant prostate cancer (CRPC), the AR transcriptional program diverges substantially from that in normal prostate (Sharma et al., 2012). A more thorough understanding of the factors influencing this "oncogenic switch" in AR behavior at both early and late disease stages is critical.

Androgen Receptor Variation in Prostate Cancer and Other Human Syndromes

The human *AR* gene is on the X chromosome and contains a CAG repeat in exon 1 that encodes a polyglutamine tract (Q-tract) in the N-terminal domain of the AR protein. Length of the CAG repeat (and thus Q-tract) is polymorphic in the population, with a median length of 21 repeats and a normal range of 9 to 37 Qs (Zitzmann and Nieschlag, 2003). Association of Q-tract variation with several syndromes is well established. Extremely long tracts (38 or more repeats) cause spinobulbar muscular atrophy (SBMA), a neurodegenerative condition also known as Kennedy disease (La Spada et al., 1991). SBMA patients suffer from motor neuron and skeletal muscle degeneration beginning any time after puberty, but more frequently in adults in their fifties. Molecular pathogenesis of SBMA occurs in part through proteotoxic gain of function of the expanded polyglutamine AR over time, in a ligand-dependent manner (Chua and Lieberman, 2013), hence the absence before puberty and the tendency for later onset. SBMA occurs only in men, and even women with homozygous mutations remain unaffected, highlighting the androgen dependence of the phenotype. The toxic gain of function mechanism has parallels with Huntington disease and other expanded polyglutamine-associated neurological syndromes (Zoghbi and Orr, 2000).

AR transcriptional activity is inversely proportional to the length of the Q-tract in model systems *in vitro* and *in vivo* (Albertelli et al., 2006; Simanainen et al., 2011; Wang et al., 2004). This occurs in part due to decreased AR-coactivator interaction with the expanded tract (Irvine et al., 2000) and greater intramolecular interaction between the N- and C-termini with fewer repeats, facilitating coactivator recruitment (Buchanan et al., 2004; Ding et al., 2004). Men with SBMA may display partial androgen insensitivity syndrome (PAIS) including infertility,

hypogonadism or impotence (Chua and Lieberman, 2013) due to decreased AR transcriptional function.

AR Q-tract length varies with ethnicity, with the shortest average length in African Americans. That population also has a higher incidence of PCa, which in combination with the *in vitro* findings led to the early hypothesis that a short Q-tract increases PCa risk through a lifetime of increased AR signaling (Coetzee and Ross, 1994). Furthermore, the Q-tract has been observed to somatically shorten during cancer progression, suggesting a role in oncogenesis (Alvarado et al., 2005). Despite an initial association in some studies, large studies showed that the Q-tract alone was not associated with PCa risk (Lindstrom et al., 2010; Price et al., 2010). However, a short Q-tract in combination with specific haplotypes in genes along the androgen synthesis pathway, including *CYP17A1* and *SRD5A2*, is associated with an increased risk of PCa (Lindstrom et al., 2006a; Lindstrom et al., 2006b). A short Q-tract has also recently been associated with a higher frequency of PCa that is positive for the recurrent TMPRSS2-ERG gene fusion (Bastus et al., 2010; Yoo et al., 2014), which will be discussed below, suggesting that AR variation may play a role in certain subtypes of PCa.

Proper AR activity is critical to normal prostate differentiation and function. In men and mice, inherited mutations in *AR* that truncate the protein prior to the LBD, or that otherwise inactivate the protein, cause partial or complete androgen insensitivity syndrome (PAIS, CAIS) depending on the severity of the mutation. These males may display infertility, hypogonadism, or lack male secondary sex traits despite the presence of a normal Y chromosome. Intriguingly, in PCa an AR protein lacking the LBD due to either alternative splicing or a somatic truncating mutation may promote resistance to hormonal therapy due to constitutive activity (see below) (Dehm et al., 2008), highlighting the divergent functional capability of AR in different contexts.

Prostate Cancer

The prostate is a gland approximately the size of a large walnut, surrounding the urethra just below the urinary bladder. It is composed of 4 zones: the peripheral zone, which is the largest portion of the prostate and the site of the majority of PCa, the transition zone, where benign prostatic hyperplasia (BPH) originates, the central zone and the anterior fibromuscular stroma. The tissue is structured histologically as glands comprised of luminal and basal epithelial cells, surrounded by stromal smooth muscle cells. The first stage of cancer progression is the onset of prostatic intraepithelial neoplasia (PIN), a "precursor lesion" where epithelial cells become atypical with enlarged nucleoli and increased proliferation, but the neoplastic cells remain contained within the basement membrane (Brawer, 2005). Adenocarcinoma is defined as the invasion of epithelial cells into the surrounding stromal tissue, and metastasis is the spread of these cells to distal sites, often bone or lymph nodes (Figure 1.2) (Abate-Shen and Shen, 2002).

PCa is the most common non-cutaneous cancer and the second-deadliest cancer among men in the United States and other Western countries. This year it is estimated that over 220,000 men will be diagnosed with PCa and more than 27,000 men will die in the United States as a result of the disease (Siegel et al., 2015). If detected early, localized PCa can generally be cured with radiation or radical prostatectomy. However, metastatic disease often becomes resistant to current therapies despite an initial favorable response, and these patients succumb to their treatment-refractory cancer. Thus, a deeper understanding of the molecular interactions underlying disease progression is necessary in order to improve upon existing treatments and to develop new ones.

Beyond developing novel therapeutics for PCa patients, a primary question is which patients require aggressive treatment. Age is the biggest risk factor for PCa, and the majority of

localized tumors are indolent, meaning that often the cancer will not substantially affect the patient's overall health within their lifetime. The majority of men over 70 show some degree of PIN or even localized PCa upon autopsy, regardless of a diagnosis within their lifetime. In other words, most PCa patients die with, not because of, their localized tumor (Waterbor and Bueschen, 1995). However, it is difficult to distinguish early PCa that will metastasize from that which will not. Improved biomarkers for aggressive vs. indolent disease could spare substantial healthcare resources by identifying those for whom watchful waiting would suffice.

Prostate Cancer Detection, Post-Metastatic Therapy and Resistance

Because prostate tumors are dependent on androgen signaling, previous therapies have targeted circulating androgen production or the AR protein. Testicular testosterone is the primary circulating androgen, however the adrenal gland secretes a low amount of androgens and testosterone precursors as well (Labrie, 2011). Hence, the original hormone treatment for PCa developed by Drs. Huggins and Hodges in 1941 was orchiectomy, which involves surgical removal of the testes (castration) (Huggins and Hodges, 2002). In the present day, "medical castration" is often performed with drugs that reduce circulating testosterone to levels equivalent to surgical castration. In most patients, this "androgen ablation" monotherapy temporarily results in tumor regression and a drop in prostate-specific antigen (PSA) levels.

Previously primary PCa was detected by digital palpation, but a more sensitive marker proved to be serum levels of the PSA protein, encoded by the *KLK3* gene and a direct target of AR. Rising PSA levels are a clinical indicator of resistance to androgen ablation therapy and resurgent AR activity. While useful for tracking disease progression in PCa patients, PSA screening for PCa risk in otherwise healthy men is very controversial and screening

9

recommendations vary (Etzioni et al., 2002; Etzioni and Thompson, 2014). Some studies have revealed a high rate of overdiagnosis, i.e. men with elevated PSA but no sign of PCa upon an invasive biopsy, such that there may be high cost but little overall survival benefit from screening the general population absent additional risk factors.

The feedback system of the hypo-pituitary-adrenal-gonadal axis maintains testosterone levels within a normal physiological range and offers opportunities for clinical intervention, i.e. targets for androgen ablation therapy. When the hypothalamus detects low testosterone levels, it produces luteinizing hormone-releasing hormone (LHRH), which signals to the pituitary to produce luteinizing hormone (LH), which signals to the testes to produce testosterone. Rising testosterone signals back to the hypothalamus to slow LHRH production (Kluth et al., 2014). LHRH agonists or antagonists are drugs commonly used to disrupt testosterone production in PCa patients. LHRH antagonists prevent the pituitary from responding to LHRH, causing reduced LH production and thus reduced testosterone production. LHRH agonists stimulate the system to temporarily increase testosterone production, yet this "burst" ultimately leads to reduced LHRH and reduced testosterone over time (Kluth et al., 2014). Reducing testosterone production in this manner is initially effective in causing regression of prostate tumors.

Antiandrogens are non-steroidal competitive inhibitors that bind the LBD of the AR protein and may be given in combination with androgen ablation, resulting in total androgen blockade. Hydroxyflutamide and bicalutamide are among the earlier antiandrogens, and more recently Enzalutamide (MDV3100) was developed as a more potent compound (Mukherji et al., 2012). Antiandrogens act by binding to the AR LBD and competitively inhibiting agonist binding, while Enzalutamide blocks nuclear entry as well. The conformation of antiandrogen-bound AR is altered such that it disrupts AF-2 and prevents interaction with the normal

complement of coregulators, and thus normal transcriptional activity is abrogated despite nuclear translocation and DNA binding. In addition, antagonists induce a partially distinct AR genomic binding profile (Chen et al., 2014).

Androgen synthesis enzymes have been targeted with small molecules as well. Abiraterone acetate is a rationally designed drug that directly inhibits the CYP17A1 enzyme that catalyzes the initial steps of testosterone production, and is given after failure of androgen ablation therapy (Bryce and Ryan, 2011). While this drug successfully reduces androgen synthesis in the adrenal gland and tumor, as well as the testes like Lupron, and extends life by several months in CRPC patients, resistance can also develop. Dutasteride and finasteride are inhibitors of the DHT conversion enzymes SRD5A1 and SRD5A2, and are used in treatment of BPH (Wu et al., 2014). To determine whether a long-term decrease in androgen signaling could reduce PCa risk, men in the Prostate Cancer Prevention Trial were given finasteride or placebo and followed for up to 18 years (Thompson et al., 2013). The finasteride group had a lower rate of PCa but a greater proportion with high-grade disease, and there was no significant difference in long-term survival. This finding highlights the heterogeneity of PCa and suggests that a given therapy may benefit or harm different subsets of patients.

As implied by the name CRPC, AR remains active despite ongoing therapy (Culig et al., 1998). This can occur through several mechanisms, including treatment-selected mutations in AR (O'Mahony et al., 2008; Steinkamp et al., 2009). Somatic mutations in the AR LBD can result in a promiscuous receptor able to be activated rather than repressed by antiandrogens, e.g. the T877A mutation that is activated by hydroxyflutamide as well as adrenal androgens (Tan et al., 1997). Similarly, AR-V716M can be activated by adrenal androgens and progesterone (Culig et al., 1993), and in a patient treated with hydroxyflutamide this mutation was the dominant AR

expressed in multiple metastases (Steinkamp et al., 2009). Furthermore, truncating mutations can introduce a stop codon prior to the LBD (Ceraline et al., 2004), or tumor cells can express alternatively spliced isoforms of AR that incorporate novel exons after the DBD and truncate prior to the LBD (Dehm and Tindall, 2011; Dehm et al., 2008). These AR variants cannot bind hormone, and are constitutively nuclear and transcriptionally active despite androgen ablation or antiandrogen therapy. In a small study, expression of truncated splice variant ARs is associated with Enzalutamide and abiraterone acetate resistance and decreased survival (Antonarakis et al., 2014). Missense mutations in AR can also facilitate abnormal transactivation of targets. The N-terminal transactivation domain mutants E231G (seen in mice) and E255K (the corresponding residue in humans) promote increased stability and nuclear localization of AR (Han et al., 2005; Steinkamp et al., 2009), due in part to decreased interaction with the ubiquitin ligase C-terminal HSP-interacting protein (CHIP) (Han et al., 2005). The W435L mutation in the WxxLF motif promotes increased transactivation via enhanced N-C interaction (Steinkamp et al., 2009).

Genes encoding androgen synthesis enzymes can be aberrantly activated in PCa, resulting in intra-tumor androgen synthesis which circumvents the normal feedback loop. AR can also become overexpressed in tumor cells due to gene locus amplification or other dysregulation, allowing a hypersensitive response to minute levels of circulating androgens or even to antiandrogens. Overexpression of AR coactivators can also sensitize the androgen response (Feldman and Feldman, 2001; Heinlein and Chang, 2004; Shen and Abate-Shen, 2010). AR can also be activated in a ligand-independent manner through phosphorylation by epidermal growth factor (EGF) or insulin-like growth factor (IGF) signaling (Culig et al., 1994). Finally, the requirement for AR signaling can be bypassed via upregulation of alternative signaling pathways in the tumor cell such as BCL2 (Feldman and Feldman, 2001; Furuya et al., 1996).

Mouse Models of Prostate Cancer

The mouse has proven to be a valuable experimental system in which to study AR and PCa (Abate-Shen and Shen, 2002; Robins, 2011), particularly at early disease stages for which human samples are unavailable. Furthermore, mice allow genetic manipulation within a homogeneous background. However, autochthonous mouse models of PCa rarely metastasize to bone, the most frequent metastatic site in humans. Additionally, the initiating genetic lesion is uniformly present, in contrast to human disease which likely originates in one or a subset of cells.

While the physiological role of the mouse prostate is similar to humans, the structure is distinct. Unlike the zonal human prostate, the mouse prostate is comprised of 4 pairs of lobes: the anterior prostate (AP), ventral prostate (VP) and the dorsal prostate (DP) and lateral prostate (LP), which are often dissected and analyzed together as the dorsolateral prostate (DLP) (Cunha et al., 1987). While mice do not naturally develop PCa in their lifetime, in contrast to the high frequency in humans, a number of genetically engineered mouse models (GEMMs) of PCa have been established. An early model of aggressive, metastatic PCa was the transgenic adenocarcinoma of the mouse prostate (TRAMP) mouse (Greenberg et al., 1995). TRAMP mice harbor a transgene expressing the SV-40 T antigen under control of the rat probasin promoter, which drives prostate-specific androgen-induced expression. The disease course in TRAMP parallels that in humans, with lesions initiating as PIN before progressing to invasive adenocarcinoma and metastasis, and with CRPC developing in castrated mice (Gingrich et al., 1996). However, TRAMP tumors show frequent neuroendocrine differentiation (Kaplan-Lefko et al., 2003), which is less common in humans. Importantly, this mouse model helped to establish that PIN is a precursor to adenocarcinoma.

More accurate mouse models of PCa reflect mutations seen in patients, including loss of *Nkx3-1*, a tumor suppressor and prostate differentiation gene (Bowen et al., 2000). *Nkx3-1*$^{-/-}$ and even *Nkx3-1*$^{+/-}$ mice develop PIN but do not progress to adenocarcinoma (Kim et al., 2002a). Mice expressing a prostate-targeted *c-Myc* transgene, modeling the oncogenic *MYC* overexpression seen in human PCa, develop PIN with progression to adenocarcinoma, suggesting a driver role (Ellwood-Yen et al., 2003). Notably, tumors in the *c-Myc* mice show reduced *Nkx3-1* expression.

Mice with one allele of the tumor suppressor *Pten* knocked out in the germline (*Pten*$^{+/-}$) develop PIN but do not progress to adenocarcinoma. The mice are predisposed to additional cancers as well, including lymphoma (Alimonti et al., 2010; Trotman et al., 2003). However, *Nkx3-1*$^{+/-}$;*Pten*$^{+/-}$ mice progress to adenocarcinoma, while mice with either single lesion do not (Kim et al., 2002b). This suggests that reduced expression of multiple tumor suppressors can accelerate cancer progression, and supports the notion that multiple alterations are required for tumorigenesis.

In addition to the autochthonous mouse models described above, immunodeficient mice may be implanted with malignant cells as xenografts. The cells may first be transduced with viral constructs to stably overexpress or knock down a given gene, or may be otherwise manipulated (Bertram et al., 2006; Chen et al., 2004; Thomas et al., 2013). Compared to GEMMs, these models can use human cells and facilitate rapid experiments to test the effects of drug treatment or gene over- or underexpression on tumor growth and metastasis. However, such experiments may not consider the influence of the microenvironment.

Androgen Receptor Variation in Mouse Models of PCa

In work led by Megan Albertelli, the Robins lab previously asked how naturally

occurring variation in AR, reflecting a stronger or weaker androgen axis, could influence PCa

initiation and progression, using the mouse for its homogeneous genetic background (Albertelli

et al., 2008; Albertelli et al., 2006). The mouse AR protein is approximately 15% divergent from

the human AR in the N-terminal domain, including an interrupted Q-tract, but otherwise the

protein sequences are nearly identical. Exon 1 of the human *AR* gene, which encodes the entire

N-terminal domain including the Q-tract, was knocked into the mouse *Ar* locus to produce a

"humanized AR" mouse, with alleles encoding short (*hAR^{12Q}*), medium (*hAR^{21Q}*) or long

(*hAR^{48Q}*) Q-tracts. The Q-tract variants alone did not affect survival or fertility, and the mice did

not develop PCa. However, several androgen-induced genes in the prostate showed a trend

toward increased expression with the "stronger" *hAR^{12Q}* allele or reduced expression with the

"weaker" *hAR^{48Q}* allele, reflecting differences at the molecular level due to AR transcriptional

activity (Albertelli et al., 2006). The varying strength of the androgen axis was also evident as

increased seminal vesicle weight or overall prostate weight with the stronger allele (Albertelli et

al., 2006; Simanainen et al., 2011). While a 48Q AR would cause SBMA in man, mice require at

least an 112Q AR to develop a similar neurodegenerative phenotype (Chevalier-Larsen et al.,

2004).

When the humanized AR mice were crossed onto the TRAMP background, effects on

cancer initiation, progression and treatment response were observed (Albertelli et al., 2008;

Robins et al., 2008). Histological analysis revealed a higher percentage of the prostate epithelium

composed of PIN at 12 weeks in *hAR^{12Q}* mice. Palpable tumors were detected later in the *hAR^{48Q}*

than *hAR^{12Q}* mice. Interestingly, the *hAR^{12Q}* mice had increased survival from the time of tumor

detection and had more well-differentiated tumors. This finding may reflect opposing functions of AR in promoting growth and proliferation as well as differentiation. Furthermore, the Q-tract affected response to castration therapy. Tumors in the hAR^{48Q} TRAMP mice did not respond to castration, and these mice died earlier. In contrast, half of the castrated hAR^{12Q} mice showed a survival benefit, but half never developed a palpable primary prostate tumor and died of aggressive metastatic disease (Albertelli et al., 2008; Robins et al., 2008). As before, these results show the divergent function of AR. In hAR^{48Q} mice, the weaker AR permits progression by AR-independent growth pathways. The divergent response of castrated hAR^{12Q} mice highlights the heterogeneity and stochastic nature of PCa. This echoes the findings of the Prostate Cancer Prevention Trial, where finasteride treatment successfully lowered the overall rate of PCa but resulted in more aggressive tumors (Thompson et al., 2013).

In additional transgenic mouse models, wildtype and mutant AR have been overexpressed. One group reported that transgenic overexpression of the AR-E231G mutant resulted in metastatic PCa and altered prostate gene expression while AR-WT did not (Han et al., 2005; Thompson et al., 2011). Transgenic expression of a truncated AR splice variant that is constitutively active *in vitro* caused PIN with upregulation of epithelial to mesenchymal transition (EMT) genes (Sun et al., 2014). These results suggest that AR dysregulation may promote oncogenesis, while an increase in wildtype AR activity via a short Q-tract (Albertelli et al., 2006) or overexpression (Thompson et al., 2011; Zong et al., 2009) does not. However in a xenograft study using AR-positive PCa cell lines, an increase in AR expression was sufficient to drive progression to CRPC (Chen et al., 2004). Moreover, AR can cooperate with additional mutations to alter disease progression (Albertelli et al., 2008; Zong et al., 2009).

These findings highlight the duality of AR; it normally promotes cell differentiation and tissue maintenance, but can also enhance cell proliferation and tumorigenesis (Gao et al., 2001). In TRAMP mice, the stronger AR drove earlier tumor growth yet also maintained better differentiation of those tumor cells, and resulted in differential response to therapy. Therefore, an "oncogenic switch" seems to occur early in prostate tumorigenesis in which AR is redirected from its normal pro-differentiation gene expression program to favor expression of genes promoting proliferation and invasion. Understanding the factors that contribute to this oncogenic switch requires determining the impact on AR signaling from additional somatic mutations that are commonly observed in tumors from human PCa patients.

Recurrent Gene Fusions in Prostate Cancer

Scott Tomlins and Arul Chinnaiyan at the University of Michigan opened up a new field in PCa research when they discovered recurrent gene fusions involving E26 transformation-specific (ETS) transcription factor genes fused to androgen-responsive promoters. The structure of these fusions immediately suggested how AR may drive oncogene activation to initiate PCa. The ETS genes *ERG* and *ETV1* were first identified as highly expressed outliers in a bioinformatic analysis of several patient data sets (Tomlins et al., 2005). After ruling out amplification of the *ERG* and *ETV1* genomic loci and showing reduced expression of the 5' exons relative to the rest of the gene, Tomlins et al. used 5' RNA ligase-mediated rapid amplification of cDNA ends (RLM-RACE) to identify potential upstream gene fusion partners. The 5' noncoding exons and upstream regulatory region of the *TMPRSS2* gene were found to be fused to the 3' coding exons of *ERG* or *ETV1* via genomic translocation (Tomlins et al., 2005).

TMPRSS2 is an androgen-induced gene, which explained the upregulation of *ERG* and *ETV1*, neither of which are highly expressed in normal prostate.

ETS transcription factors are cell cycle regulators capable of controlling growth, development and proliferation, and ETV1 is important for muscle and nervous system development. *In vitro*, overexpression of exogenous ERG or ETV1 in benign prostate cell lines results in increased invasion, while knockdown in fusion-positive PCa cell lines decreases invasion (Mesquita et al., 2014; Tomlins et al., 2007; Tomlins et al., 2008a). ERG and ETV1 overexpression mimic RAS/MAPK signaling in benign prostate cells (Hollenhorst et al., 2011a). A recent study attaining ERG knockdown with an inducible short hairpin RNA (shRNA) demonstrated that ERG drives proliferation and inhibits luminal and neuronal differentiation (Mounir et al., 2014). Furthermore, the matrix metalloproteinase genes *MMP7* and *MMP9* are transcriptional targets of ERG and ETV1 (Shin et al., 2012; Tian et al., 2013), which suggests that promoting a breakdown of the extracellular matrix is one way that overexpressed ETS factors increase invasiveness.

Recurrent gene fusions such as BCR-ABL have been previously identified in leukemia, and the BCR-ABL protein has proven to be a valuable therapeutic target (Jabbour and Kantarjian, 2014). ETS genes were known to be involved in gene fusions in Ewing's sarcoma, most frequently FLI1 but also ERG and ETV1 (Jeon et al., 1995; May et al., 1993; Sorensen et al., 1994). ETV1 is also a key transcription factor in gastrointestinal stromal tumors (GIST) (Ran et al., 2015). The identification of ETS fusions in PCa suggested that it may be possible to stratify patients by molecular alteration and design new targeted therapies.

ERG is fused to *TMPRSS2* in approximately 50% of prostate tumors, and occasionally to alternative upstream partners (Han et al., 2008). *ETV1* is fused to *TMPRSS2* in some cases, but

more often to a broader spectrum of upstream partners, collectively in 5-10% of tumors. The ETS genes *ELK4*, *ETV4* and *ETV5* are each similarly rearranged in 2-5% of tumors (Rubin et al., 2011). A distinct class of prostate tumors overexpress SPINK1, though not mediated by a gene fusion event, in approximately 10% of patients (Tomlins et al., 2008b). Importantly, the vast majority of upstream ETS fusion partners are androgen-induced genes, though housekeeping genes or human endogenous retroviruses (HERVs) drive high expression in a subset of ETS fusions (Rubin et al., 2011).

Not only is expression of the ETS fusions generally androgen-induced, but androgen stimulation of benign prostate cells can promote formation of the TMPRSS2-ERG fusion (Bastus et al., 2010; Lin et al., 2009; Mani et al., 2009). The *TMPRSS2* and *ERG* genes lie 2.8 Mb apart on chromosome 21. Concomitant recruitment of AR and topoisomerase II beta (TOP2B) induces double-strand breaks, and inappropriate repair results in excision of the intervening sequence and formation of the fusion product (Haffner et al., 2011). Despite the high frequency of ETS gene rearrangements in prostate tumors, it remains questionable whether the presence of a fusion alone indicates poor prognosis. A large study showed no association between the TMPRSS2-ERG fusion and biochemical recurrence after prostatectomy (Pettersson et al., 2012; Rubin et al., 2011; Taris et al., 2014a). However, TMPRSS2-ERG has diagnostic utility, and is useful in distinguishing high-grade PIN (HG-PIN) and PCa from other histological abnormalities (Barbieri and Tomlins, 2014).

In mice transgenic overexpression of ERG or ETV1 in the prostate is insufficient for PCa but results in PIN at variable penetrance, reflecting heterogeneous disease even in a homogeneous genetic background (Carver et al., 2009; King et al., 2009; Klezovitch et al., 2008; Shin et al., 2009; Tomlins et al., 2007; Tomlins et al., 2008a). Similarly when mouse prostate

cells overexpressing ERG are transplanted into the prostate of immunocompromised mice, ERG overexpression induces PIN (Zong et al., 2009). These *in vitro* and *in vivo* results suggest that ETS factors play a role in early neoplasia. However, similar to overexpression of AR alone, an increase in activity may not be sufficient to drive complete transformation. Additional dysregulation or cooperating genomic insults such as tumor suppressor loss may be required to promote progression to overt PCa, at least in mouse models.

PTEN Loss in Prostate Cancer

Expression of the phosphatase and tensin homolog gene (*PTEN*) is reduced or lost due to genomic deletion or inactivating mutations in more than half of prostate tumors, and it is frequently lost in other cancers as well (Taylor et al., 2010). *PTEN* is a tumor suppressor gene whose protein product is a phosphatase that targets the signaling molecule phosphatidylinositol-3,4,5-trisphosphate (PIP3). In turn, PIP3 reduction inhibits activation of the phosphoinositide 3-kinase (PI3K) / protein kinase B (AKT) signaling pathway (Stiles et al., 2004). PI3K phosphorylates AKT at Serine-473, and phospho-AKT (pAKT) activates mammalian target of rapamycin (mTOR) signaling as well as other pro-survival, pro-proliferation pathways. PTEN loss is associated with worse clinical prognosis in PCa patients (Bismar et al., 2011) and progression to CRPC, as shown in xenograft experiments where PTEN-deficient tumors continued to grow despite castration (Bertram et al., 2006).

Complete germline deletion of *Pten* in mice is lethal, but hypomorphic alleles reveal that even 30% *Pten* expression ($Pten^{hy/-}$) is viable. Furthermore, penetrance of multiple cancers including PCa is inversely correlated with *Pten* expression level, with PIN developing in $Pten^{+/-}$ mice and progression to prostate adenocarcinoma occurring in $Pten^{hy/-}$ mice (Alimonti et al.,

2010; Trotman et al., 2003). Conditional *Pten* knockout in the mouse prostate, achieved with

floxed *Pten* (*Pten^{flox/flox}*) and a probasin-driven Cre recombinase transgene, avoids the lethality

caused by germline deletion and results in high-penetrance adenocarcinoma (Ma et al., 2005;

Wang et al., 2003).

The AR and PI3K/AKT pathways reciprocally inhibit one another, meaning that

treatments targeting one pathway can lead to enhanced activity of the other (Carver et al., 2011;

Mulholland et al., 2011). AR inhibits pAKT indirectly via the androgen-induced gene *FKBP5*,

whose protein product upregulates PHLPP, the phosphatase for pAKT. Likewise, PTEN loss

inhibits AR transcriptional activity indirectly via activation of the polycomb repressive complex

member EZH2, as well as c-JUN and EGR1 (Mulholland et al., 2011). Combination therapy, i.e.

inhibiting AR and PI3K/AKT signaling simultaneously, more potently represses the growth of

PCa cells *in vitro* and in xenograft models and may have therapeutic utility in patients (Carver et

al., 2011; Mulholland et al., 2011; Thomas et al., 2013).

Cooperation Between ETS Fusions and PTEN Loss

In patient tumors, genomic loss of one or both copies of *PTEN* is significantly correlated

with the presence of the TMPRSS2-ERG fusion (Bismar et al., 2011; King et al., 2009; Krohn et

al., 2012), leading to the hypothesis that the two lesions cooperate in oncogenesis. Prostatic ERG

overexpression in *Pten^{+/-}* mice results in progression to adenocarcinoma (Carver et al., 2009) or

at least higher penetrance PIN (Baena et al., 2013; King et al., 2009) than in *Pten^{+/-}* mice alone,

supporting cooperation. In a report published while this thesis project was ongoing, prostatic

ETV1 overexpression in *Pten^{+/-}* mice resulted in higher-penetrance PIN compared to *Pten*

reduction alone, but still without progression to adenocarcinoma (Baena et al., 2013). In

Pten^{flox/flox} mice, concurrent ERG overexpression resulted in greater progression to adenocarcinoma (Chen et al., 2013) or no additive effect (Baena et al., 2013). The combination of ETV1 overexpression and prostatic *Pten* deletion resulted in earlier death than in *Pten^{flox/flox}* mice alone (Baena et al., 2013). In experiments where mouse prostate cells were transduced with lentiviral constructs and re-implanted into immunocompromised mice, stable overexpression of ERG alone in the implanted cells resulted in PIN, but simultaneous AKT overexpression or PTEN knockdown resulted in progression to adenocarcinoma (Zong et al., 2009). While it appears that ETV1 and ERG have the potential to cooperate with *Pten* loss or reduction in prostate oncogenesis, results vary between studies. This may reflect differences in mouse strain background, time points and the nature of the transgene or knocked-in construct, as well as human-mouse differences.

Intriguingly, in the mouse prostate tissue re-implantation experiments, lentiviral AR overexpression alone did not induce any neoplasia, but stable AR plus ERG overexpression resulted in adenocarcinoma (Zong et al., 2009). This particular finding suggests that increased activity level of wildtype AR can influence PCa progression in the context of oncogene activation, which is in line with the results in *hAR;TRAMP* mice (Albertelli et al., 2008). Together, those discoveries beg the question of how variation in AR or the androgen axis (modeled by polymorphic Q-tract length) affects PCa progression driven by ETS overexpression and PTEN reduction.

Cell Culture Models of Prostate Cancer

Cell lines derived from human PCa metastases as well as normal prostate tissue have also been important for molecular studies of AR and other important signaling pathways, facilitating

biochemical analyses not possible *in vivo*. Numerous PCa cell lines are commercially available and commonly used (Sobel and Sadar, 2005a, b). Some cell lines were cultured directly from tumors, while others were immortalized from normal prostate tissue or passaged through mouse xenografts. Each line has distinct properties such as mutated, overexpressed or absent AR, loss or overexpression of AR cofactors, ETS fusions, or other features that suit different cell lines to specific experimental questions. A disadvantage of cell lines is that they generally represent late stage disease from a single tumor. Therefore, biological replicates in most cell culture experiments represent responses to culture conditions rather than individual variation. Cell lines can also acquire mutations in culture, and experiments with the same cell line in different labs may not give uniform results. Finally, a monolayer of cells does not recapitulate the complex milieu of cell types and signaling factors present in tissue. Nevertheless, PCa cells are a valuable tool in AR and PCa biology.

LNCaP cells, derived from a lymph node PCa metastasis, are used frequently to study AR and PCa (Horoszewicz et al., 1983). LNCaP cells express AR and respond to androgen stimulation, and a number of androgen-regulated gene sets have been characterized in LNCaP (DePrimo et al., 2002; Jones et al., 2005). Withdrawing androgen slows cell growth, but long-term androgen ablation selects for androgen-independent cells, such as the LNCaP-abl line. Interestingly, LNCaP cells exhibit a biphasic androgen response where superphysiological levels inhibit growth, again highlighting the dual capacity of AR to promote proliferation or differentiation. The LNCaP AR harbors the T877A mutation in the LBD that allows activation by the antiandrogen hydroxyflutamide. This mutation likely arose in the patient in response to antiandrogen treatment, which selects for LBD mutations as a means of evading therapy

(O'Mahony et al., 2008; Steinkamp et al., 2009). The T877A mutation is found in post-treatment PCa patients and additional PCa cell lines as well.

LNCaP cells have lost PTEN expression, and overexpress ETV1 due to a genomic rearrangement placing the entire ETV1 locus in an androgen-responsive region (Tomlins et al., 2007). Previous studies in LNCaP have reported that ETV1 enhances AR genomic binding and target gene induction (Baena et al., 2013; Chen et al., 2013; Shin et al., 2009). Predicted ETS and AR binding sites overlap throughout the genome, and indeed ETV1 and AR binding overlap in ChIP-seq experiments (Chen et al., 2013). The ETV1 and AR proteins can physically interact in a DNA-independent manner as well (Shin et al., 2009).

VCaP cells, derived from a vertebral metastasis, express wild-type but amplified AR, exemplifying another means to evade hormone therapy: androgen hypersensitivity through AR overexpression. VCaP cells retain PTEN expression and harbor a canonical TMPRSS2-ERG fusion gene. AR transactivation is strongly induced by androgen treatment, and ERG knockdown enhances AR activity, suggesting that ERG is repressing AR in this context (Baena et al., 2013; Mounir et al., 2014; Tomlins et al., 2008a; Yu et al., 2010). ChIP-seq experiments revealed that not only do ERG and AR binding sites significantly overlap, but ERG recruits the polycomb repressive complex (PRC), which places repressive histone 3 lysine 27 trimethylation (H3K27me3) marks near AR target genes (Yu et al., 2010). Exogenous ERG expression represses AR activity in additional PCa cell lines as well (Tomlins et al., 2008a; Yu et al., 2010).

Several other PCa cell lines such as PC3 and DU-145 have lost AR expression, but can exhibit androgen responsiveness when exogenous AR is introduced. Of note, some AR-negative PCa cell lines are more proliferative, invasive and tumorigenic than AR-positive cells. Expressing AR in PC3 cells and stimulating with DHT indeed slows proliferation (Mirochnik et

al., 2012), again highlighting the dual nature of AR: in some contexts it promotes proliferation and tumorigenesis, yet even in tumors and metastatic PCa cells it can promote differentiation.

Based on the *in vitro* studies described above, it has been suggested that while ERG and ETV1 both promote cell invasion, they have mainly divergent interactions with AR at the molecular level; ETV1 enhances AR activity while ERG represses it (Baena et al., 2013). However, in a mouse model ERG appears to promote activation of AR target genes, but only in prostate tumors of *Pten$^{flox/flox}$* mice (Chen et al., 2013). This suggests that interactions may differ *in vivo* vs. *in vitro*, and may depend on disease stage or the status of additional signaling pathways. Furthermore, the relationship between ETV1 and AR in contexts outside of LNCaP cells remains largely unexplored.

AR Variation and ETS-Induced or PTEN Loss-Induced Neoplasia

In my thesis work I have explored how changes in the strength of the androgen axis, exemplified by Q-tract variation modeling the extremes in the human population, affect pathology resulting from oncogene activation and tumor suppressor loss in PCa. Mice expressing a short, median or long Q-tract AR were crossed with mice carrying a prostate-targeted ETV1 transgene, or harboring germline loss of one *Pten* allele. These mice reflect human genetic variation in AR combined with common somatic mutations occurring in prostate tumors, and were examined with or without androgen ablation. Thus, this strategy encompasses the heterogeneity in human PCa, particularly in early-stage disease and the transition to malignancy, in the context of a varying androgen axis.

Global gene expression profiling by RNA-seq was performed to identify the downstream molecular consequences of interaction between the key transcription factors AR and ETV1 at

early and later stages of PCa progression. Particular attention was paid to genes and pathways dysregulated by ETV1 that are potentially targetable in therapy or that may have prognostic value. The effects observed in mice were directly tested *in vitro* with benign and malignant prostate cell lines modeling early, intermediate and late disease stages. Knockdown or overexpression of AR and ETV1 were performed to study direct interactions, with upstream genomic binding and downstream gene expression output analyzed.

Chapter 2 presents the mouse studies, which were recently published in the journal *Hormones and Cancer* (Higgins et al., 2015). Chapter 3 describes *in vitro* experiments that directly examine whether ETV1 alters AR target gene expression in different cellular contexts. Chapter 4 discusses the collective results and explores future scientific questions.
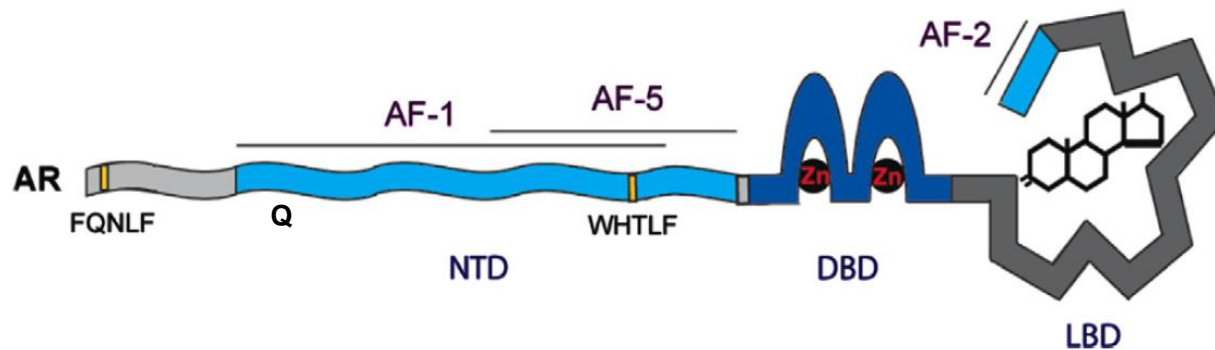
Figure 1.1: Functional Domains of Androgen Receptor

The 110 kDa AR protein contains distinct functional domains. The N-terminal transactivation domain (NTD) contains the ligand-independent activation functions AF-1 and AF-5. The DNA binding domain (DBD) consists of two zinc fingers. A hinge domain lies between the DBD and the ligand binding domain (LBD). Ligand binding induces a conformational change in the LBD, forming AF-2 which recruits transcriptional cofactors. The FQNLF and WHTLF motifs facilitate N-terminal C-terminal interaction and further facilitate cofactor binding. Adapted from (Robins, 2011).
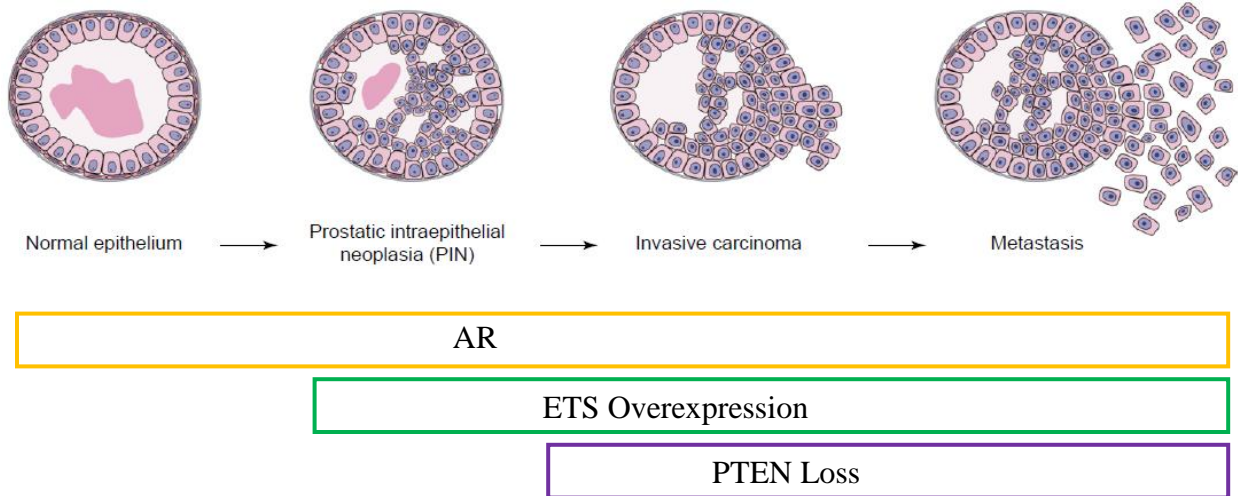
Figure 1.2: Model of Prostate Cancer Progression

The normal prostate gland consists of luminal and basal epithelial cells surrounded by stromal smooth muscle. PIN, a PCa precursor lesion, occurs with atypia and uncontrolled proliferation of epithelial cells that remain contained within the basement membrane. Invasion through the basement membrane and into the stromal tissue constitutes adenocarcinoma (PCa). The invasive cells can eventually metastasize to distant sites. Adapted from (Abate-Shen and Shen, 2002).

AR is expressed throughout PCa progression, including in CRPC. ETS fusions generally occur as a relatively early event and are clonal within a given tumor focus. PTEN loss can occur as an early or late event, but is more frequent in advanced PCa. PTEN loss is associated with progression to CRPC.

Chapter 2

Interaction of the androgen receptor, ETV1 and PTEN pathways in mouse prostate varies with pathological stage and predicts cancer progression

Acknowledgements

Abstract

To examine the impact of common somatic mutations in prostate cancer (PCa) on

androgen receptor (AR) signaling, mouse models were designed to perturb sequentially the AR,

ETV1 and PTEN pathways. Mice with "humanized" AR (*hAR*) alleles that modified AR

transcriptional strength by varying polyglutamine tract (Q-tract) length were crossed with mice expressing a prostate-specific, AR-responsive ETV1 transgene ($ETV1^{Tg}$). While *hAR* allele did not grossly affect ETV1-induced neoplasia, ETV1 strongly antagonized global AR regulation and repressed critical androgen-induced differentiation and tumor suppressor genes, such as *Nkx3-1* and *Hoxb13*. When *Pten* was varied to determine its impact on disease progression, mice lacking one *Pten* allele ($Pten^{+/-}$) developed more frequent prostatic intraepithelial neoplasia (PIN). Yet only those with the ETV1 transgene progressed to invasive adenocarcinoma. Furthermore, progression was more frequent with the short Q-tract (stronger) AR, suggesting that the AR, ETV1 and PTEN pathways cooperate in aggressive disease. On the $Pten^{+/-}$ background, ETV1 had markedly less effect on AR target genes. However, a strong inflammatory expression signature, notably upregulation of *Cxcl16*, was induced by ETV1. Comparison of mouse and human patient data stratified by presence of ETS fusion genes highlighted additional factors, some not previously associated with prostate cancer but for which targeted therapies are in development for other diseases. In sum, concerted use of these mouse models illuminates the complex interplay of AR, ETV1 and PTEN pathways in pre-cancerous neoplasia and early tumorigenesis, disease stages difficult to analyze in man.

Introduction

Signaling through the androgen receptor (AR), a hormone-activated transcription factor in the nuclear receptor superfamily, is critical for normal prostate development and prostate cancer (PCa) progression (Abate-Shen and Shen, 2000). Androgen ablation therapy initially abrogates AR signaling and induces tumor regression, but tumors invariably recur despite

ongoing therapy and with continued AR expression and signaling (Shen and Abate-Shen, 2010).

Even with recently developed therapies, disease progressing despite castrate levels of serum

testosterone (termed castration-resistant prostate cancer [CRPC]) remains incurable (Knudsen

and Kelly, 2011). A more thorough understanding of the interaction between AR and additional

oncogenic pathways commonly dysregulated in PCa will be critical in identifying novel targets

for therapeutic intervention.

Well known genetic variation in the AR protein occurs in the length of a polyglutamine

tract (Q-tract) in the N-terminal domain. As shown by us and others, Q-tract length is inversely

proportional to AR transcriptional strength *in vitro* and *in vivo*, as seen molecularly in

differential target gene expression and physiologically in seminal vesicle weight (Albertelli et al.,

2006; Chamberlain et al., 1994; Simanainen et al., 2011). Q-tract length alone has not proven to

be associated with PCa risk in humans but in combination with alleles of the androgen synthesis

genes *CYP17* and *SRD5A2* the stronger AR increases PCa risk, supporting the notion that the

androgen axis overall influences disease (Lindstrom et al., 2006a; Lindstrom et al., 2006b). We

have previously shown that altering AR strength via Q-tract length variation on a homogenous

genetic background modifies PCa onset and progression in an aggressive transgenic mouse

model (Albertelli et al., 2008). Interestingly, AR genetic variation has recently been reported to

be associated with the frequency of recurrent gene fusions in PCa (see below) (Bastus et al.,

2010; Yoo et al., 2014). This led us to examine the *in vivo* effect of AR variation on PCa driven

by alterations commonly seen in human tumors.

Recurrent genomic rearrangements that fuse 5' regulatory elements of androgen-

responsive genes to the coding region of E26 transformation-specific (ETS) transcription factor

genes occur in approximately half of human prostate tumors (Tomlins et al., 2007; Tomlins et

al., 2005). These fusions drive robust androgen-induced prostatic expression of ETS factors otherwise not expressed in the prostate. Fusions involving the *ERG* and *ETV1* genes occur in approximately 50% and 5-10% of PCa, respectively (Tomlins et al., 2007; Tomlins et al., 2008a; Tomlins et al., 2005). ERG fusion events themselves are AR-mediated (Bastus et al., 2010), and prostate tumors are more likely to be ERG+ in patients harboring a short Q-tract (strong) *AR* allele (Bastus et al., 2010; Yoo et al., 2014), further suggesting cooperation between ETS and AR pathways. These fusions occur early in PCa ontogeny, and individual cancer foci or metastases are generally clonal for a given rearrangement, suggesting selection (Mehra et al., 2007; Svensson et al., 2011). Prostatic overexpression of ETS factors induces PIN in some mouse models (Baena et al., 2013; Carver et al., 2009; King et al., 2009; Shin et al., 2009; Tomlins et al., 2007), and ETS factors promote invasion and alter gene expression *in vitro* (Baena et al., 2013; Hollenhorst et al., 2011a; Tomlins et al., 2007; Yu et al., 2010). However, it is unknown how modulation of the androgen axis, such as by AR genetic variation, alters the effect of ETS overexpression on tumorigenesis.

Perturbation of AR and ETS pathways alone does not lead to PCa in mice but additional genetic events cooperate in tumorigenesis. The tumor suppressor *PTEN* is frequently deleted or inactivated in a variety of human cancers, including PCa (Taylor et al., 2010). PTEN is a phosphatase that inactivates the PI3K target PIP3, in turn preventing phosphorylation of AKT and activation of downstream proliferation and survival pathways (Stiles et al., 2004). Furthermore, the AKT and AR signaling pathways can repress one another in a reciprocal manner (Carver et al., 2011; Mulholland et al., 2011). In PCa, *PTEN* loss is associated with poor prognosis and progression to CRPC (Bertram et al., 2006; Bismar et al., 2011). In mice *Pten* reduction causes PIN in a dose-dependent manner, while prostate-targeted *Pten* homozygous

deletion leads to adenocarcinoma (Alimonti et al., 2010; Carver et al., 2009; Lesche et al., 2002; Trotman et al., 2003). Several additional genetic hits can cooperate with *Pten* reduction to promote PCa, such as further tumor suppressor loss (as of *Nkx3-1*) (Abate-Shen et al., 2003) or oncogene activation (as of *ERG*) (Carver et al., 2009; King et al., 2009). *ETV1* overexpression cooperates with prostate-specific *Pten* deletion to drive aggressive adenocarcinoma (Baena et al., 2013). However, the interaction of ETV1 overexpression and *Pten* reduction, which is more common in patients than homozygous loss (Whang et al., 1998), is not fully understood, with recently reported results (Baena et al., 2013) differing from the findings described here. Further, the extent to which altered AR signaling influences disease progression in these contexts has not been addressed.

In the current study we used gene expression profiling to determine how varying the strength of the androgen axis would alter prostate pathology initiated by ETV1 overexpression and/or PTEN reduction in mice. A marked antagonism of the normal AR-regulated transcriptome in ETV1-transgenic prostates was largely abrogated on a *Pten*-hemizygous background. With reduced PTEN, ETV1 overexpression induced disease progression, as well as a pro-inflammatory gene signature, both of which were impacted by AR strength. Integration of mouse and patient data revealed potential ETV1 regulation of known and novel PCa-associated genes, highlighting novel targets for therapeutic intervention.

Results

Effect of AR allele strength on ETV1-induced PIN

To test the role of AR in PCa initiation, we examined the effect of variation in AR transcriptional strength on ETV1-induced neoplasia. "Humanized" AR (*hAR*) mice were previously engineered by germline knockin to express an AR protein essentially identical to human, including either a short (*hAR^{12Q}*), average (*hAR^{21Q}*) or long (*hAR^{48Q}*) polyglutamine tract (Q-tract) in the N-terminal domain, modeling the extremes of human variation (Albertelli et al., 2006). As the mouse Ar lacks a contiguous Q-tract, which is known to affect AR activity, the *hAR* mice more accurately reflect human AR variation and biology. Q-tract length inversely correlates with AR transcriptional activity *in vitro*, seen as altered prostatic gene expression and endpoints of androgen action such as seminal vesicle weight (Albertelli et al., 2006; Chamberlain et al., 1994; Simanainen et al., 2011). Previously, we showed that AR Q-tract length modifies PCa onset, progression and treatment response in the aggressive TRAMP mouse model (Albertelli et al., 2008). Thus, variable AR transcriptional activity has the potential to modulate the effect of additional oncogenic events and alter the course of disease.

To test the interaction of AR with an oncogene activated in human PCa, *hAR^{12Q}* and *hAR^{48Q}* mice were crossed with ETV1 transgenic (*ETV1^{Tg}*) mice, in which a probasin-derived promoter drives androgen-inducible prostatic expression of human ETV1 (Figure 2.1a) (Tomlins et al., 2007). *hAR;ETV1^{Tg}* male offspring were castrated at 12 weeks (to ablate androgen signaling) or left intact, and prostate lobes were microdissected at 24 weeks and compared to those of intact non-transgenic *hAR* controls. Unlike the alobular human prostate, the mouse gland is comprised of three paired dorsolateral, ventral and anterior prostate lobes, referred to as DLP,

VP and AP, respectively. Morphologically there is not a particular mouse prostate lobe that is most similar to the human prostate (Shappell et al., 2004).

Histopathological analysis (n = 5-8 lobes per group) revealed PIN and substantial hyperplasia in prostates of intact *hAR;ETV1*^{Tg} mice (Figure 2.1b). Prostates of intact non-transgenic *hAR* controls were either normal or showed focal hyperplasia, and castrated *hAR;ETV1*^{Tg} mice had atrophic glands as expected (data not shown). In intact mice, 25% of *hAR*^{12Q}*;ETV1*^{Tg} and 20% of *hAR*^{48Q}*;ETV1*^{Tg} animals developed PIN by 24 weeks in the VP (Figure 2.1b). All of the remaining intact transgenic mice showed hyperplasia in either the DLP or VP (Figure 2.1b). Representative examples of each stage are shown in Figure 2.1c. These results are consistent with previous reports in which mice overexpressing ETV1 in the prostate via transgene or knock-in developed PIN but did not progress to adenocarcinoma (Baena et al., 2013; Shin et al., 2009; Tomlins et al., 2007). Here we show that the incidence of PIN was not affected substantially by AR Q-tract length.

AR regulation is antagonized by overexpression of ETV1

Despite driving only early neoplasia, the ETV1 transgene had a pronounced effect on prostatic gene expression. The DLP was chosen for analysis because the expression pattern in mouse DLP is most similar to that of the human prostate peripheral zone (Berquin et al., 2005), where most human PCa arises. Additionally, as shown below in *Pten* hemizygous mice, the DLP harbored substantially more PIN and adenocarcinoma than other lobes (Figure 2.10). In the previously reported *hAR* TRAMP mice, PIN is most apparent in the DLP as well (Albertelli et al., 2008).

qRT-PCR analysis showed that the androgen-induced genes *Tmprss2*, *Pbsn* and *Nkx3-1* were downregulated in prostates of intact *hAR;ETV1^{Tg}* mice, similar to the expected decrease in castrated controls (Figure 2.2a). Conversely, *Clu*, which is normally repressed by AR and thus upregulated following androgen ablation, was upregulated in prostates of intact *ETV1^{Tg}* mice as well as in castrated mice (Figure 2.2a). *Nkx3-1* is a well-established tumor suppressor gene in the prostate and a marker of luminal epithelial cell differentiation (Wang et al., 2009). *Nkx3-1* null mice develop PIN, and *Nkx3-1* is frequently downregulated in human PCa (Kim et al., 2002a). Its downregulation in *hAR;ETV1^{Tg}* mice here suggested a role in ETV1-mediated oncogenesis.

Examination of global gene expression differences by RNA-seq revealed striking and widespread molecular changes in the prostates of *hAR;ETV1^{Tg}* relative to *hAR* mice. DLP RNA samples were divided into 3 unique pools per group (2 pools for castrate groups), and a library was prepared for each pool. Along with samples from the *Pten^{+/-}* mice (see below), indexed libraries were divided across 4 lanes on the Illumina Hi-Seq 2000 for an average of 11.94 million reads per library. 95.8% of bases had quality scores $\geq$ Q30. Principal component analysis of all genes in all libraries was performed to gauge overall expression differences between groups. Three distinct clusters were observed, with samples segregated by ETV1 transgene and castration, while AR genotype had a substantially smaller effect (*hAR^{12Q}* and *hAR^{48Q}* samples were intermixed), as shown in Figure 2.2b.

Differential expression was performed between pairs of groups, or between multiple groups using a generalized linear model (GLM). Genes with a false-discovery rate (FDR) of 0.05 or less were considered significant. When the *hAR^{12Q}* and *hAR^{48Q}* mice were analyzed separately, 1145 and 2419 genes were upregulated and 757 and 2028 genes were downregulated, respectively, in transgenics vs. non-transgenics (Figure 2.2a,c). The majority of genes, 943

upregulated (82%) and 571 downregulated (75%), were shared among the hAR^{12Q} and hAR^{48Q} mice (Figure 2.2d), consistent with the principal component plot. However, a greater number of genes were significantly altered in the hAR^{48Q} mice. This may be because the weaker hAR^{48Q} is more susceptible to perturbation by ETV1 overexpression, resulting in greater differential expression in transgenic mice.

Using the GLM tools to combine hAR^{12Q} and hAR^{48Q} mice for differential expression, 2368 genes were upregulated and 2196 downregulated in intact $hAR;ETV1^{Tg}$ relative to hAR mice (Figure 2.3a). A comparable number of genes were differentially expressed among the castrated mice relative to intact, serving to highlight androgen-regulated genes (whether direct or indirect targets) by the effects of androgen ablation (data not shown). Such extensive differential expression in castrated mice was expected, but the magnitude of the effect in intact ETV1 transgenics was striking. The differential expression patterns between transgenic and non-transgenic DLP revealed that the intact $hAR;ETV1^{Tg}$ mice displayed a pattern similar to that of castrated mice, with many expression changes in the same direction (Figure 2.3a). Along with the initial qRT-PCR data, this suggested that ETV1 may inhibit normal AR function in a manner akin to androgen ablation. However, some ETV1-induced changes were "reverted" by castration (middle portion of Figure 2.3a), suggesting that ETV1 also controls a number of non-AR target genes.

To determine which pathways were altered in $hAR;ETV1^{Tg}$ DLP, functional annotation of differentially expressed genes was performed with the Database for Annotation, Visualization and Integrated Discovery (DAVID) (Huang Da et al., 2009) (http://david.abcc.ncifcrf.gov). "Prostate development" and "prostate morphogenesis" were among the gene ontology (GO) terms significantly enriched among ETV1-downregulated genes in intact mice. Relative

expression of genes annotated with these GO terms is shown in Figure 2.3b and a complete list

of enriched GO terms is in Online Resource 2

(http://link.springer.com/article/10.1007%2Fs12672-014-0215-9) (Higgins et al., 2015).

Importantly, this gene list includes the tumor suppressors *Nkx3-1* and *Pten*. Furthermore, the AR

pioneer factor *Foxa1* (Gao et al., 2003; Lupien and Brown, 2009) was downregulated in

hAR;ETV1^{Tg} mice. As downregulation of *Pten* or *Foxa1* would be predicted to result in

diminished AR transcriptional activity (Carver et al., 2011; Mulholland et al., 2011), the

expression pattern in *hAR;ETV1^{Tg}* mice suggests a possible upstream mechanism by which

ETV1 overexpression could antagonize AR.

To examine the significance of these DLP expression differences in the context of human

cancer, differentially expressed mouse gene sets were converted to human official gene symbols

and uploaded to Oncomine (Rhodes et al., 2004). The Oncomine database contains thousands of

"molecular concepts", which are gene sets annotated as being overexpressed in a certain cancer

subtype, induced by a certain drug treatment, or some other biologically meaningful annotation.

Mouse gene IDs from significant gene sets were converted to unique human gene symbols using

the HCOP tool at www.genenames.org, and then uploaded to Oncomine as "custom concepts".

Each custom concept was queried against the public Oncomine concept database and our custom

concepts. Notably, genes downregulated in *hAR;ETV1^{Tg}* mice relative to *hAR* mice were

significantly associated with the following concepts: "upregulated genes in prostate cancer cells

in response to synthetic androgen R1881" (DePrimo et al., 2002), "upregulated genes (time

dependent) in prostate cancer cells in response to androgen" (Jones et al., 2005), "downregulated

genes in prostate cancer after androgen ablation therapy" (Holzbeierlein et al., 2004), and custom

concepts containing genes downregulated in the castrated mice (Figure 2.3c). Similarly, genes

upregulated in *hAR;ETV1^{Tg}* mice relative to *hAR* mice were significantly associated with the concept: "upregulated genes in prostate cancer after androgen ablation therapy" (Holzbeierlein et al., 2004) as well as custom concepts containing genes upregulated in the castrated mice (Figure 2.3c). A complete list of significantly associated concepts can be found in Online Resource 3 (http://link.springer.com/article/10.1007%2Fs12672-014-0215-9) (Higgins et al., 2015). Thus, a significant subset of androgen-responsive genes, including those altered in human PCa patients, are affected by the ETV1 transgene in these mice. Furthermore, a large number of muscle-associated genes were upregulated in the prostates of *hAR;ETV1^{Tg}* mice (Figure 2.3b). This could reflect stromal smooth muscle cell gene expression that is affected in a paracrine manner by ETV1 activity in the epithelial compartment, disrupting normal pro-differentiation signals (Singh et al., 2014). Finally, ETV1-upregulated genes were significantly enriched for targets of the polycomb repressive complex (PRC) (Figure 2.3b). Co-regulation by the PRC, AR and the ETS factor ERG has been reported previously, however ERG repressed those shared targets in human PCa cells (Yu et al., 2010). These results could indicate divergent functions of ETV1 and ERG, their differential action at early vs. late disease stages or discrepancies between *in vitro* and *in vivo* results.

In sum, ETV1 overexpression in mouse prostate antagonized AR transcriptional activity and disrupted the normal prostate expression program. This included the repression of important prostate tumor suppressors, differentiation genes and AR coregulators as well as derepression of polycomb target genes.

Pten reduction and ETV1 overexpression cooperate to promote PCa progression

ETV1 overexpression was previously shown to exacerbate PCa progression in mice with total knockout of *Pten* in the prostate (Baena et al., 2013). Because many human prostate tumors show deletion of only one allele or a partial decrease in expression of PTEN, we asked whether reduction of this key tumor suppressor would cooperate with ETV1 overexpression in oncogenesis. Further, we queried whether varying AR transcriptional strength would impact disease progression. ETV1 transgenic mice carrying short, median or long Q-tract AR alleles were backcrossed at least five generations onto the FVB background, and then crossed with FVB mice bearing germline deletion of one *Pten* allele (*Pten*$^{+/-}$) for optimal genetic homogeneity (Figure 2.1a). Cohorts of each genotype were castrated at 12 weeks or left intact, and aged until moribund or until PTEN-dependent disease (generally lymphoma (Trotman et al., 2003)) necessitated euthanization (median age of 41 weeks, range 20-83 weeks).

Pten$^{+/-}$ mice developed more frequent PIN than the *Pten*$^{+/+}$ mice regardless of ETV1 transgene or AR allele (Figure 2.4). The majority of intact mice developed PIN, as did a subset of castrates. Of note, the *hAR*^{21Q} mice developed slightly less PIN overall, regardless of the ETV1 transgene, and showed no PIN in the absence of androgen. PIN was graded from PIN2 to PIN4, with PIN4 being the most severe (Ittmann et al., 2013; Park et al., 2002). Among intact mice, progression to adenocarcinoma occurred exclusively in ETV1 transgenics (Figure 2.4). Macroscopic DLP tumors were identified upon dissection in one *hAR*^{12Q} and one *hAR*^{21Q} mouse. Histopathological analysis detected adenocarcinoma in the VP of one additional transgenic *hAR*^{12Q} mouse (Figures 2.10, 2.11). Intriguingly, adenocarcinoma was observed in two castrated *hAR*^{12Q} mice (one with and one without the ETV1 transgene) (Figure 2.4). Castration-resistant disease has been observed in TRAMP mice (Albertelli et al., 2008) and in prostate-specific *Pten*

knockout mice (Mulholland et al., 2011), but not in *Pten* heterozygous animals. These data suggest that even a partial reduction in PTEN may be sufficient to promote CRPC.

The DLP had markedly greater frequency and severity of neoplasia than the VP among intact mice, while among castrated mice the rates of PIN were lower overall but similar between lobes (Figure 2.10). There was a trend toward more frequent and severe disease in intact mice older than the median age of 41 weeks, while among castrates there was a greater trend for disease incidence in mice 41 weeks or younger (Figure 2.10). While it was previously reported that ETV1 promoted PCa progression in *Pten*-null mouse prostates (Baena et al., 2013), these results show that ETV1 overexpression cooperated with even partial PTEN loss (see below) to promote aggressive PCa. Additionally, these results indicated that even heterozygous PTEN loss promoted castration-resistant neoplasia and adenocarcinoma. Furthermore, the stronger AR carried by *hAR^{12Q}* mice promoted greater PCa progression despite similar overall rates of PIN.

Immunohistochemical (IHC) staining for AR protein revealed nuclear expression in prostate epithelial cells in normal regions as well as in PIN and adenocarcinoma foci, similar to human disease where AR is present throughout PCa progression (Figure 2.5). Analysis of ETV1 expression by RNA *in situ* hybridization (RNA-ISH), performed by a pathologist blinded to genotype, confirmed ETV1 expression in prostate epithelial cells of *hAR;ETV1^{Tg};Pten^{+/-}* mice and undetectable ETV1 expression in non-transgenics (Figure 2.5, 2.11). ETV1 expression varied somewhat between individual transgenic animals, with a trend for higher expression in mice with more advanced PIN or adenocarcinoma. This could be because high ETV1 expression promotes more aggressive disease, or alternatively because AR signaling is partially increased in neoplastic cells, resulting in increased expression of the AR-driven ETV1 transgene. Interestingly, there was substantial heterogeneity between the two DLP tumors, with the *hAR^{12Q}*

tumor (Figure 2.5, row 4) appearing less differentiated than the hAR^{21Q} tumor (Figure 2.5, row 5). Thus, in this small sample, adenocarcinoma tended to be more frequent and aggressive in the hAR^{12Q} mice.

Despite the germline loss of one *Pten* allele and an approximately 50% reduction in *Pten* mRNA (see below), robust PTEN protein expression was detected in all samples tested. However, locally reduced PTEN expression was seen in a subset of PIN and adenocarcinoma foci (Figure 2.5). PTEN normally dephosphorylates and inactivates PI3K, in turn preventing phosphorylation and activation of Akt and thus inhibiting Akt-mediated cell growth and proliferation (Stambolic et al., 1998). Despite maintenance of PTEN protein expression even in neoplastic foci, phospho-Akt (pAkt) protein was present exclusively in regions of PIN or adenocarcinoma (Figure 2.5). Greater pAkt staining correlated with more advanced disease, as expected. Therefore, in this model complete PTEN loss is not necessary for AKT activation.

Reduction of PTEN leads to abrogated effect of ETV1 on AR

We next examined the effect of ETV1 on gene expression in this model of PCa progression. qRT-PCR analysis of AR target genes *Tmprss2*, *Pbsn*, and *Nkx3-1* revealed markedly attenuated ETV1 influence in prostates of $Pten^{+/-}$ relative to $Pten^{+/+}$ mice (Figure 2.6a, note that expression in $Pten^{+/+}$ mice is shown in lanes 1-3 of each gene for reference). However, overall repression of AR target genes was observed when one *Pten* allele was deleted, and those targets were still strongly repressed in castrated $Pten^{+/-}$ mice (Figure 2.6a). Prostatic *Pten* expression was indeed about half on the $Pten^{+/-}$ background, and was repressed by ETV1 (or castration) in prostates of $Pten^{+/+}$ but not $Pten^{+/-}$ mice (Figure 2.6b). This observation revealed that even a partial reduction in prostatic PTEN inhibited AR, extending a previous finding that

total PTEN loss in the prostate leads to reduced AR activity (Carver et al., 2011; Mulholland et al., 2011).

To further compare the molecular effects of *hAR* allele and ETV1 overexpression in the *Pten*$^{+/-}$ background, global gene expression was analyzed by RNA-seq. DLP RNA samples from ETV1 transgenic vs. non-transgenic mice as well as from the individual macroscopic tumors were assayed. Principal component analysis of the RNA-seq data showed that samples from all castrated mice and one macroscopic tumor clustered together (Figure 2.7a). The remaining tumor from a *hAR*^{12Q} mouse mapped separately, suggesting a disparate expression pattern, as might be expected from the poorly differentiated phenotype (see Figure 2.5). Samples from intact mice showed substantial heterogeneity within and between groups and did not form distinct clusters regardless of the transgene, suggesting that ETV1 had a more moderate and/or variable effect in this background (Figure 2.7a).

Overall, fewer genes were significantly differentially expressed between the prostates of transgenic and non-transgenic mice on the *Pten*$^{+/-}$ background. 59 genes were upregulated and 3 downregulated when all intact transgenics were contrasted with all intact non-transgenics by GLM analysis (Figure 2.7b). Interestingly, this set was enriched with 15 genes also upregulated by ETV1 in the *Pten*$^{+/+}$ mice, including orthologs of the PCa-associated genes *PSCA*, *SOX4* and *HPN* (Figure 2.7c). In particular, *HPN* is highly overexpressed in human PCa, promotes metastasis in a mouse model, and can be effectively targeted with a small molecule inhibitor (Tang et al., 2014). Additionally, these 59 genes were enriched for genes further upregulated in the macroscopic DLP tumors (see below), suggesting that ETV1 induces oncogenic expression changes prior to invasive disease, and that these genes may serve as biomarkers of impending

tumorigenesis. Androgen ablation affected a similar number of genes as in the $Pten^{+/+}$ mice (data not shown).

In contrast to little apparent effect of Q-tract length on the $Pten^{+/+}$ background (see Figure 2.2a), separating the groups by hAR allele revealed notable differences in expression due to androgen axis variation in $Pten^{+/-}$ mice. Analysis of individual hAR genotypes revealed 39, 156 and 303 genes upregulated and 180, 51 and 30 genes downregulated between transgenic and non-transgenic hAR^{12Q}, hAR^{21Q} and hAR^{48Q} prostates, respectively (Figures 2.7d, 2.12). Unlike in the $Pten^{+/+}$ background, the majority of differentially expressed genes showed little overlap, indicating they were unique to a single hAR genotype. There was a general trend toward greater repression by ETV1 in the context of the stronger hAR^{12Q} allele, and greater activation by ETV1 with the weaker hAR^{48Q} allele. Fewer differences in gene expression between ETV1-transgenic and non-transgenic $Pten^{+/-}$ mice could result in part from larger variance in age and disease stage among mice, or more heterogeneous ETV1 effects overall, in turn resulting in the variation seen in Figure 2.7b and thus reduced statistical sensitivity. Additionally, ETV1 could have a directly reduced influence on gene expression on the $Pten^{+/-}$ background. This latter explanation is supported by the qPCR data (Figure 2.6a), suggesting an abrogation of the effect of ETV1 on AR targets. Concept mapping confirmed that the broad ETV1-AR antagonism observed in the $Pten^{+/+}$ mice was diminished by loss of one $Pten$ allele (Online Resource 3, Higgins et al., 2015).

ETV1 induced inflammatory gene expression

Genes upregulated in prostates of ETV1-transgenic vs. nontransgenic $hAR;Pten^{+/-}$ mice were significantly enriched with inflammation-associated GO terms (Figure 2.7a). Relative expression of these genes is illustrated in the heatmap of Figure 2.8a, including expression levels

in the macroscopic DLP tumors. Many of the inflammatory genes were upregulated further in one or both tumors. The chemokines CXCL5 and CXCL16 are known to be associated with human PCa progression (Begley et al., 2008; Jung et al., 2013), and NUPR1 is associated with a variety of cancers including breast, pancreatic and lung cancer (Guo et al., 2012; Hamidi et al., 2012; Jung et al., 2012). Because a significant inflammation signature was seen in prostates of ETV1 transgenic mice prior to overt tumorigenesis, it is possible that ETV1-dependent inflammation may contribute to oncogenesis. Regardless, these factors may be biomarkers of impending tumorigenesis in ETV1^{+} prostates. In support of the functional significance of this gene signature, histologic evidence of inflammation has been previously noted in ETV1 knockin mice (Baena et al., 2013).

Direct ETV1 regulation of *CXCL16* and *NUPR1* was tested in human prostate cells. The benign human prostate epithelial cell line RWPE-1 was transduced with lentiviral vectors that stably express AR, as well as either ETV1 or LACZ (Tomlins et al., 2007; Tomlins et al., 2008a). qRT-PCR revealed that the ETV1-transduced cells expressed the endogenous *CXCL16* and *NUPR1* genes at significantly higher levels than the LACZ controls (Figure 2.8b), providing evidence of direct gene regulation by ETV1. This upregulation was observed with or without stimulation with the synthetic androgen R1881, suggesting that ETV1 induction of *CXCL16* in these cells is not AR-dependent. In contrast, *NUPR1* was sensitive to androgen in the absence but not the presence of exogenous ETV1.

ETV1 effects in mouse DLP parallel those in ETS[+] and aggressive human PCa

We explored the significance of these data by comparison to human PCa expression patterns and sought novel ETV1-regulated genes. Molecular concept analysis in Oncomine

revealed significant overlap between androgen-induced genes (see Figure 2.3), genes downregulated in DLP tumors and genes downregulated by ETV1 in $Pten^{+/+}$ mice. Relative expression of these shared genes is shown in the heatmap in Figure 2.9a. This pattern suggests that expression patterns in late ETV1/PTEN-induced tumorigenesis recapitulate early ETV1-induced signatures. Thus, selective AR repression may be important at multiple disease stages. Notably, the tumor suppressor and luminal epithelial differentiation marker *Nkx3-1* (Wang et al., 2009) is among androgen-induced transcripts downregulated in the tumors as well as prostates of early-stage $ETV1^{Tg}$ mice. Genes differentially expressed in $ETV1^{Tg};Pten^{+/-}$ prostates were not significantly enriched for this set of androgen-induced genes, yet overlapped with early-stage mouse disease, DLP tumors and human PCa (see Figs. 7 and 8). When genes differentially expressed in the macroscopic DLP tumors were further queried in Oncomine, significant enrichment with aggressive human PCa was observed. Genes downregulated in the $hAR^{21Q};ETV1^{Tg};Pten^{+/-}$ DLP tumor were significantly enriched for downregulated genes in human PCa metastases and advanced Gleason grade tumors (Figure 2.9b) (Grasso et al., 2012; Holzbeierlein et al., 2004; Lapointe et al., 2004; Nakagawa et al., 2008; Yu et al., 2004).

Two recent large-scale studies profiled gene expression in localized and metastatic PCa from over 200 total patients (Grasso et al., 2012; Taylor et al., 2010). These microarray data were stratified by ETS status, *PTEN* expression level and localized vs. metastatic tumors, and compared with the mouse RNA-seq data. Molecular concept analysis of the dataset from Taylor, *et. al.*, with ERG$^+$ and ETV1$^+$ patients combined as "ETS$^+$", revealed that genes downregulated in ETS$^+$, PTEN-normal localized tumors vs. non-ETS tumors were significantly enriched among genes downregulated in prostates of $hAR;ETV1^{Tg}$ mice or in DLP tumors (Figure 2.9c). While many transcripts were present in patterns unique to DLP tumors or $hAR;ETV1^{Tg}$ prostates, a

number were repressed in both groups (Figure 2.9c, middle horizontal rows). As with important androgen-regulated genes (see Figure 2.9a), this overlap once again suggests common ETV1 action in early neoplasia and in tumors, in contrast to intermediate stages of tumorigenesis.

Genes downregulated in ETS$^+$ patients that are also downregulated in *hAR;ETV1*^{Tg} mice as well as DLP tumors include a number of genes associated with various cancers, but not yet with PCa (Figure 2.9c). For example, *REC8* is a meiotic recombination gene whose hypermethylation is associated with poor prognosis in gastrointestinal stromal tumors (Okamoto et al., 2012). Downregulation of the stromal cell-derived factor 2-like 1 (*SDF2L1*) gene is associated with poor prognosis in breast cancer (Kang et al., 2009). *SEMA4G* was one of the few candidate tumor suppressor genes on the colorectal cancer (CRC) associated chromosome 10 loss of heterozygosity (LOH) region to be significantly downregulated in CRC tumors (Wang et al., 2008). This suggests potential roles for these genes in PCa, and potential regulation by ETS factors.

Of note, several genes were dysregulated in opposite directions in the two DLP tumors, including *H19*, *SEMA4G* and *KCNN4* (Figure 2.9c,d). This highlights the heterogeneity between the tumors and among these mice in general, similar to heterogeneity among human PCa patients. Furthermore, many genes were repressed in *hAR;ETV1*^{Tg} mice but upregulated in DLP tumors, or vice-versa (Figure 2.9c). This pattern emphasizes that while there is substantial overlap between early and late stages, as described above, there is a great deal of divergence as well, and different ETV1 targets may be more important or play different roles at one stage of disease progression than another.

PCa patient expression data from the study by Grasso *et. al.* (Grasso et al., 2012) was stratified as above by ETS status, PTEN expression level and localized vs. metastatic tumor site,

and differential expression was re-calculated. Overlap with the mouse RNA-seq data is shown in Figure 2.9d. *KCNN4*, a potassium channel gene, was upregulated in localized ETV1$^+$ vs. ETS$^-$ tumors in human PCa patients with normal PTEN levels (Grasso et al., 2012), as well as in *hAR;ETV1^{Tg}* vs. prostates and in DLP tumors (Figure 2.9d). KCNN4 expression is increased in benign prostatic hyperplasia (BPH) and intermediate Gleason grade PCa, but not high Gleason grade PCa (Ohya et al., 2009; Ohya et al., 2011). Additionally, *LRP8*, a low density lipoprotein receptor, is upregulated in localized ETV1$^+$ human tumors with normal PTEN (Grasso et al., 2012) and in mouse DLP tumors (Figure 2.9d). High *LRP8* expression is associated with several human cancers, including lung and gastric cancer, but has not yet been linked to PCa (Dun et al., 2013; Garnis et al., 2005; Pencheva et al., 2012). As before, these genes showed variable upregulation between the DLP tumors, highlighting heterogeneity in mouse as well as in human patients.

Expression in the intermediate-stage *ETV1^{Tg}/Pten$^{+/-}$* mice showed little overlap with the human data in these particular comparisons. In part, this could be due to fewer differentially expressed genes at that intermediate stage (see above). However, as seen in Figures 2.7 and 2.8, ETV1 induced a notable inflammatory signature in *Pten*-hemizygous mice, along with a number of individual PCa-associated genes and genes shared with both the early *ETV1^{Tg}* mice and the later DLP tumors. In sum, these studies shed light on distinct ETV1 gene regulatory networks at different disease stages, and highlight novel ETV1 targets when filtered against human data.

Discussion

This study examined in mice the degree to which AR genetic variation and ETV1 overexpression interact early in neoplasia, and their subsequent interaction with PTEN reduction in PCa progression. In both patients and transgenic mice, ETS overexpression is AR-driven, and AR activity is affected by factors downstream of PTEN. The molecular consequences of altering AR and ETV1 transcriptional regulation was queried with high-throughput gene expression analysis. Marked antagonism of the normal AR-regulated transcriptome occurred in prostates of ETV1 transgenic mice despite mild pathology. This antagonism was largely abrogated on a *Pten*-hemizygous background. In the *Pten*-hemizygous mice concurrent ETV1 overexpression induced progression to adenocarcinoma in a subset of mice as well as a striking pro-inflammatory gene signature. AR variation had little impact on early neoplasia driven by ETV1, but a stronger AR allele impacted gene expression and PCa progression in the *Pten*-hemizygous model. These results suggest that ETV1 cooperates with even reduced PTEN signaling to drive cancer progression in mice, and that partially antagonizing AR and promoting inflammation may be key components of the ETV1-driven oncogenic program. Integration of mouse and patient data revealed potential ETV1 regulation of known and novel PCa-associated genes, suggesting novel targets for therapeutic intervention.

Despite substantial AR antagonism similar to the effects of castration, prostates of $ETV1^{Tg}$ mice do not show atrophy, suggesting selective action favoring survival and proliferation. While ETV1 overexpression is insufficient to cause invasive PCa in mice, disruption of the normal AR-regulated, pro-differentiation gene expression program drives PIN and hyperplasia. This may "prime" the prostate for further dedifferentiation and tumor

50

progression following additional oncogenic insults, such as PTEN reduction or loss. In the case of ERG, it has been reported that PTEN loss is correlated with ERG fusions in patients (King et al., 2009) and that ERG fusion precedes PTEN loss (Gumuskaya et al., 2013).

We have previously shown an influence of the androgen axis on PCa onset and progression in TRAMP mice, where oncogenesis is driven by prostatic expression of an SV40 Large-T antigen transgene (Albertelli et al., 2008). While AR strength does not impact the early stages of ETV1-induced neoplasia in the current model, the rate of progression to adenocarcinoma is impacted when combined with *Pten* reduction. Confirmation here of the influence of AR in a model reflecting recurrent events in human PCa adds to the recent discovery that ETS^{+} PCa is more common in men with a stronger AR (Yoo et al., 2014).

While fewer genes are affected by ETV1 overexpression in the *Pten*$^{+/-}$ background overall, a greater number of differentially expressed genes are identified when Q-tract variants are analyzed individually, revealing divergent effects of the androgen axis on gene expression and disease progression. The *hAR*^{12Q} mice show significant repression of polycomb target genes with ETV1 overexpression, as do the DLP tumors, where most other groups show the opposite pattern (Online Resource 3, Higgins et al., 2015). As ETS factors can interact with the polycomb repressive complex (Yu et al., 2010), perhaps the greater repression seen with *hAR*^{12Q} indicates a greater cooperation in the context of the stronger AR and low PTEN, and could signify impending tumorigenesis. Induction of inflammatory genes is more pronounced in the *hAR*^{21Q} and *hAR*^{48Q} mice (Online Resources 2 and 3, Higgins et al., 2015). A number of those inflammatory genes are further upregulated in the tumors, indicating that they may be potential early biomarkers of aggressive disease. While a number of mouse models of PCa show inflammation during tumorigenesis, the expression signature specifically in *ETV1*^{Tg} mice relative

to non-transgenics suggests a role of ETV1. Confirmation of regulation by ETV1 *in vitro* supports inflammation as a factor in ETV1^{+} neoplasia.

A "core" set of targets is upregulated by ETV1 in both *Pten*^{+/+} and *Pten*^{+/-} mice, including a number of genes known to be upregulated in human PCa. Several of these genes including *PSCA* and *HPN* encode proteins that are druggable *in vitro* and in preclinical models (Tang et al., 2014; Yu et al., 2013). ETS[+] patients with particularly high expression of these genes may respond more favorably in future targeted therapy. ERG promotes *SOX4* expression to stimulate epithelial to mesenchymal transition in PCa (Wang et al., 2014), and these mouse data suggest that ETV1 may promote *SOX4* expression as a common component of ETS-driven oncogenesis.

Combined inhibition of the AR and PI3K/AKT pathways in PCa has been recently shown to be a potentially effective treatment strategy, as these pathways reciprocally repress one another, and either pathway can compensate when the other is inhibited (Carver et al., 2011; Mulholland et al., 2011). Since the AR, PTEN and ETV1 pathways all cooperate in PCa progression, dual inhibition of AR and PI3K/AKT may be more effective for some patients following stratification by ETS fusion status.

The CRPC seen in castrated *Pten*-hemizygous mice highlights the fact that hormone ablation generally slows disease progression in mice and patients, but in some cases can accelerate it (Albertelli et al., 2008; Johnson et al., 2005). In the previous TRAMP study, CRPC varied with AR strength, with half of castrated *hAR^{12Q}* mice failing to evince a palpable tumor prior to dying of metastatic castrate-resistant disease (Albertelli et al., 2008). Not only did a number of castrated *Pten*-hemizygous mice develop PIN or adenocarcinoma, but disease tended to arise earlier than in the intact mice, and greater progression was seen with the stronger *hAR*

allele. While CRPC has been previously reported in mice with a prostate-specific *Pten* deletion, these results suggest that even *Pten* reduction can promote CRPC. These findings support clinical data that hemizygous *PTEN* deletion predicts more rapid disease recurrence following radical prostatectomy and hormone therapy (Choucair et al., 2012). Further, this raises the question of whether AR genotyping might have predictive value in these situations.

Whether ETS fusion status in patients is associated with poor prognosis remains controversial and depends heavily on cohorts studied and definitions of disease aggressiveness (Rubin et al., 2011; Taris et al., 2014b). Results from the current study suggest that a stronger AR promotes ETV1-driven PCa progression, in line with the androgen regulation of the transgene in mice and of fusion genes in patients. Castration eliminates ETV1-driven disease in $Pten^{+/+}$ mice, and significantly reduces overall disease in $Pten^{+/-}$ mice. In one study, a subset of ERG^+ patients had a very favorable response to abiraterone acetate, which targets androgen synthesis via CYP17 inhibition (Attard et al., 2009). This underscores the androgen regulation of ETS fusion genes, and suggests that those tumors may be more dependent on AR activity than fusion-negative tumors.

Genes downregulated in the DLP tumors relative to PIN show the same expression pattern in high Gleason grade and metastatic human PCa (see Figure 2.9b). This finding suggests that the genes and pathways altered in the mouse models described here are not only generally relevant to human PCa, but may indicate aggressive disease. Genes downregulated in DLP tumors are enriched for androgen-induced targets, and in particular those that are also repressed by ETV1 in prostates of $Pten^{+/+}$ mice. These data suggest that the selective antagonism of AR in early neoplasia becomes a redirection of AR activity in later stage tumorigenesis.

Direct comparison of the mouse data to several human PCa patient data sets stratified by ETS status and PTEN expression level (Grasso et al., 2012; Taylor et al., 2010) reveal a number of known and novel PCa-associated genes potentially regulated by ETV1. One of these, *KCNN4*, is targetable with a potassium channel inhibitor in a rat model of BPH (Ohya et al., 2011), suggesting that it may have utility in ETV1^{+} PCa patients. Additional genes including *LRP8*, *SEMA4G*, *REC8* and *SDF2L1* are associated with other cancers but not yet PCa, and not yet with ETS regulation (Dun et al., 2013; Garnis et al., 2005; Kang et al., 2009; Okamoto et al., 2012; Pencheva et al., 2012; Wang et al., 2008). *H19* has a known role in PCa (Zhu et al., 2014) but no known ETS regulation. These data suggest potentially novel roles for these genes in PCa, as well as regulation by ETV1, warranting their further exploration as biomarkers or in therapeutic strategies.

Recently, ERG overexpression was shown to have little effect on AR signaling in the mouse prostate, but after *Pten* deletion ERG enhanced AR activity and stimulated tumorigenesis (Chen et al., 2013). The same effect was observed in human PCa expression sets stratified by these factors, with ERG-AR cooperation found in PTEN-low tumors (Chen et al., 2013). *In vitro*, ERG is a strong repressor of AR in several PCa cell lines with or without functional PTEN (Yu et al., 2010). Further data show that ERG blocks AR-induced differentiation in luminal epithelial cells (Mounir et al., 2014; Tomlins et al., 2008a). These studies suggest that the ERG-AR interaction is context-dependent, with different outcomes observed *in vitro* and *in vivo*, and dependent on PTEN status and cancer stage. Based on findings here, ETV1 also appears to behave in a highly context-dependent manner. In part, our *in vivo* AR-ETV1 results fall along a similar "spectrum" as the AR-ERG interaction described by Chen, *et. al.* (Chen et al., 2013). However, we observe ETV1 antagonism of AR that is lost with reduced *Pten*, yet in the DLP

tumors strong repression of AR targets recurs. The different interactions could result from PTEN

dose (hemizygous vs. prostate-specific knockout) or reflect distinct properties of ETV1 vs. ERG.

ETV1 has been reported to enhance AR activity *in vitro* (Baena et al., 2013; Chen et al., 2013;

Shin et al., 2009). However, such studies have been limited to LNCaP cells, which lack

functional PTEN. Further investigation of the AR-ETV1 interaction in additional models is

needed to clarify the effect *in vivo* vs. *in vitro*, as well as the influence of AR variation and

PTEN status.

In conclusion, the mouse models described here provide novel insight into the interaction

of key pathways driving early-intermediate stage PCa, and also reflect aggressive human disease.

A role of the androgen axis in disease progression is confirmed in PCa models driven by

recurrent somatic genetic alterations seen in patients. A number of known and druggable PCa-

associated factors show potential ETV1 regulation and warrant further investigation in patients

stratified by AR, ETS and PTEN status as novel therapeutic targets or prognostic biomarkers.

Materials and Methods

Mice

All animal work was performed in accordance with protocols approved by the University

Committee on Use and Care of Animals (UCUCA) at the University of Michigan. ETV1-

transgenic FVB mice expressing the human *ETV1* coding region driven by the ARR_2-Pb

promoter ($ETV1^{Tg}$) were a gift from Dr. Arul Chinnaiyan (University of Michigan) (Tomlins et

al., 2007). In the first experimental cohort, $ETV1^{Tg}$ males were crossed with C57BL/6 females

expressing a "humanized" androgen receptor (*hAR*) (Albertelli et al., 2006) with a short (12Q) or

long (48Q) polyglutamine tract. Transgenic males ($hAR;ETV1^{Tg}$) were castrated at 12 weeks or left intact, and aged to 24 weeks. Intact, non-transgenic hAR mice were used as controls. For the second series, $Pten^{flox/flox}$ mice (Lesche et al., 2002), on an FVB background, a gift from Dr. William Muller (McGill University), were crossed with FVB/N-Tg(EIIa-cre)C5379Lmgd/J mice (Jackson Labs # 003314) to excise the floxed $Pten$. $Pten$-deleted offspring were maintained as hemizygotes ($Pten^{+/-}$). $hAR;ETV1^{Tg}$ mice carrying 12Q, 21Q or 48Q hAR alleles were backcrossed for at least five generations onto the FVB background and then female transgenics crossed with $Pten^{+/-}$ males. Resulting $hAR;ETV1^{Tg};Pten^{+/-}$ and $hAR;Pten^{+/-}$ males were either castrated at 12 weeks or left intact, and aged to a median of 41 weeks (range 20-83 weeks). Genotyping primers are listed in Table 2.1.

Microdissection and sample preparation

Anterior prostate (AP), dorsolateral prostate (DLP) and ventral prostate (VP) lobes were individually microdissected from experimental mice. For the $hAR;ETV1^{Tg}$ mice, lobes were frozen in Optimal Cutting Temperature (OCT) compound (Sakura). 5 μm sections were cut and stained with hematoxylin and eosin (H&E) for histology, and RNA was extracted from the remaining tissue (see below). For $hAR;ETV1^{Tg};Pten^{+/-}$ mice, one lobe per pair was fixed in 10% neutral-buffered formalin for 24 hours, then transferred to 70% ethanol until embedding in paraffin and cutting of 5 μm sections for H&E staining. The other lobe was frozen in RNA-later (Ambion). All prostate RNA was purified with the RNeasy kit with on-column DNase digestion (Qiagen) following tissue homogenization in Buffer RLT. Macroscopic prostate tumors were divided in half, with one half prepared for histology and the other half prepared for RNA analysis as described above.

qRT-PCR

cDNA was reverse-transcribed from total RNA using random hexamers and either the SuperScript II 1st-Strand Synthesis kit (Invitrogen) for mouse prostate RNA, or the High Capacity cDNA Reverse Transcription kit (Applied Biosystems) for human cell line RNA. qRT-PCR samples were run on an AB7300 or AB7500 thermal cycler (Applied Biosystems) using Power SYBR Green Master Mix (Applied Biosystems) or ABSolute Blue SYBR Green Rox Master Mix (Thermo Scientific) according to the manufacturer's instructions. Following normalization to *Actb* for mice, and *ACTB* or *GAPDH* for human cells, relative expression was calculated using the $2^{-\Delta\Delta Ct}$ method. All primer sequences are listed in Table 2.1.

RNA-seq analysis

Mouse DLP RNA was used for Illumina mRNA-seq library construction. For each genotype/treatment group (n = 4-13 mice per group), individual RNA samples were divided amongst 3 unique pools (2 unique pools for castrated groups due to low RNA yield) and a library was prepared from each pool. Individual libraries were prepared for each macroscopic DLP tumor as well (n = 2). For each library, poly-A$^+$ RNA was first purified from 200 ng total RNA with Dynabeads Oligo(dT)$_{25}$ (Invitrogen). Libraries were constructed with NEBNext mRNA-seq Master Mix reagents and NEBNext Multiplex Oligos for Illumina (New England Biolabs). Multiplexed libraries were sequenced on an Illumina HiSeq 2000 with the SE-50 module at the University of Michigan Sequencing Core. Four lanes were sequenced, each containing 11-12 indexed libraries. Reads were aligned to the mouse mm10 genome with TopHat2 (Kim et al., 2013), transcript counts were generated with the HT-Seq Python script (http://www-huber.embl.de/users/anders/HTSeq/doc/index.html) and differential expression was calculated in

the Bioconductor package edgeR, which utilizes counts rather than FPKM (Anders et al., 2013). Contrasts were performed between pairs of genotype/treatment groups, or between multiple genotype/treatment groups using the generalized linear model (GLM) tools in edgeR. Genes differentially expressed at a false-discovery rate (FDR) ≤ 0.05 were considered significant.

Bioinformatics functional annotation and pathway analysis

Functional annotation of significant gene sets was performed with DAVID (http://david.abcc.ncifcrf.gov) (Huang Da et al., 2009). The following gene ontology (GO) terms and pathways were tested for enrichment: GOTERM_BP_ALL, GOTERM_CC_ALL, GOTERM_MF_ALL, PANTHER_BP, PANTHER_MF, BIOCARTA, KEGG_PATHWAY and PANTHER_PATHWAY. GO terms and pathways with a Benjamini-adjusted FDR ≤ 0.05 were considered significantly enriched relative to the *Mus musculus* background gene list.

Enrichment with human cancer-related gene sets was performed with Oncomine (https://www.oncomine.org) (Rhodes et al., 2004). Mouse gene IDs from significant gene sets were converted to unique human gene symbols using the HCOP tool at www.genenames.org, and uploaded to Oncomine as "custom concepts". For gene sets with more than 1000 genes, the top 1000 were used for custom concepts. Each custom concept was queried against the "Biology Concepts", "My Concepts", "Literature-defined Concepts" and "Oncomine Gene Expression Signatures" concept databases in Oncomine with "All Entrez Genes" as the background list. Significant enrichment was set as an odds ratio (OR) ≥ 4 and a p-value ≤ 10^{-6}. Oncomine output was used to generate molecular concept maps (Rhodes et al., 2007) in Cytoscape (www.cytoscape.org), with edges representing significant enrichment between concepts and node size proportional to overlap with the primary custom concept.

Pathological analysis of mouse prostates

Mouse prostate lesions were classified and graded based on the recent consensus criteria established by the Mouse Models of Human Cancer prostate pathology committee (Ittmann et al., 2013; Park et al., 2002).

Immunohistochemistry

Slides were prepared with 5 μM sections from FFPE mouse prostates. The antibodies used in this study included AR N-20 (Santa Cruz # sc-816, 1:500 dilution), phospho-AKT (Ser473) (Cell Signaling #9271, 1:100 dilution), and PTEN (Cell Signaling #9188, 1:80 dilution). Immunohistochemistry (IHC) was performed essentially as described for AR and pAKT (Albertelli et al., 2008), and for PTEN (Bhalla et al., 2013; Sathyanarayana et al., 2014).

In situ **hybridization**

A custom RNA probe against human *ETV1* transcript (Advanced Cell Diagnostics) was hybridized to 5 μM FFPE mouse prostate sections essentially as described (Kunju et al., 2014).

Cell Lines

RWPE-1 cells stably overexpressing ETV1 or LACZ (Tomlins et al., 2007; Tomlins et al., 2008a) were a gift from Dr. Arul Chinnaiyan (University of Michigan) and were maintained in KSFM (Gibco # 10724-011) supplemented with BPE and EGF, 1:100 penicillin/streptomycin (Gibco # 15140-122) and 3 μg/ml blasticidin (Life Technologies # R21001) to maintain stable expression of the transduced ETS construct or control. 293T cells were a gift from Dr. Margaret

Gnegy (University of Michigan) and were maintained in DMEM (Gibco # 11995-065) with 10% FBS (GeneMate # S-1200-500) and 1:100 penicillin/streptomycin.

Lentiviral Packaging and Transduction

The FG9 lentiviral expression plasmid was previously derived from FUGW (Addgene # 14883) (Lois et al., 2002; Qin et al., 2003) and was a gift from Dr. David Baltimore (California Institute of Technology). FG9 was linearized with BamHI, and a BglII-3xFLAG-BamHI fragment was inserted, destroying the 5' BamHI site but preserving the 3' site. AR was excised as a BamHI fragment from the pCMV5-AR plasmid (Steinkamp et al., 2009) and ligated into FG9-3xFLAG to produce the final FG9-3xFLAG-AR plasmid. For transduction, 5×10^6 293T cells were seeded in a poly-L-lysine coated 10 cm dish. The following day, cells were transfected with 10 µg FG9-3xFLAG-AR plasmid or FG9-vector control, 3 µg pHCMVG, 2 µg pRSV-rev, 6 µg pRRE and 80 µg polyethylenimine, suspended in 150 mM NaCl. Virus-containing medium was harvested 48 and 72 hours post-transfection, filtered through a 0.45 µM filter and applied directly to RWPE-ETV1 or RWPE-LACZ cells. After transduction of the AR construct, 100 µg/ml Hygromycin B (Life Technologies #10687-010) was added to maintain expression of AR or the vector control.

Androgen Stimulation and RNA Purification

5×10^4 RWPE-ETV1-AR or RWPE-LACZ-AR cells were seeded in 12-well dishes in complete growth medium without antibiotic selection. Beginning the following day, cells were deprived of BPE for 48 hours. Cells were then stimulated with 1 nM R1881 or methanol vehicle

for 24 hours before lysis and RNA purification with TRIzol reagent (Ambion # 15596018). The experiment was performed in biological triplicate.

Conflict of Interest

The University of Michigan has been issued a patent on the detection of ETS gene fusions in prostate cancer, on which R.M. and S.A.T are listed as co-inventors. The University of Michigan licensed the diagnostic field of use to Gen-Probe, Inc., who has sublicensed some rights to Ventana/Roche. S.A.T. has served as a consultant to, and has received honoraria from, Ventana/Roche. The remaining authors declare that they have no conflicts of interest.

Table 2.1 Primer sequences for genotyping and real-time PCR

Mouse Genotyping Primers

Primer	sequence 5'-3'
Qtract.g F	ACCCAGAGGCCGCGAGCGC
Qtract.g R	GCACTCCAGGGCCGACTGCG
ETV1.g F	GCCAACTGGGATGCAAGACACT
ETV1.g R	AGAAAGCTGGCGGCGAAATC
Pten.g 1	ACTCAAGGCAGGGATGAGC
Pten.g 2	AATCTAGGGCCTCTTGTGCC
Pten.g 3	GCTTGATATCGAATTCCTGCAGC

Mouse qRT-PCR Primers

Primer	sequence 5'-3'
Pbsn F	AGGGACTAAGTGCCAACTGTA
Pbsn R	ACTCCAGCCACTCGTGTGA
Tmprss2 F	CAGTCTGAGCACATCTGTCCT
Tmprss2 R	CTCGGAGCATACTGAGGCA
Nkx3-1 F	GACTGTGAACATAATCCAGGGG
Nkx3-1 R	TGATGGCTGAACTTCCTCTCC
Clu F	TCCCGGAAGTGTGTAACGAGA
Clu R	CGCCGTTCATCCAGAAGTAGA
Pten F	TGCACAGTATCCTTTTGAAGACC
Pten R	GAATTGCTGCAACATGATTGTCA
hAR F	AAGCACTGCTGCTCTTCAGC
hAR R	GAACTGATGCAGCTCTCTTGC
Actb F	AGTGTGACGTTGACATCCGTA
Actb R	GCCAGAGCAGTAATCTCCTTCT

Human qRT-PCR Primers

Primer	sequence 5'-3'
CXCL16 F	GCAGCGTCACTGGAAGTTG
CXCL16 F	ATCCCCGAGTAAGCATGTCC
NUPR1 F	ATGGCCACCTTCCCAC
NUPR1 R	TCAGCGCCGTGCCCCTCG
ACTB F	CAAAGACCTGTACGCCAACA
ACTB R	TCAGGAGGAGCAATGATC
GAPDH F	TGCACCACCAACTGCTTAGC
GAPDH R	GGCATGGACTGTGGTCATGAG
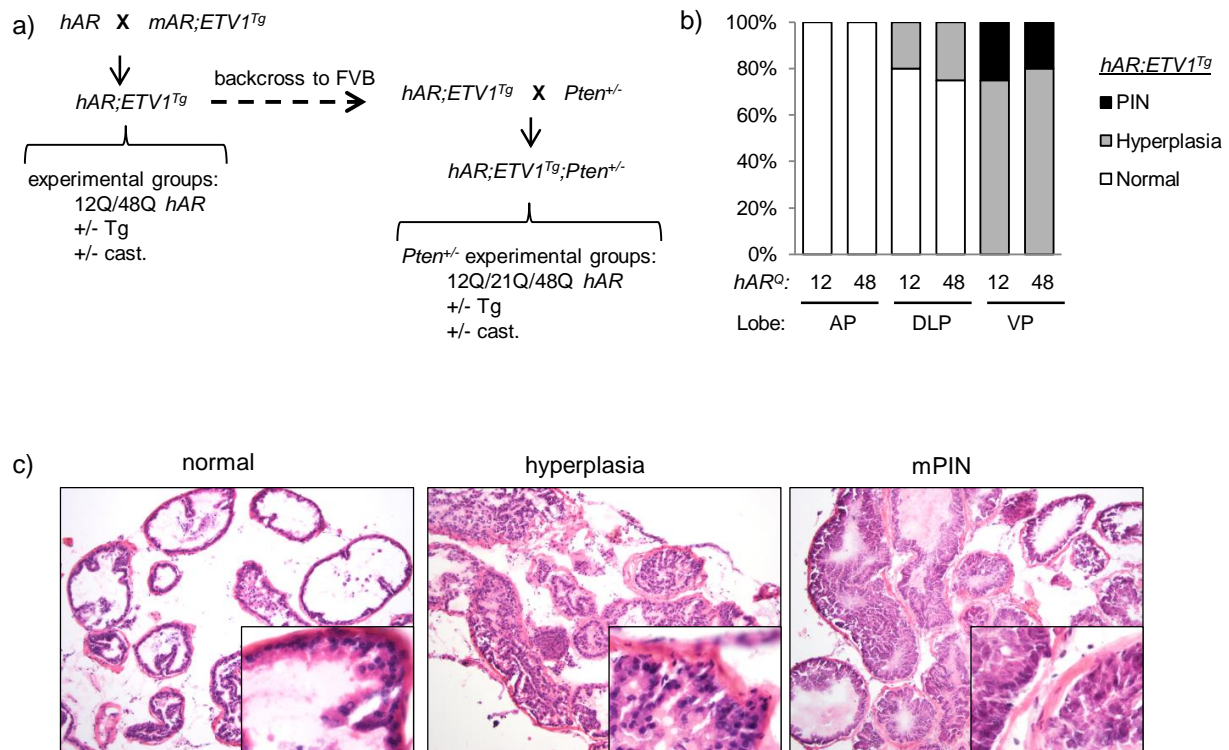
Figure 2.1: Effect of AR allele strength on ETV1-induced PIN

A) C57BL/6 mice carrying a "humanized" *AR* gene with a short (hAR^{12Q}) or long (hAR^{48Q}) polyglutamine tract were crossed with ETV1-transgenic FVB mice ($ETV1^{Tg}$) to generate $hAR;ETV1^{Tg}$ mice. Experimental mice were castrated or left intact at 12 weeks, aged to 24 weeks and compared to intact *hAR* controls. $hAR;ETV1^{Tg}$ mice were then backcrossed to FVB and crossed with $Pten^{+/-}$ mice to generate $hAR;ETV1^{Tg};Pten^{+/-}$ experimental mice with short (12Q), median (21Q) or long (48Q) Q-tracts. Experimental $hAR;ETV1^{Tg};Pten^{+/-}$ mice were castrated or left intact at 12 weeks, aged to an average of 43 weeks and compared to $hAR;Pten^{+/-}$ controls. B) Representative H&E stained prostates from $hAR;ETV1^{Tg}$ mice. Normal tissue (DLP), hyperplasia (DLP) and mPIN (VP) are shown. Images are 10x with 40x insets. **c** The proportion of mice with hyperplasia and mPIN in AP, DLP and VP among $hAR^{12Q};ETV1^{Tg}$ and $hAR^{48Q};ETV1^{Tg}$ mice. 5-8 lobes per group were analyzed.

a)

b)

c)

d) Up-regulated by ETV1

Down-regulated by ETV1

64
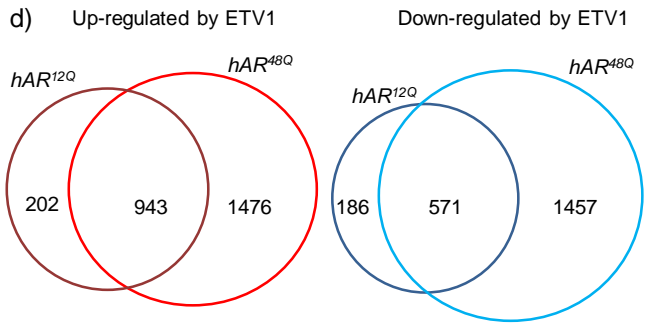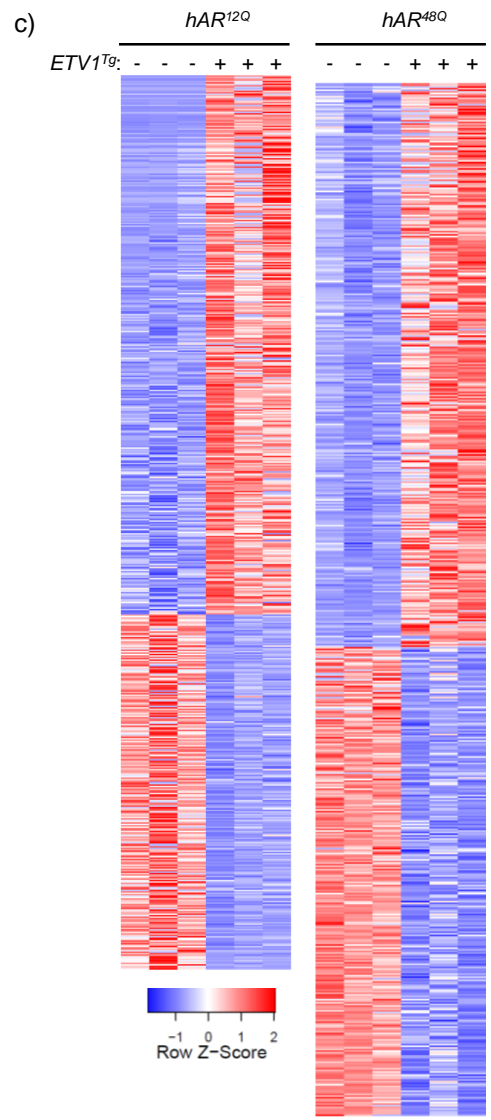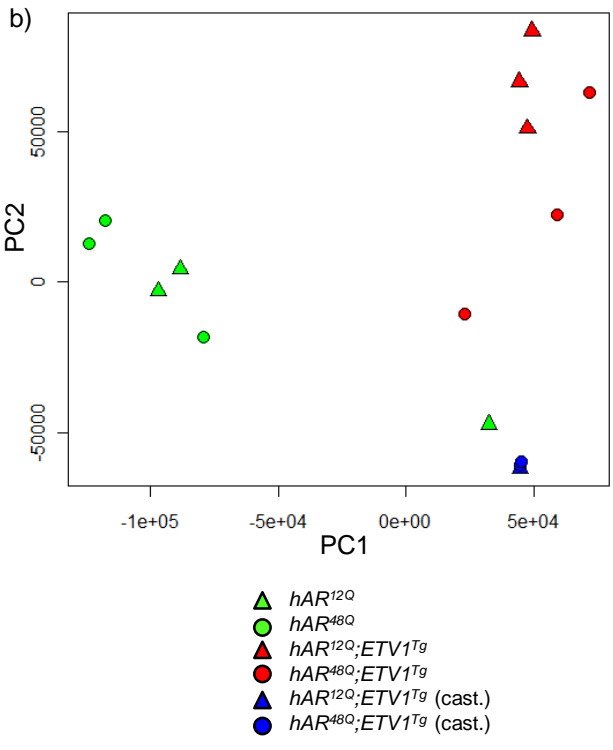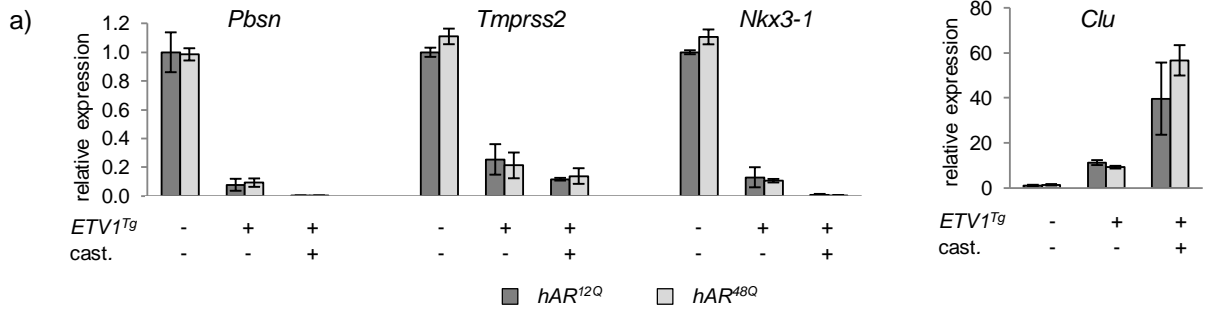
Figure 2.2: ETV1 overexpression alters prostatic gene expression

A) 2 unique pools of DLP RNA from each group were analyzed by qRT-PCR. Expression of the AR target genes *Pbsn*, *Tmprss2*, *Nkx3-1* and *Clu* was normalized to *Actb* expression and plotted relative to the intact *hAR^{12Q}* group using the 2^{-ddCt} method. Mean +/- SEM are plotted. B) Principal component analysis was performed for all genes among the 16 individual RNA-seq libraries. *hAR^{12Q}* and *hAR^{48Q}* mice are represented as triangles and circles, respectively. Green, red and blue represent intact non-transgenic, intact transgenic and castrated transgenic mice, respectively. C) RNA-seq analysis was performed on DLP RNA. Samples from intact groups were divided into 3 unique RNA pools for library construction (2 unique pools for castrated groups). Heatmaps include differentially expressed genes between the groups shown (FDR ≤ 0.05). Individual libraries are shown for differentially expressed genes among intact *hAR^{12Q};ETV1^{Tg}* vs. *hAR^{12Q}* (1145 up, 757 down) or intact *hAR^{48Q};ETV1^{Tg}* vs. *hAR^{48Q}* (2419 up, 2028 down). Red and blue represent high or low expression, respectively, relative to the mean expression level in the samples shown. Columns and rows represent samples and genes, respectively. D) Overlap between genes differentially expressed in *hAR^{12Q};ETV1^{Tg}* and *hAR^{48Q};ETV1^{Tg}* is illustrated by Venn diagram.

a)

hAR^Q: 12 48 12 48 12 48
$ETV1^{Tg}$: - - + + + +
cast. - - - - + +
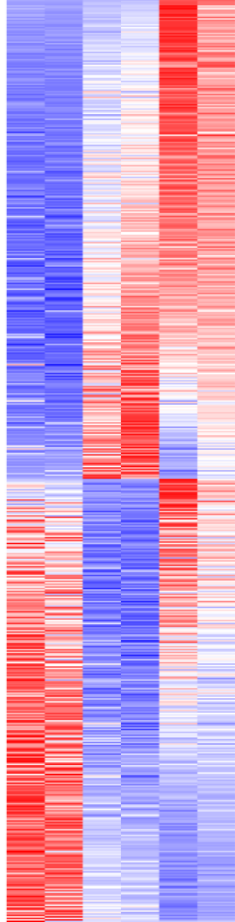
Row Z-Score
-1 0 1 2

b)

hAR^Q: 12 48 12 48 12 48
$ETV1^{Tg}$: - - + + + +
cast.: - - - - + +
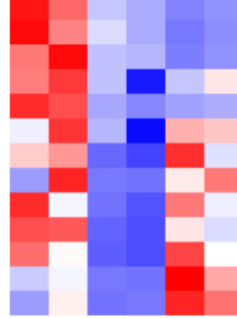
Nkx3-1*
Hoxb13*
Stat5a
Sox9
Foxa1*
Notch1
Pten*
Cd44
Serpinb5
Esr1
Tnc
Trp63
Ahr

GO:
"Prostate Development"
"Prostate Morphogenesis"

-1.5 -0.5 0.5 1.5
Row Z-Score

c)

Up in PCa cells with Resveratrol treatment

Down in PCa cells with MSA treatment

Up in PCa cells with androgen treatment

Down in fibroblasts expressing EWS/FLI fusion

Down in PCa after androgen ablation

Down in castrated mice

DOWN in ETV1-Tg mice

Striated muscle contraction

Stirated muscle thick filament

Muscle myosin

Down in muscle after aerobic exercise

Structural component of muscle

Muscle development

UP in ETV1-Tg mice

Up in castrated mice

Up in clear cell renal cell carcinoma

EED target genes in hESC

H3K27me3 target genes in hESC

SUZ12 target genes in hESC

SUZ12 target genes in hEF

H3K27me3 target genes in hEF

Polycomb target genes in hESC

CBX8 target genes in hEF

66

Figure 2.3: AR regulation is antagonized by ETV1 overexpression

A) The generalized linear model (GLM) tools in edgeR were used to test differential expression between all *hAR;ETV1^{Tg}* and all *hAR* mice. 2368 genes were upregulated and 2196 downregulated in prostates of *hAR;ETV1^{Tg}* mice (FDR ≤ 0.05) and are shown in the heatmap. Relative expression in prostates of castrated mice is included. The heatmap is plotted as in Figure 2.2a, except that each column represents the average expression among biological replicate libraries. B) Genes significantly upregulated or downregulated in prostates of *hAR;ETV1^{Tg}* relative to *hAR* mice were uploaded to DAVID for functional annotation with gene ontology (GO) terms. The heatmap shows genes annotated with select significantly enriched GO terms (Benjamini FDR ≤ 0.05) among the downregulated genes. See Online Resource 2 (Higgins et al., 2015) for the complete list of significant GO terms. C) The top 1000 upregulated and downregulated genes in prostates of *hAR;ETV1^{Tg}* relative to *hAR* mice were converted to human gene symbols, uploaded to Oncomine as "custom concepts" and queried against the Oncomine concept database. Significantly enriched concepts, defined as having an odds ratio (OR) ≥ 4 and p ≤ 10^{-6}, are shown as molecular concept maps. Node size is proportional to overlap with the primary concept. Similar concepts have the same color and are clustered together. See Online Resource 3 (Higgins et al., 2015) for a complete list of significant concepts.
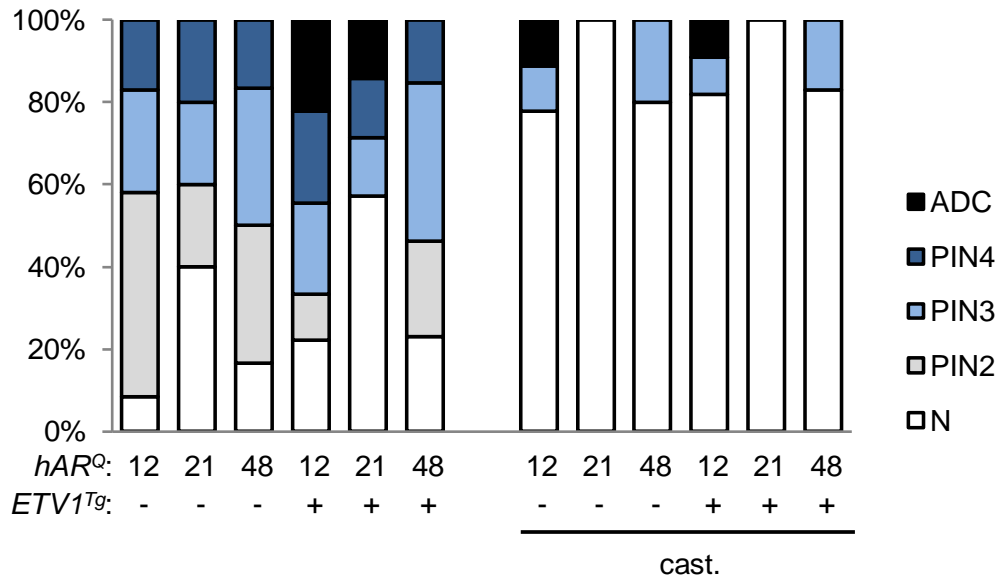
Figure 2.4: ETV1 overexpression with *Pten* reduction promotes progression to adenocarcinoma

H&E stained DLP and VP sections were scored by the pathologist as normal, mPIN2-4 or adenocarcinoma (ADC). The graph represents the proportion of mice per group (n = 5-14) at each disease stage, with the most severely diseased prostate lobe per mouse used to plot the data. See Figure 2.10 for stratification by age and individual prostate lobe.
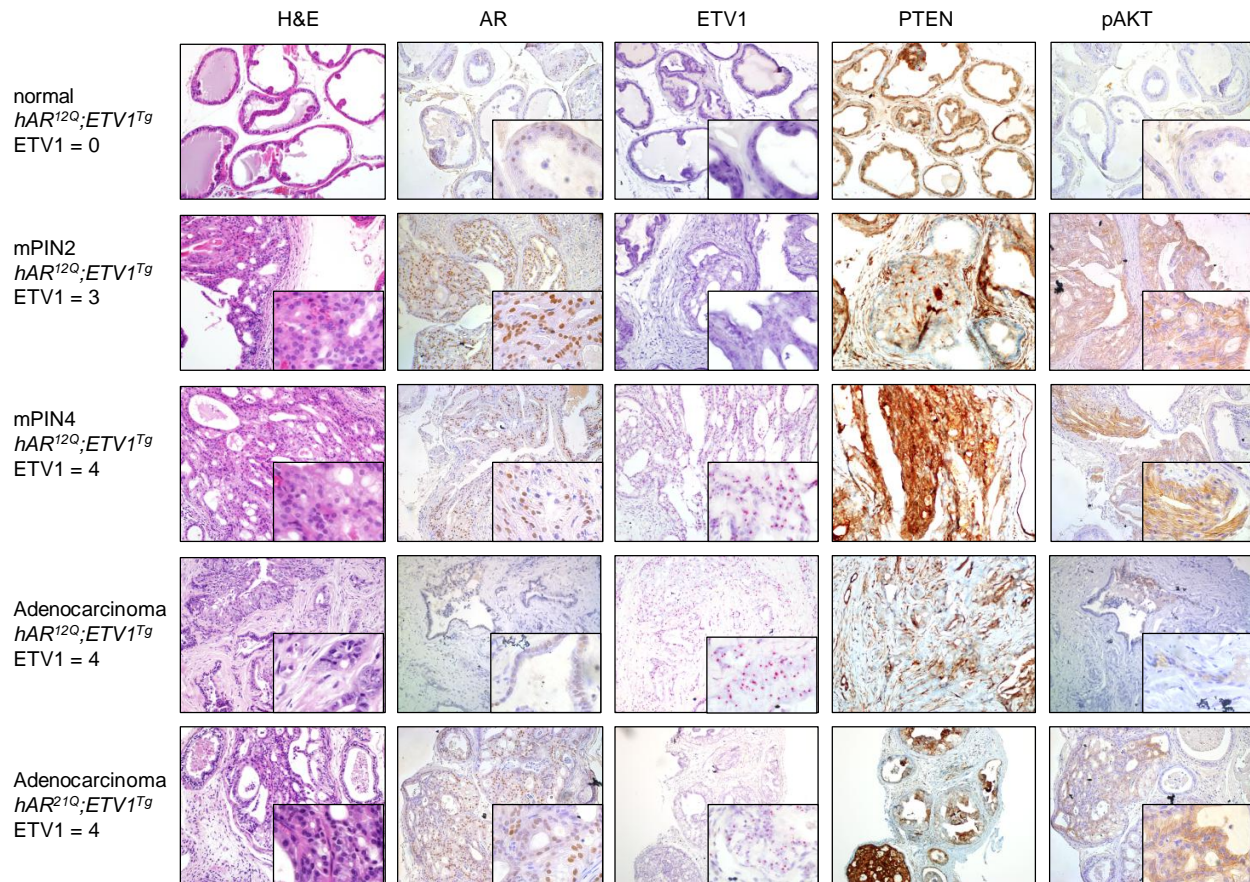
Figure 2.5: Histopathology in *Pten*-hemizygous mice

Representative prostate sections are shown from, in order, intact $hAR^{12Q};ETV1^{Tg};Pten^{+/-}$ mice with normal, PIN2 or PIN4 DLP, as well as macroscopic DLP tumors (adenocarcinoma) from $hAR^{12Q};ETV1^{Tg};Pten^{+/-}$ and $hAR^{21Q};ETV1^{Tg};Pten^{+/-}$ mice. Sections were stained with H&E. Immunohistochemical (IHC) staining was performed with antibodies to AR, PTEN or pAKT protein (brown staining). *In situ* hybridization (ISH) was performed with a probe against the human ETV1 transcript (red staining). ETV1 expression level is scored as 0-4, with 4 being highest. Images are shown at 10x-20x magnification with 60x inset. Consecutive sections were used when possible, and each row of images shows stained sections from a single mouse prostate.
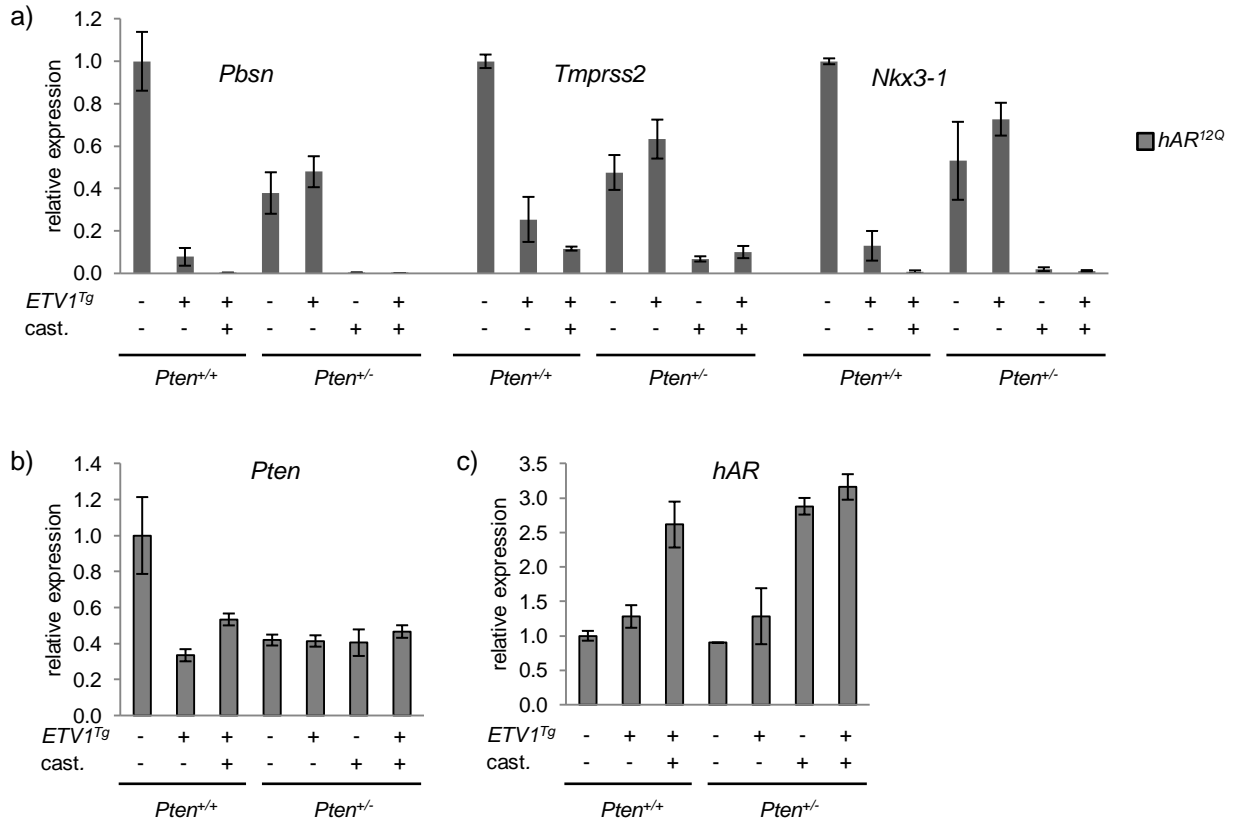
Figure 2.6: Effect of ETV1 on AR targets is muted with reduced *Pten*

A) *hAR^{12Q}* mice are shown as representative data in all panels. Expression of AR target genes *Pbsn*, *Tmprss2*, and *Nkx3-1* in DLP was measured by qRT-PCR and normalized to *Actb*. Expression levels in intact and castrate *hAR^{12Q};ETV1^{Tg}*, *hAR^{12Q};Pten^{+/-}* and *hAR^{12Q};ETV1^{Tg};Pten^{+/-}* are plotted relative to intact *hAR^{12Q}*. Lanes 1, 2 and 3 for each gene are repeated from Figure 2.2a for comparison between backgrounds. B) *Pten* expression in DLP was measured by qRT-PCR as above. C) *hAR* expression was measured by qRT-PCR as above. For all qRT-PCR, DLP RNA samples were divided into 2 unique pools for analysis. Mean and SEM are plotted. The 2^{-ddCt} method was used to calculate relative expression.

a)

b)

$Pten^{+/-}$

| hAR^Q: | 12 | 21 | 48 | 12 | 21 | 48 |
| $ETV1^{Tg}$: | - | - | - | + | + | + |

Row Z−Score

GO: Inflammatory Response
Chemokine Activity
Chemokine Receptor Activity
Cytokine Activity
Response to Stimulus

Legend:
△ hAR^{12Q}
■ hAR^{21Q}
● hAR^{48Q}
▲ $hAR^{12Q};ETV1^{Tg}$
■ $hAR^{21Q};ETV1^{Tg}$
● $hAR^{48Q};ETV1^{Tg}$

△ hAR^{12Q} (cast.)
■ hAR^{21Q} (cast.)
● hAR^{48Q} (cast.)
▲ $hAR^{12Q};ETV1^{Tg}$ (cast.)
■ $hAR^{21Q};ETV1^{Tg}$ (cast.)
● $hAR^{48Q};ETV1^{Tg}$ (cast.)
■ $hAR^{21Q};ETV1^{Tg}$ (TUM)
▲ $hAR^{12Q};ETV1^{Tg}$ (TUM)
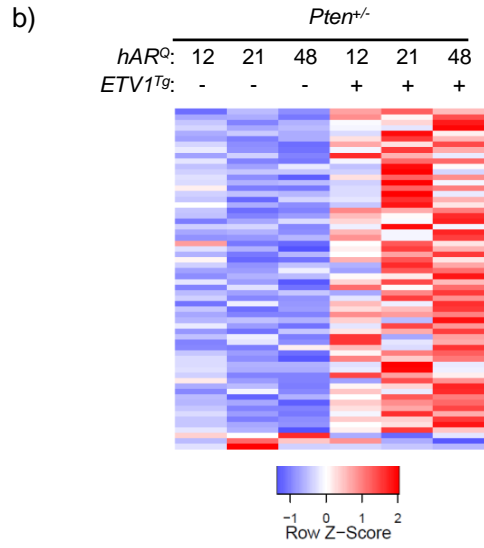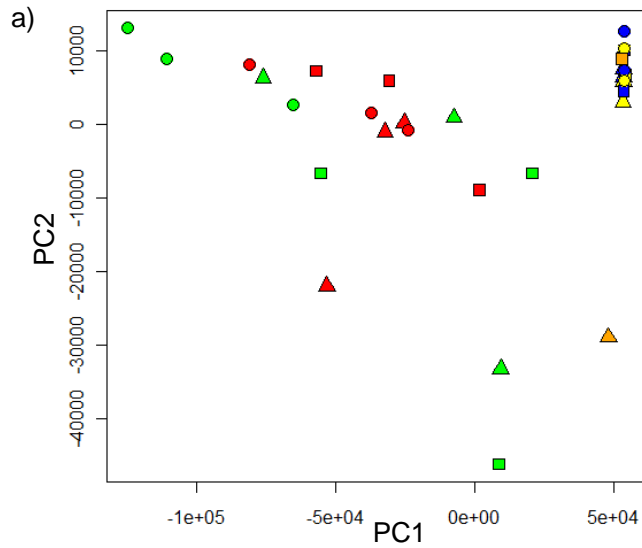
c)
Atp2a3
*Hpn**
Lcn2
Mb
Mybpc2
Neurl3
*Nupr1**
Padi2
Pglyrp1
Pmepa1
Ppp1r3b
*Psca**
S100a11
*Sox4**
Sphk1

d)

Up-regulated by ETV1

hAR^{12Q} hAR^{21Q}
13
3
23   45
108
232
hAR^{48Q}

Down-regulated by ETV1

hAR^{12Q} hAR^{21Q}
171   8   42
1   28   1
hAR^{48Q}

71
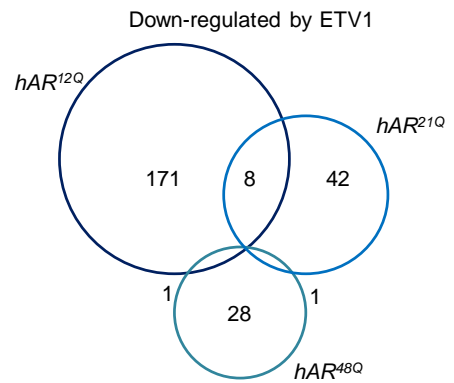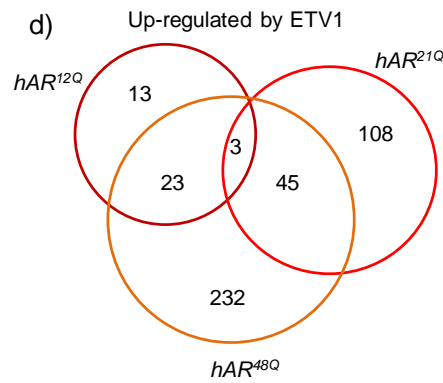
Figure 2.7: ETV1 overexpression alters genome-wide expression in *Pten*-hemizygous mice

A) Principal component analysis was performed for all genes among the individual RNA-seq libraries. hAR^{12Q}, hAR^{21Q} and hAR^{48Q} mice are represented as triangles, squares and circles, respectively. Green and red represent intact non-transgenic and transgenic mice, yellow and blue represent castrated non-transgenic and transgenic mice, and orange represents macroscopic tumors, respectively. B) RNA-seq analysis was performed on DLP RNA as before. Heatmaps include differentially expressed genes between the groups shown (FDR ≤ 0.05), with columns representing the average among biological replicate libraries. By GLM analysis of all $hAR;ETV1^{Tg};Pten^{+/-}$ libraries vs. all $hAR;Pten^{+/-}$ libraries, 59 genes are upregulated and 3 downregulated in prostates of $hAR;ETV1^{Tg};Pten^{+/-}$ mice. Select significantly enriched GO terms are listed. C) ETV1-upregulated genes shared among $Pten^{+/-}$ and $Pten^{+/+}$ mice are listed. D) Differential expression was performed between transgenics and non-transgenics for each AR Q-tract group individually. Overlap between genes differentially expressed in $hAR^{12Q};ETV1^{Tg}$, $hAR^{21Q};ETV1^{Tg}$ or $hAR^{48Q};ETV1^{Tg}$ relative to non-transgenics is illustrated by Venn diagram.
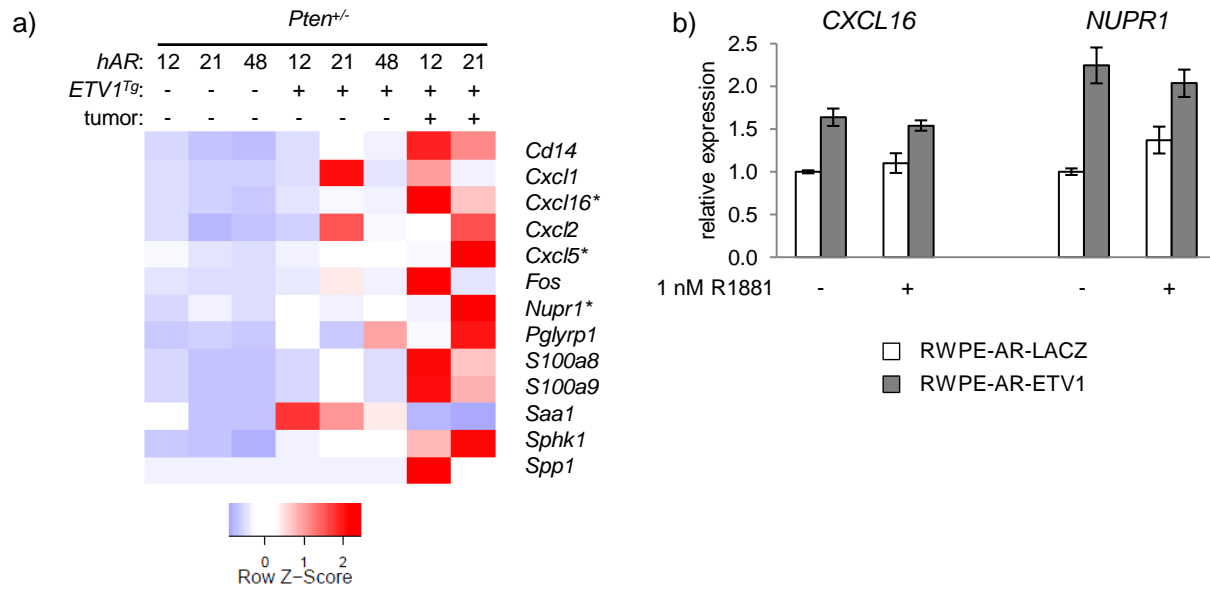
Figure 2.8: ETV1-induced inflammatory expression signature precedes tumorigenesis

A) Genes that are differentially expressed between $hAR;Pten^{+/-}$ and $hAR;ETV1^{Tg};Pten^{+/-}$ mice and annotated with inflammation-related GO terms (see Figure 2.7a) are shown in the heatmap. Relative expression in prostates of $hAR;Pten^{+/-}$ and $hAR;ETV1^{Tg};Pten^{+/-}$ mice is shown, as well as expression in the macroscopic prostate tumors. B) RWPE-1 cells stably expressing AR and either ETV1 or LACZ were stimulated with 1 nM R1881 or methanol vehicle, and RNA was prepared for qRT-PCR analysis. Expression of the inflammatory genes *CXCL16* and *NUPR1* were normalized to *GAPDH* or *ACTB*, respectively, and plotted relative to RWPE-AR-LACZ cells. Mean and SEM are plotted for biological triplicate samples.

a)

	Pten+/+						*Pten*+/-								
Abca5
Acsl3
Dnajb9
Edem2
Erp44
Gdf15
Iqgap2
Mccc2
Nkx3-1*
Pdia4
Pgm3
Ppapdc1b
Rab11fip4
Sec24d
Slc33a1
Zbtb10

ETV1^*Tg*: - - + + + + - - + + + + + +
cast: - - - - + + - - - - - - - -
hAR^Q: 12 48 12 48 12 48 12 21 48 12 21 48 12 21

DLP   Tumor

-1 0 1 2
Row Z-Score

b)

Advanced Gleason Score: Top 1% Under-expressed (Nakagawa)

Metastasis: Top 1% Under-expressed (Grasso)

Metastasis: Top 1% Under-expressed (Lapointe)

Down in mouse DLP tumor

Carcinoma vs. Normal: Top 1% Underexpressed (Liu)

Metastasis: Top 1% Under-expressed (Yu)

Metastasis: Top 1% Under-expressed (Holzbeierlein)

c)

	Pten+/+						*Pten*+/-								
Cd28
Snx24
Sytl5
C17orf58
Bcar3
Slc39a11
Gpr155
Ctsc
Fxyd3
Mar3
Raph1
Magi3
Dach2
Nostrin
Pof1b
Gipc2
Slc10a5
Fam107b
Fabp5
Upk3b
Gnmt
Slc26a3
Stxbp6
Cntnap2
Adhfe1
Sdf2l1*
Dennd3
Sema4g*
Rpgrip1
Rec8*
Sp5
Auh
Dkga
Acad8
Mthfr
Syt1
Mapk10
Dlg2
Ryr2
Stk32a
Ttn
Foxf2
Hpgd
Slc35f3
Ppp1r12b
Corin
Frmd3
Colq
C7orf31
Ggt7
H19*
Nkd1
Dclk2
Kazald1
Myom2
Casc1
Itm2a
Scin
Col28a1

ETV1^*Tg*: - - + + - - - + + + + +
hAR^Q: 12 48 12 48 12 21 48 12 21 48 12 21

DLP   Tumor

-2 0 1 2 3
Row Z-Score

d)

	Pten+/+				*Pten*+/-							
Sdk1
Kcnn4*
Lrp8*
F3
Myo1e
Smpd3

ETV1^*Tg*: - - + + - - - + + + + +
hAR^Q: 12 48 12 48 12 21 48 12 21 48 12 21

DLP   Tumor

-1 0 1 2 3
Row Z-Score

74

Figure 2.9: ETV1 effects in mouse DLP parallel those in ETS$^+$ and aggressive human PCa

A) A set of androgen-induced genes is significantly repressed in *hAR;ETV1^{Tg}* prostates and in *Pten$^{+/-}$* tumors. Relative expression across groups is represented in the heatmap. B) Genes downregulated in *hAR^{21Q};ETV1^{Tg};Pten$^{+/-}$* tumor tissue were uploaded to Oncomine and queried against "Oncomine gene expression signatures". Significant enrichment of genes downregulated in human PCa metastases and advanced Gleason grade PCa was observed, and select concepts are shown in the molecular concept map. Node size is proportional to the number of genes shared with the primary concept. O.R. $\geq$ 4.0. p $\leq 10^{-6}$. C) The heatmap shows the relative expression pattern of genes that are significantly downregulated in ETS$^+$ vs. non-ETS localized tumors from the Taylor Prostate data set as well as in *hAR;ETV1^{Tg}* mouse prostates or DLP tumors. D) The heatmap shows relative expression of genes that are significantly overexpressed in ETV1$^+$ vs. non-ETS localized tumors from the Grasso Prostate data set as well as in *hAR;ETV1^{Tg}* mouse prostates or DLP tumors.
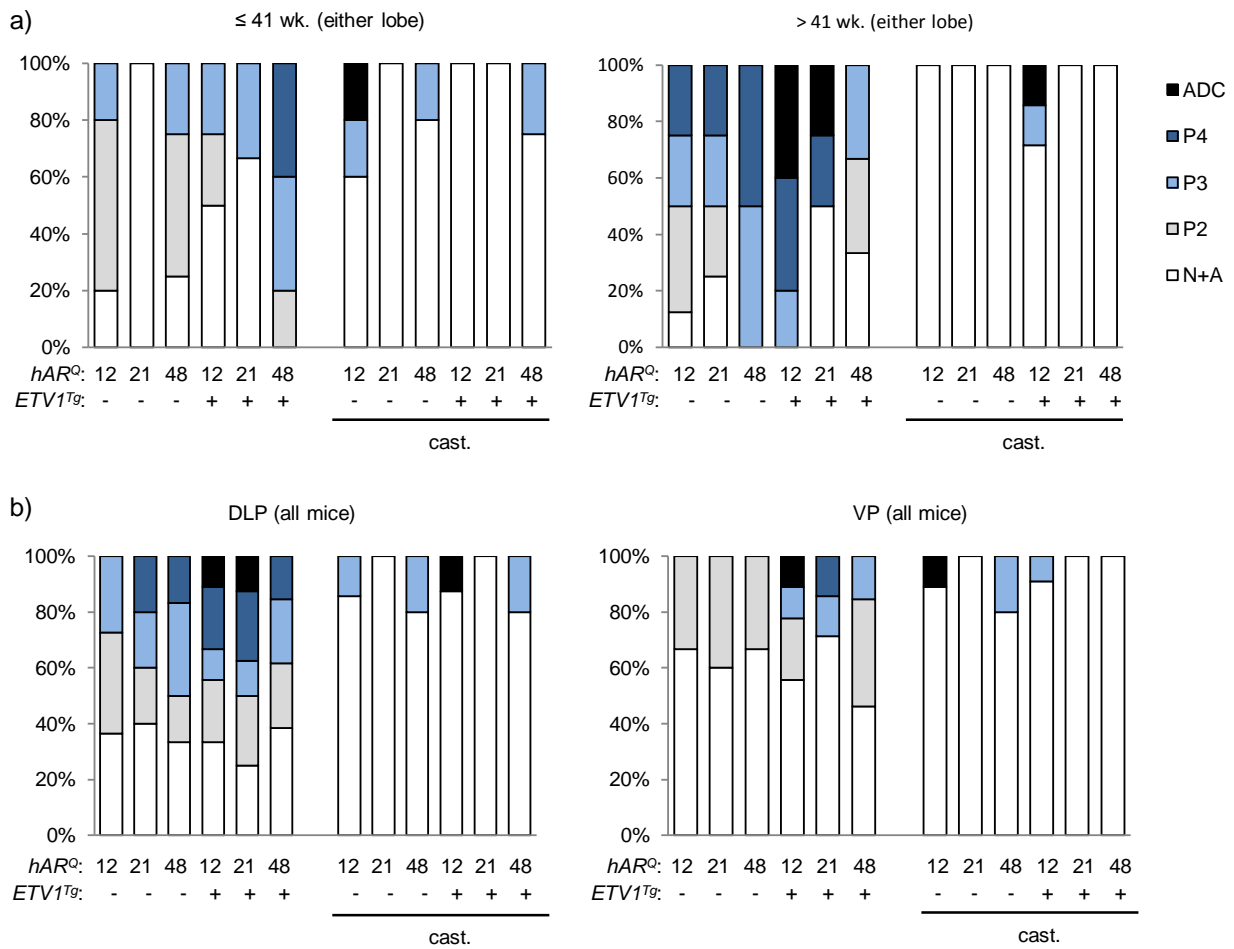
Figure 2.10: Prostate pathology in *Pten*-hemizygous mice varies with age and lobe

A) DLP and VP sections were scored as normal or atrophy (N+A), mPIN2-4 (P2-4) or adenocarcinoma (ADC). The median age at sacrifice was 41 weeks, and samples were divided into subsets ≤ 41 weeks or > 41 weeks of age. The proportion of samples at each stage was plotted per experimental group. Samples were plotted according to the most severely diseased lobe. Prostates from 5-14 mice per group were analyzed. B) As in panel A, but DLP and VP sections from each mouse were plotted separately for mice of any age.
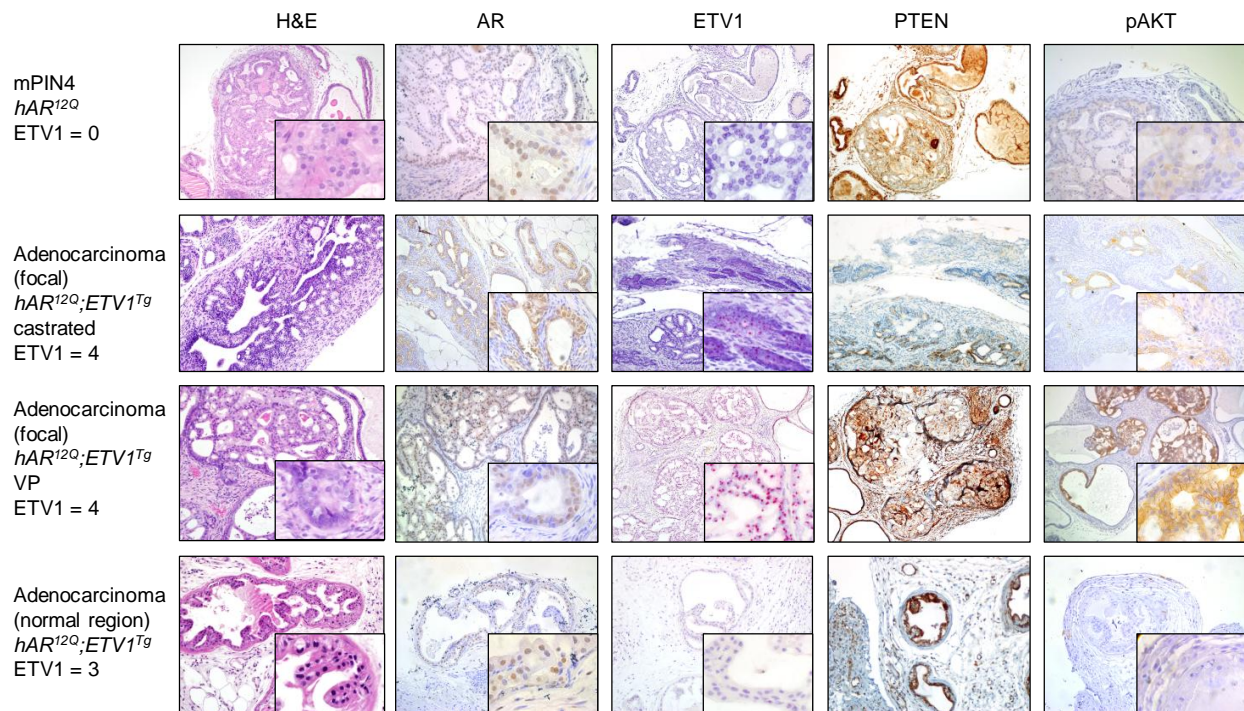
Figure 2.11: Histopathology in *Pten*-hemizygous mice

Additional prostate sections are shown from, in order, an intact $hAR^{12Q};Pten^{+/-}$ DLP, a castrated $hAR^{12Q};ETV1^{Tg};Pten^{+/-}$ DLP, an intact $hAR^{12Q};Pten^{+/-}$ VP and a normal region of a macroscopic $hAR^{12Q};ETV1^{Tg};Pten^{+/-}$ DLP tumor. Sections were stained with H&E. Immunohistochemical (IHC) staining was performed with antibodies to AR, PTEN or pAKT protein (brown staining). *In situ* hybridization (ISH) was performed with a probe against the human ETV1 transcript (red staining). ETV1 expression level is scored as 0-4, with 4 being highest. Images are shown at 10x-20x magnification with 60x inset. Consecutive sections were used when possible, and each row of images shows sections from a single mouse prostate.
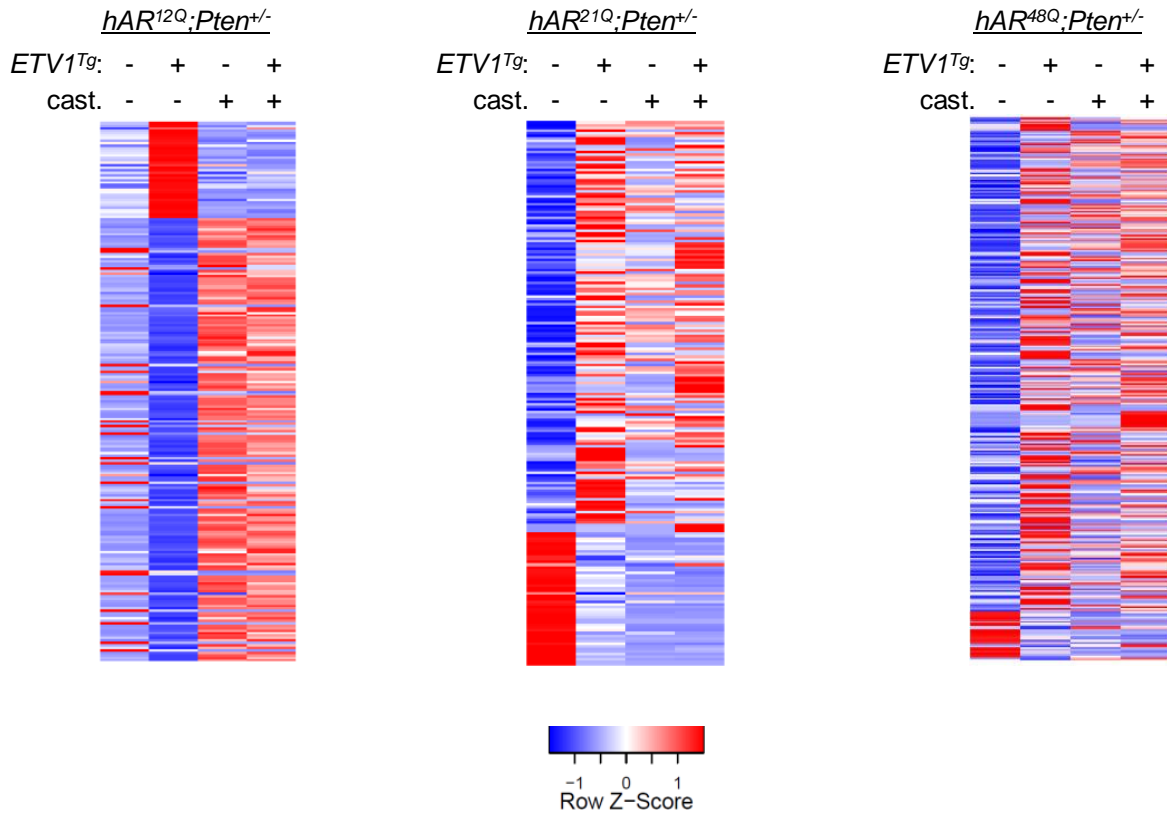
Figure 2.12: Differential expression by *hAR* allele in *ETV1*^{*Tg*}*;Pten*^{*+/-*} mice

The heatmaps show relative expression of genes differentially expressed (FDR ≤ 0.05) in intact ETV1-transgenic vs. non-transgenic mice on the *Pten*-hemizygous background. Each *hAR* Q-tract allele was analyzed separately. For each group, relative expression in castrated mice is included. Each lane represents the average expression from of 2-3 pools of RNA per group. See Figure 2.7d for the number of shared and unique genes in each contrast.

Chapter 3

**Selective antagonism of androgen receptor by ETV1
in benign and malignant human prostate cells**

Acknowledgements

Stable RWPE-ETV1, RWPE-ERG and RWPE-LACZ cells (Tomlins et al., 2007; Tomlins et al., 2008a) were a gift from Dr. Arul Chinnaiyan (University of Michigan). The FG9 plasmid (see Chapter 2) was a gift from Dr. David Baltimore (California Institute of Technology). The p5HBhARcDNA plasmid was a gift from Dr. Andrew Lieberman (University of Michigan).

Abstract

Androgen receptor (AR) signaling, which is central to prostate cancer (PCa) onset and progression, cooperates with oncogene activation and tumor suppressor loss to drive tumorigenesis. Common somatic alterations include gene fusions that place ETS cell cycle transcription factors under AR control, driving elevated expression, or loss of the tumor suppressor PTEN. Disruption of either pathway can impact AR activity, but many questions remain as to the specific molecular interactions at early vs. late disease stages.

It has been suggested that while the ETS factors ETV1 and ERG promote the same physiological endpoint, i.e. early neoplasia and invasion, they do so via different molecular mechanisms. Chiefly, ERG was thought to repress AR while ETV1 plays a more cooperative role. Additional studies suggest that interactions with AR may not be inherently divergent, but may depend more on disease stage or the activity of additional signaling pathways such as PTEN.

In this study, the effect of ETS factors on AR action was explored in benign and malignant human prostate cells. In benign RWPE-1 cells, overexpression of either ETV1 or ERG repressed androgen induction of luciferase reporters, yet enhanced AR regulation of endogenous

chromosomal targets, suggesting that within this cell line ETV1 and ERG have a similar effect on AR-regulated gene expression. In malignant PCa cell lines with or without functional PTEN, ETV1 knockdown resulted in greater AR activation or repression of target genes, indicating that ETV1 was repressing AR action. This included repression of the tumor suppressor gene *NKX3-1*, which was previously noted in ETV1-transgenic mice. Targeted inhibition of PTEN-regulated factors (such as AKT) as a proxy for restoring PTEN function in PTEN-null PCa cells did not significantly affect the ETV1-AR interaction. ETV1 repression of AR was not achieved through differential genomic binding of AR at affected targets, nor was repression associated with altered enhancer RNA (eRNA) expression.

Together, these results suggest that ETV1 and ERG impact AR signaling in a similar direction in multiple experimental systems. ETV1 repression of AR transcriptional activity *in vitro* is highlighted in multiple malignant cell lines, yet appeared to be largely independent of PTEN, in contrast to previous *in vivo* findings.

Introduction

Multiple aberrant signaling pathways converge to promote PCa progression, with different molecular subtypes of prostate tumors harboring disruptions of specific combinations of factors (Barbieri et al., 2013; Barbieri and Tomlins, 2014). One of the most common classes of somatic alterations in prostate tumors involves genomic rearrangement of oncogenic ETS transcription factors early in tumorigenesis. These rearrangements result in fusion of the coding region of an ETS gene to androgen-responsive regulatory elements that drive high prostatic expression. The ETS factors ERG and ETV1 are rearranged in approximately 50% and 5-10% of

tumors, respectively, among PSA-screened Caucasian cohorts (Rubin et al., 2011; Tomlins et al., 2005).

As transgenes or knock-ins in mice, ETV1 and ERG promote prostatic intraepithelial neoplasia (PIN) at variable penetrance without progression to adenocarcinoma, confirming a role in early neoplasia (Higgins et al., 2015; Shin et al., 2009; Tomlins et al., 2007; Tomlins et al., 2008a). In combination with *Pten* deletion, ETV1 and ERG promote more aggressive PIN or progression to adenocarcinoma, showing that oncogenic ETS activation can cooperate with tumor suppressor loss in PCa (Baena et al., 2013; Carver et al., 2009; Chen et al., 2013; Higgins et al., 2015; King et al., 2009).

In benign human prostate cells, ETV1 or ERG overexpression increase invasiveness without a concomitant increase in proliferation (Baena et al., 2013; Hollenhorst et al., 2011a; Tomlins et al., 2007; Tomlins et al., 2008a). ETS rearrangements have been detected in human PCa cell lines, including the ERG-positive VCaP line and ETV1-positive LNCaP and MDA-PCa-2b cells. ERG or ETV1 knockdown in these cells inhibits invasion and anchorage-independent growth, as well as proliferation in some models, and alters AR transcriptional activity (Baena et al., 2013; Chen et al., 2013; Mesquita et al., 2014; Mounir et al., 2014; Shin et al., 2009; Tomlins et al., 2007; Tomlins et al., 2008a; Yu et al., 2010). *In vitro* experiments suggest that ERG primarily represses AR by binding near AR binding sites in the genome and recruiting the polycomb repressive complex (PRC) to place repressive H3K27me3 marks on histones (Baena et al., 2013; Tomlins et al., 2008a; Yu et al., 2010). On the other hand, ETV1 enhances AR genomic binding and target gene activation *in vitro* (Baena et al., 2013; Chen et al., 2013; Shin et al., 2009).

While the interaction between AR and ERG has been studied in several different PCa cell lines and consistent AR repression by ERG is observed, experiments focusing on ETV1 and AR have primarily been performed in a single cell line (LNCaP) (Baena et al., 2013; Chen et al., 2013; Shin et al., 2009). It is unclear whether those findings extrapolate to different cellular contexts, including whether the PTEN signaling pathway impacts AR-ETV1 interaction. Furthermore, little is known about the mechanism by which ETV1 enhances AR genomic binding. In previous ETS overexpression experiments in benign cells, AR was absent. Given the central role of AR in prostate differentiation and throughout PCa progression, examining ETS factors in the context of functional AR is critical.

We previously characterized the interaction between genetic variation in AR, overexpression of oncogenic ETV1 and reduction of the PTEN tumor suppressor in mice (Higgins et al., 2015). ETV1 exhibits a striking antagonism of AR transcriptional activity in the context of benign or early neoplastic prostate tissue with normal PTEN levels. With reduced PTEN the strong ETV1-AR interaction at the level of AR target gene expression is largely abrogated, but there is a general mild reduction in AR activity. Furthermore, the stronger AR allele cooperates physiologically with ETV1 overexpression and PTEN reduction to promote progression to prostate adenocarcinoma. In macroscopic tumors, AR repression by ETV1 is observed as it is in early neoplasia (Higgins et al., 2015). These findings suggest that ETV1 and PTEN repression of AR may be important in early as well as later oncogenesis. This is in contrast to existing *in vitro* data primarily showing cooperation between ETV1 and AR (Baena et al., 2013; Chen et al., 2013; Shin et al., 2009). These apparent incongruities could be due to *in vivo* vs. *in vitro* differences, PTEN status, or disease stage of the cells or tissue. To extend the *in vivo* discoveries from the *hAR;ETV1^{Tg};Pten$^{+/-}$* mice and elucidate the reasons behind divergent

findings, we explored the ETV1-AR interaction in benign and malignant human prostate cell lines.

Lentiviruses and siRNAs were used to overexpress or knock down AR and ETS factors to model direct interaction between these proteins at early, intermediate and late disease stages. AR transcriptional regulation of target genes in different cellular contexts was the primary experimental endpoint. In benign AR-expressing cells, ETV1 and ERG were studied in parallel to determine whether they impact AR signaling in a similar or opposing manner. To test the hypothesis that PTEN impacts the ETV1-AR interaction, experiments were performed in malignant cell lines with intact vs. absent endogenous PTEN signaling, or following inhibition of PTEN-repressed factors as a proxy for restoring PTEN activity. Chromatin immunoprecipitation (ChIP) assays were employed to test whether ETV1-driven alterations in AR target gene expression are achieved through differential binding of AR or other factors. Together these experiments aim to clarify the cellular features influencing the context-dependent interaction of ETV1 and AR in human prostate cells.

Results

ETS factors impact AR transactivation in benign prostate cells

The effect of ETV1 and ERG on AR transcriptional activity was first tested in immortalized benign prostate cells that lack endogenous expression of these factors. Despite their origin as normal prostate epithelial cells, in contrast to an early report (Bello et al., 1997), RWPE-1 cells do not express of AR (Table 3.1, Figure 3.1). Microsatellite profiling confirmed the identity of our RWPE-1 cell line (data not shown). Loss of AR expression is a common

phenomenon in cultured benign prostate epithelial cells, also occurring in PrEc cells (Vander Griend et al., 2014).

RWPE-1 cells were transduced with lentiviral constructs to stably express AR or an FG9 empty vector control. AR protein in transduced cells was expressed at levels comparable to endogenous AR in LNCaP cells (Figure 3.1A), with no AR expression in the empty vector control cells (Figure 3.1B). RWPE-AR cells were further transduced with lentiviral constructs to stably express truncated ETV1 or ERG, compared with either empty vector or one expressing LACZ as a control (Tomlins et al., 2007; Tomlins et al., 2008a). Transduction with ETV1 lentivirus resulted in 12-fold higher expression, and ERG transduction resulted in a 400-fold increase in expression in the absence of hormone (Figure 3.1B). Treatment with the synthetic androgen R1881 resulted in a further expression increase (1.4 fold for ETV1, 2-fold for ERG) (Figure 3.1B).

Interaction of AR and ETS factors was tested first on transfected plasmids as sensitive reporter genes. A luciferase reporter driven by a minimal thymidine kinase promoter combined with steroid hormone response elements (HRE3-tk-Luc) (Steinkamp et al., 2009) was strongly induced by androgen stimulation in the RWPE-AR cells (Figure 3.2A). An additional reporter containing approximately 500 bp of the PSA (*KLK3*) promoter along with 1.3 kb of its enhancer cloned from LNCaP cells (PSA-Luc) (Perez-Stable et al., 2000) was also robustly induced in the stable RWPE-AR cells (Figure 3.2A). RWPE-FG9 cells showed no luciferase induction following androgen treatment, reaffirming the absence of endogenous AR activity (Figure 3.2A). Together, these results confirm that while RWPE-1 cells do not express endogenous AR, they retain other cellular components necessary to respond to androgen with exogenous AR.

When ETV1 or ERG were stably overexpressed, androgen induction of the HRE3-tk-Luc reporter was inhibited by approximately 50%, with greater inhibition of PSA-Luc (Figure 3.2B). This result shows that both ETS factors are capable of antagonizing AR transactivation in response to androgen. Of note, baseline activity of the PSA-Luc reporter was also reduced approximately 50% with ERG or ETV1 overexpression (Figure 3.2B). The PSA sequences contain ETS binding sites (Shin et al., 2009) as well as sites for transcription factors in addition to AR, suggesting that binding of ETV1 or ERG may inhibit transcription independent of AR. These findings are consistent with the striking antagonism of AR by ETV1 seen in normal and early neoplastic prostate tissue in the transgenic mice (Figures 2.2A, 2.3A,C) (Higgins et al., 2015). Furthermore ETV1 and ERG impacted AR activity in the same direction in these experiments (Figure 3.2B), whereas they have been reported to have opposite effects on AR in malignant PCa cells (Baena et al., 2013; Yu et al., 2010).

We next examined how ETV1 or ERG overexpression impacted AR transcriptional activity at endogenous target genes. A number of canonical AR target genes are not androgen-regulated in RWPE-AR cells, including *TMPRSS2* and *KLK3* (data not shown). However, exogenous AR regulates a broader set of targets in these cells (Altintas et al., 2011). In RWPE-AR-LACZ control cells, stimulation with 1 or 10 nM R1881 resulted in induction of *AQP3* and *MME* expression, as well as repression of *NT5E* (Figure 3.3). Stable overexpression of ETV1 or ERG enhanced activation or repression of these AR targets (Figure 3.3). Intriguingly, these effects were seen in the absence of hormone and were greater with 1 nM R1881. This suggests that ETV1 and ERG may influence the activity of the basal transcriptional machinery or other transcription factors independent of AR. As with the luciferase reporters, ETV1 and ERG act in

the same direction on the endogenous targets with regard to their effect on androgen signaling, although in this case it is accentuating rather than countering AR action.

ETV1 antagonizes AR in metastatic PCa cell lines

The ETV1-AR interaction was next probed in two cell lines, MDA-PCa-2b and LNCaP, derived from human PCa metastases (Table 3.1). Both lines overexpress ETV1 due to genomic rearrangements, and both express AR, allowing study of the endogenous factors. MDA-PCa-2b cells retain PTEN expression and represent an earlier disease stage, while LNCaP cells have lost PTEN and represent a later, though still androgen-dependent, phase. siRNA was used to knock down ETV1 and the impact on AR transcriptional activity tested.

Transfection of siRNA targeting ETV1 (siETV1) in MDA-PCa-2b cells resulted in approximately 60% ETV1 knockdown relative to non-targeted siRNA (siScr) (Figure 3.4). MDA-PCa-2b cells express high levels of ETV1and this level of knockdown was not increased up to 25 nM siETV1 (data not shown), suggesting that the 60% knockdown of ETV1 was also the maximum achievable with a short hairpin RNA (shRNA) in these cells (Mesquita et al., 2014). shRNA data suggest that total knockdown can be lethal, at least in the case of ERG (Scott Tomlins, personal communication).

Following siETV1 transfection, treatment of MDA-PCa-2b cells with 10nM R1881 induced up to a 7-fold increase in expression of the AR targets tested (Figure 3.4). *FKBP5*, *NKX3-1* and *AQP3* expression levels increased above androgen-induced levels with ETV1 knockdown. *KLK3* showed a trend toward decreased expression, while *TMPRSS2* and *MME* were unaffected (Figure 3.4). *MME*, which is strongly androgen-induced in RWPE-AR cells, is modestly androgen-repressed in MDA-PCa-2b. siETV1 altered expression of *AQP3* and *NKX3-1*

in the absence of androgen as well, suggesting that ETV1 is capable of interacting with the basal

transcriptional machinery or other factors. While not all AR target genes queried showed a

significant effect of ETV1 knockdown, those that did suggested that ETV1 was inhibiting AR

transcriptional activity. Importantly, the ETV1-repressed genes include the tumor suppressor

NKX3-1, which was also inhibited in pre-neoplastic prostates and tumors of *ETV1^{Tg}* mice

(Figures 2.2A, 2.3B, 2.9A) (Higgins et al., 2015).

LNCaP cells were used to test the ETV1-AR interaction in the context of PTEN loss.

Transfection with siETV1 reduced expression by approximately 80% at the transcript level

relative to cells transfected with siScr or to untransfected cells (Figure 3.5A). Effective

knockdown persisted for at least 48-96 hours post-transfection (data not shown). A reduction in

ETV1 protein was verified by Western blot (Figure 3.5A, compare left 4 bands to right 4 bands),

but due to the high level of background with the ETV1 antibody, qRT-PCR was more routinely

used to gauge knockdown. Following ETV1 knockdown, cells were stimulated with 1 nM or 10

nM DHT to replicate the experimental conditions of a recent report as closely as possible (Baena

et al., 2013).

ETV1 knockdown significantly enhanced AR activation of the target genes *KLK3*, *NKX3-*

1 and *TMPRSS2* following androgen stimulation, with a trend toward increased *FKBP5*

expression (Figure 3.5B). *MME* is not normally androgen-induced in LNCaP cells, but siETV1

significantly increased *MME* expression with 10 nM DHT. ETV1 knockdown enhanced AR-

mediated repression of *AQP3* (Figure 3.5B). These results implied that endogenous ETV1

antagonizes AR activation as well as repression of target genes in LNCaP cells. This finding was

consistently obtained for multiple experimental conditions, despite reports of ETV1-AR

cooperation in LNCaP cells (Baena et al., 2013; Chen et al., 2013; Shin et al., 2009) (see

discussion). ETV1 knockdown similarly affected basal transcription of *TMPRSS2*, *NKX3-1* and *AQP3*, again suggesting the influence of other factors.

Interaction between ETV1 and PI3K/AKT pathways

Given the striking antagonism of AR by ETV1 and the loss of that antagonism with reduced PTEN in mice (Higgins et al., 2015), we hypothesized that PTEN signaling could act, in some contexts, as a "switch" that influenced ETV1-AR interaction. Despite the unexpectedly similar results in MDA-PCa-2b (PTEN$^+$) and LNCaP (PTEN$^-$) cells, the ETV1-AR interaction was further probed to determine whether altered PTEN activity exerted an influence within this cell line. As a proxy for restoring PTEN signaling in the PTEN-null LNCaP cells, AKT and PI3K signaling were inhibited, either with AKT siRNA (siAKT) or with the dual PI3K/mTOR inhibitor NVP-BEZ235 (BEZ235) (Serra et al., 2008).

Treatment with siAKT led to almost complete loss of total AKT protein, but levels of phospho-AKT (pAKT), the active form of the protein, were reduced only 2-4 fold (Figure 3.6A). This suggests that pAKT is more stable than the un-phosphorylated protein, or that there is high kinase or low phosphatase activity targeting AKT.

Treatment with either siAKT or siETV1 resulted in a trend toward increased androgen-stimulated expression of the AR target genes *TMPRSS2* and *FKBP5* (Figure 3.6B). This is consistent with reports describing inhibition of AR activity by the PI3K/AKT pathway (Carver et al., 2011; Mulholland et al., 2011). Simultaneous knockdown of both ETV1 and AKT trended toward an additive increase in androgen-stimulated expression of *FKBP5*, while *TMPRSS2* expression was no greater than with siETV1 alone (Figure 3.6B). Intriguingly, siAKT increased expression of the androgen-repressed gene *AQP3* while siETV1 trended toward reduced

expression even in combination with siAKT. This result shows that AKT inhibition may affect AR-mediated activation and repression differently. Furthermore, at these targets AKT and ETV1 appear to act independently, with a trend to additivity in some cases. While variance was large and effect sizes small, this experiment did not provide evidence that AKT signaling is a switch controlling the effect of ETV1 on AR target gene regulation.

Treatment with 500 nM BEZ235 reduced pAKT protein without affecting total AKT (Figure 3.6C), confirming that the target of BEZ235 is PI3K, which results in reduced AKT activity but not expression. 500 nM BEZ235 significantly increased androgen-induced expression of *TMPRSS2* and caused a non-significant increase in *FKBP5* levels (Figure 3.6D). These results are again consistent with recent reports describing PI3K/AKT inhibition of AR (Carver et al., 2011; Mulholland et al., 2011) and with the effect of AKT knockdown by siRNA (Figure 3.6B). When BEZ235 and siETV1 were combined, androgen-induced expression of both *TMPRSS2* and *FKBP5* were greater than with siETV1 alone. For *FKBP5* there was a trend toward an additive increase in expression. Concurrent ETV1 knockdown slightly reduced the BEZ235-induced increase in *TMPRSS2* expression with DHT, but not below that seen with only siETV1. Thus neither target revealed combinatorial action of ETV1 and P13K, dampening the notion that PI3K signaling acts as a switch to control the ETV1-AR interaction, at least in LNCaP cells.

AR genomic binding is not perturbed by ETV1 in metastatic PCa cells

ETS binding sites frequently reside near AR binding sites in the genome, and ERG is known to repress AR binding *in vitro* (Yu et al., 2010). Therefore, we hypothesized that ETV1 might antagonize AR transcriptional activity by disrupting AR binding at target genes.

Chromatin immunoprecipitation (ChIP) was performed following ETV1 knockdown in LNCaP cells. Target sequences for qPCR were selected based on overlapping AR and ETV1 binding sites observed in ChIP-seq studies. Priority was given to sites where AR binding is enhanced by androgen stimulation as well as by ETV1, such as the *TMPRSS2* -13 kb enhancer (Figure 3.7A) (Baena et al., 2013; Chen et al., 2013; Yu et al., 2010).

Cells were transfected with siETV1 or siScr and treated for 4 hours with 10 nM DHT or 2 hours with 1 nM R1881 before harvesting chromatin. Genomic binding of AR or RNA PolII (PolII) was detected with specific antibodies vs. IgG-only control, and enrichment at target sequences was quantified by qPCR. In an initial experiment, DHT stimulation successfully increased binding of AR and PolII at the *TMPRSS2* and PSA (*KLK3*) enhancers relative to methanol-treated cells (Figure 3.7B). Since the synthetic androgen R1881 has a higher binding affinity for AR and is not metabolized in the cell, R1881 was used subsequently.

LNCaP cells were transfected with siETV1 or siScr and treated with 1 nM R1881 or vehicle. Enrichment above the IgG control was observed for AR and RNA PolII binding at the *TMPRSS2* -13kb enhancer with 1 nM R1881. However, ETV1 knockdown did not significantly affect AR or PolII binding at the *TMPRSS2* enhancer (Figure 3.7C) or promoter (data not shown) despite having the expected effect on *TMPRSS2* gene expression (Figure 3.7D). As a control, PolII bound to the *GAPDH* transcription start site (TSS) while AR signal was at background levels (Figure 3.7C). Unfortunately, ETV1 binding could not be detected above IgG background in any experimental run, probably due to the poor quality of the commercial antibody. In summary, there was no evidence for an impact of ETV1 on AR or PolII binding at the *TMPRSS2* promoter or enhancer.

An alternative hypothesis to explain how ETV1 inhibits expression of TMPRSS2 and other AR target genes is altered enhancer RNA (eRNA) expression, rather than a direct effect on AR binding. Next-generation sequencing applications such as global run-on sequencing (GRO-seq) (Core et al., 2008) and bromouridine sequencing (Bru-seq) (Paulsen et al., 2014) allow nascent RNA to be purified and sequenced. Such experiments have revealed that enhancers are actively transcribed, rather than simply serving as a docking site for transcription factors from which to act on distal targets. *TMPRSS2* eRNA transcription was recently characterized (Puc et al., 2015), and the primer sequences from that report were used to test for differential *TMPRSS2* eRNA expression following ETV1 knockdown in LNCaP cells. While R1881 stimulation increased eRNA expression, siETV1 had no significant effect on expression at either the basal level or following androgen treatment (Figure 3.7). The inhibition of *TMPRSS2* expression by ETV1 does not appear to be mediated by altered eRNA expression.

Discussion

The aim of these experiments was to study direct interactions between ETV1 and AR in human prostate cells representing progressive disease stages, with a focus on confirming and extending observations made in the $ETV1^{Tg}$ mice (Higgins et al., 2015). Collectively, the data reveal that ETV1 has the capacity to enhance or repress AR signaling depending on cellular context. AR activation of luciferase reporters is antagonized by both ETV1 and ERG in benign cells, yet at endogenous genes both activation and repression by AR are enhanced. In two metastatic PCa cell lines, ETV1 represses AR induction of target genes regardless of PTEN

status. This repression does not appear to be mediated through altered AR or PolII binding at the gene promoter or enhancer.

It was initially surprising to observe such repression in LNCaP cells, as cooperation between ETV1 and AR had previously been reported in that cell line (Baena et al., 2013; Shin et al., 2009). Despite mirroring experimental conditions as closely as possible, including the same siETV1 reagent and qRT-PCR primer sequences, those results could not be replicated. To verify that the LNCaP cells retained their critical features, the *AR* gene was sequenced and the presence of the T877A mutation confirmed. Additionally, Western blot analysis showed that the LNCaP cells lacked PTEN protein expression and had high pAKT expression, as expected. The cells robustly expressed ETV1 that could be knocked down with targeted siRNA. The effect was not due to differential expression of the housekeeping gene used to normalize expression levels, as *ACTB* was not significantly affected by ETV1 knockdown. The experiment was repeated with fresh LNCaP cells ordered directly from ATCC, and similar results were obtained. Cells were negative for Mycoplasma by PCR assay. In our hands, ETV1 consistently antagonized AR in LNCaP cells.

It is possible that some technical factor such as serum brand or culture condition had an influence over time. Expression of different ETS factors within the same cell line varies between labs (Hollenhorst et al., 2011b; Mesquita et al., 2014; Pellecchia et al., 2012). Subtler variation in expression level of AR, ETV1 and other factors among sublines is also possible. Nevertheless, in our hands ETV1 appears to be a repressor of AR both *in vivo* (Higgins et al., 2015) and in malignant prostate cells, similar to findings with ERG (Baena et al., 2013; Tomlins et al., 2008a; Yu et al., 2010).

While previous reports have studied ETS factors in the benign RWPE-1 cell line, this work is the first to look at the interaction between stably expressed ETV1 or ERG together with AR. Of note, ETV1 and ERG affect AR signaling in the same "direction" for a given target. Both factors inhibit androgen induction of luciferase reporters, yet enhance the induction or repression of androgen-induced or -repressed genes, respectively. For some targets these effects are seen even in the absence of hormone, suggesting that ETV1 and ERG can interact with the basal transcriptional machinery. AQP3 and MME have known roles in oncogenesis. AQP3, a water and small solute channel, promotes motility and invasion of PCa cells, in part through increased MMP3 expression and ERK signaling (Chen et al., 2015). MME, also known as CD10, NEP or neprilysin, is an endopeptidase associated with poor prognosis in esophageal squamous cell carcinoma and other cancers (Lee et al., 2015). MME was previously shown to exert tumor suppressive functions in PCa cell lines, mediated in part by facilitating inhibition of PI3K by PTEN (Sumitomo et al., 2005). On average, MME levels are reduced in both localized and metastatic tumors relative to normal tissue in PCa patients. However, increased MME in either localized or metastatic PCa is associated with poor survival (Fleischmann et al., 2011). Both AQP3 and MME are expressed in normal tissues, and perhaps their inappropriate activation by ETV1 or ERG could contribute to early disease.

ETV1 and ERG promote similar physiological outcomes, e.g. invasion *in vitro* and early neoplasia *in vivo*, but it has been suggested that they do so through divergent gene expression programs (Baena et al., 2013). The emerging picture from our work and other recent studies is that ETV1 and ERG may be more similar than different. It may largely be the cellular context that influences their differential activity rather than inherently divergent function (Chen et al., 2013).

In vitro, PTEN status does not appear to be a "switch" that controls the effect of ETV1 on AR action. In both MDA-PCa-2b and LNCaP cells (PTEN-positive and -negative, respectively) ETV1 antagonizes AR regulation of target genes, though the specific subset of affected targets varies slightly between lines. Inhibiting PI3K/pAKT signaling, in effect partially restoring PTEN function, did not significantly alter ETV1-AR antagonism in LNCaP cells. Broader differences in the transition from benign to malignant cells may be important, as AR regulation of endogenous targets was enhanced by both ETV1 and ERG in benign RWPE-1 cells. It remains to be seen whether PTEN knockdown in benign prostate cells or in malignant MDA-PCa-2b cells affects the ETV1-AR interaction.

In the AKT knockdown experiments, pAKT appeared to be more stable than the un-phosphorylated protein (Figure 3.6). This is perhaps surprising, as AKT phosphorylation at Ser473 has been reported to promote polyubiquitination and proteasomal degradation (Wu et al., 2011). However, those experiments were carried out in 293T or MEF cells with tagged, overexpressed AKT. Other groups report that dephosphorylating AKT at Ser473 does not alter stability (Liao and Hung, 2010). It is possible that the ubiquitin ligase, kinase or phosphatase that target AKT are present at different levels in LNCaP cells under the current experimental conditions.

Recent evidence suggests that eRNA transcription at enhancers plays an active role in promoting transcription of the target gene, in part through stabilization of chromatin looping (Li et al., 2013). Such eRNAs have been reported to be involved in estrogen receptor (ER) and AR-mediated transcription (Li et al., 2013; Puc et al., 2015). eRNA inhibition could affect expression of the neighboring gene, but in LNCaP cells ETV1 repression of *TMPRSS2* expression does not appear to be due to differential expression of the *TMPRSS2* eRNA. The TMPRSS2 antagonism

by ETV1 is not due to differential binding of AR or RNA PolII upstream of *TMPRSS2* either. It remains possible that ETV1 inhibits active transcription by PolII, causing it to remain "poised" at the promoter or enhancer. ChIP for histone modifications marking active transcription such as H3K36me3 (Hon et al., 2009) could address this hypothesis, as could testing for PolII binding further downstream in the *TMPRSS2* gene body.

In these experiments, both ETV1 and ERG affected expression of a number of target genes even in the absence of androgen. In PCa cells, ERG is known to recruit the polycomb repressive complex (PRC) to AR target genes, resulting in placement of H3K27me3 marks and transcriptional repression (Yu et al., 2010). ChIP for PRC components or H3K27me3 histone modifications would test the hypothesis that ETV1 utilizes a repressive mechanism similar to ERG, in effect acting as an "anti-pioneer" factor.

Thus far it has been presumed that ETV1 antagonizes AR primarily at the level of target gene transcription, as both proteins are transcription factors and are known to have overlapping binding sites. Because standard qRT-PCR and even RNA-seq represents a static "snapshot" of transcript levels, it remains possible that ETV1 affects post-transcriptional mRNA stability rather than transcription. Alternatively, the rate of extension could be slowed despite a similar rate of transcription factor binding and initiation. Bru-seq following ETV1 knockdown and androgen stimulation would clarify whether differential expression of *TMPRSS2* and other AR targets is transcriptionally mediated, as Bru-seq enriches for nascent RNA. As a more general experiment, Bru-seq combined with ChIP-seq in androgen-stimulated prostate cells would clarify which androgen-induced or -repressed genes are primary AR and ETV1 targets and which genes are induced (or repressed) secondarily.

Overall, these experiments highlight the capacity for ETV1 to selectively repress AR signaling in benign and malignant human prostate cells, with or without PTEN signaling. Consistent ETV1 inhibition of the androgen-induced tumor suppressor *NKX3-1* in multiple PCa cell lines as well as in mice (Higgins et al., 2015) supports a model in which ETV1 acts by disrupting the pro-differentiation expression program normally regulated by AR. At both early and later disease stages this push toward dedifferentiation may prime prostate cells for transformation following additional oncogenic events.

Materials and Methods

Cell lines

RWPE-1 cells (ATCC cat. # CRL-11609), as well as stably transduced RWPE-AR, RWPE-ETS and RWPE-AR-ETS cells, were maintained in KSFM (Gibco) with EGF and BPE supplements (included) plus 1:100 penicillin/streptomycin (Gibco). LNCaP cells (ATCC # CRL-1740) were maintained in RPMI1640 (Gibco) with 10% FBS (GeneMate) and 1:100 penicillin/streptomycin. MDA-PCa-2b cells (ATCC # CRL-2422) (a gift from Dr. Arul Chinnaiyan) were maintained in F12K medium (Gibco) with 20% FBS, 5 ng/ml insulin, 10 ng/ml EGF, 25 ng/ml cholera toxin, 100 pg/ml hydrocortisone and 1:100 penicillin/streptomycin.

To maintain stable expression of AR or FG9 empty vector control constructs, 100 μg/ml Hygromycin B (Invitrogen) was added to the complete growth medium. To maintain stable expression of ETV1, ERG, LACZ or pLenti empty vector control constructs, 3 μg/ml Blasticidin-HCl (Invitrogen) was added to the complete growth medium.

RWPE-ETS-AR transduction

For details regarding cloning of the FG9-3xFLAG-AR plasmid and its stable transduction into RWPE-ETS cells, see Chapter 2. In order to generate comparable RWPE cells stably expressing AR without the 3xFLAG tag, an AR fragment was first excised from the p5HBhARcDNA plasmid (gift from Dr. Andrew Lieberman) with BamHI and BglII restriction enzymes. The FG9 lentiviral plasmid was then linearized with BamHI, and the 3.1kb AR fragment was ligated to linearized FG9 to generate FG9-AR. The ligation product was transformed into One-Shot Stbl3 competent cells (Invitrogen) and colony PCR was performed with primers flanking each ligation site to check orientation. FG9-AR was packaged into a lentivirus and transduced into RWPE cells as in Chapter 2.

Western Blot

The primary antibodies and dilutions used for Western blots include AR (Santa Cruz # sc-816, 1:500), GAPDH (Millipore # MAB374, 1:10000), ETV1 (Abcam # 81086, 1:500), AKT (Cell Signaling # 9272, 1:1000), pAKT (Cell Signaling # 9271, 1:1000) and β-tubulin (Santa Cruz # sc-9104, 1:1000). The secondary antibody was HRP-conjugated anti-rabbit IgG (Santa Cruz # sc-2313, 1:5000). HRP signal was detected with ECL Western Blotting Substrate (Pierce) according to the manufacturer's instructions.

RWPE-AR-ETS Luciferase transfection and androgen stimulation

50,000 cells per well were seeded into 12-well plates in complete growth medium. In all *in vitro* experiments, cells were counted and seeded from independently maintained flasks, as well as transfected and hormone-stimulated from independently prepared solutions, in order to

obtain biological replicates. The following day, medium was changed to KSFM with only EGF supplement for 4 hours. Cells were then transfected with 400 ng Firefly luciferase reporter plasmid, 25 ng pHRL-null Renilla luciferase control plasmid and 1.275 µl ("3:1" ratio) XTremeGene9 transfection reagent (Roche) in 50 µl OPTI-MEM (Gibco). Luciferase reporters include PSA-Luc (Perez-Stable et al., 2000) and 3xHRE3-Luc (Steinkamp et al., 2009). The following day, cells were stimulated with 1-10 nM R1881 or methanol vehicle for 24 hours. Cells were gently shaken for 30 minutes in 250 µl 1x passive lysis buffer (Promega), and 10 µl per well was read on a Turner Biosystems Veritas Luminometer using Dual-Luciferase Reporter Assay reagents (Promega). Luciferase activity per sample was expressed as the ratio of Firefly luciferase counts (reporter) to Renilla .luciferase counts (control) in each well. Mean and SEM were plotted.

RWPE-ETS-AR androgen stimulation and endogenous gene expression

50,000 cells per well were seeded into 12-well plates in complete growth medium. The following day, medium was changed to KSFM with EGF supplement only for 48 hours. Cells were then stimulated with 1-10 nM R1881 or methanol vehicle for 24 hours. RNA was harvested by lysing the cells in TRIzol reagent (Invitrogen) and purifying RNA according to the standard TRIzol protocol.

siRNA knockdown of ETV1 followed by androgen stimulation

10 cm dishes (for chromatin) or 6-well plates (for RNA) were pre-coated with poly-L-lysine (Sigma) to enhance cell adherence. LNCaP cells were counted on a hemacytometer and 250,000 cells were seeded per well, or scaled up to 1,375,000 cells per 10 cm dish. After 48

hours the cells were transfected with 5 nM ETV1 siRNA (ETV1 ON-TARGET siRNA SmartPool, Dharmacon # L-003801-00-0005) or non-targeting siRNA (Non-Targeting Control siRNA #1, Dharmacon # D-001801-01-05) suspended in OPTI-MEM with DharmaFect 3 transfection reagent (Dharmacon # T-2003-03) according to the manufacturer's protocol. 24 hours later, medium was changed to RPMI 1640 with 10% charcoal-stripped Nu-Serum (Corning) to starve cells of hormones for 48 hours. Cells were then treated with 1 nM or 10 nM DHT for 4 hours or 1nM R1881 for 2 hours (for chromatin) or 16 hours (for RNA). Chromatin was harvested as described above. RNA was harvested by lysing the cells in TRIzol reagent (Invitrogen) and purifying RNA according to the standard TRIzol protocol.

For MDA-PCa-2b cells the protocol for siRNA transfection and androgen stimulation was essentially identical to that described above for LNCaP. However, cells were starved for only 24 hours in F12K medium containing 10% CSNS and all supplements except hydrocortisone.

PI3K pathway inhibition

The PI3K/mTOR inhibitor NVP-BEZ235 was obtained from Cayman Chemical Company (# 10565). LNCaP cells were seeded and transfected with siETV1 as described above. During DHT stimulation, cells were co-treated with 500 nM BEZ235 or DMSO vehicle and harvested the following day as described above.

AKT siRNA (siAKT) (Cell Signaling # 6211) was used to knock down AKT *in vitro*. LNCaP cells were seeded and hormone-stimulated as described above, and 5 nM siAKT was co-transfected with siETV1 or siScr.

Chromatin immunoprecipitation (ChIP)

  To crosslink DNA and proteins, formaldehyde was added directly to the cell culture medium to a concentration of 2% and dishes were gently shaken 30 minutes at room temperature. Crosslinking was stopped by the addition of glycine to a final concentration of 0.125 M and 5 minutes of additional shaking. Cells were rinsed twice with cold PBS, then scraped and collected twice in 3 ml cold PBS. Cells were pelleted for 4 minutes at 2,000 rpm at 4°C in a benchtop centrifuge. Pellets were resuspended in 400 ul hypotonic buffer (25 mM HEPES, 5 mM KCl, 0.5 mM $MgCl_2$, 1 mM DTT, 0.5% NP-40) with 1x Halt Protease Inhibitor cocktail (Pierce), rotated 15 minutes at 4°C and pelleted for 1 minute at 2,500 rpm at 4°C. Pelleted nuclei were resuspended in 400 μl SDS lysis buffer (1% SDS, 10 mM EDTA pH 8.0, 50 mM Tris-Cl pH 8.0) with 1x protease inhibitors and incubated on ice ≥ 10 minutes. Chromatin was sheared to 200-1,000 bp by sonication on a Branson Sonifier Cell Disruptor 185. Each sonication cycle consisted of a 10 second sonication pulse at power setting 5, followed by at least 60 seconds on ice. LNCaP cells were sonicated for 8 cycles. Cell debris was pelleted for 10 minutes at maximum speed in a microcentrifuge at 4°C and discarded. The concentration of chromatin was determined on a NanoDrop spectrophotometer.

  Protein A agarose beads (Invitrogen) were washed twice in RIPA buffer and resuspended in RIPA buffer with 1x protease inhibitors, along with 37.5 ng/μl salmon sperm DNA and 50 ng/μl BSA to block non-specific binding of DNA and proteins. For each IP, 10-25 μg chromatin was first diluted into 500 μl RIPA buffer with 1x protease inhibitors. Chromatin was pre-cleared by adding 60 μl washed/blocked protein A agarose beads and rotating 1 hour at 4°C. Beads were pelleted by spinning 2 minutes at maximum speed at 4°C and discarded, and cleared chromatin was transferred to a new tube. 2-5 μg antibody was added to each tube, and tubes were rotated

overnight at 4°C. For each sample, an "Input" tube was pre-cleared and rotated overnight with no antibody added. The antibodies used for ChIP include: AR (Abcam # ab74272, 5 μg), AR (Santa Cruz # sc-816, 5 μg), RNA PolII (Active Motif # 39097, 2 μg), ETV1 (Abcam # 81086, 2 μg) and IgG control (Santa Cruz # sc-2027, 2 μg).

Antibody/chromatin complexes were precipitated by adding 30 μl washed/blocked protein A agarose beads to each tube (except Inputs) and rotating overnight at 4°C. Beads were pelleted 2 minutes at 3,000 RPM at 4°C and the supernatant was discarded. The beads were washed with 1 ml each of: low salt immune complex wash buffer (0.1% SDS, 1% Triton X-100, 2 mM EDTA, 20 mM Tris-HCl pH 8.0, 150 mM NaCl), high salt immune complex wash buffer (0.1% SDS, 1% Triton X-100, 2 mM EDTA, 20 mM Tris-HCl pH 8.0, 500 mM NaCl), LiCl immune complex wash buffer (0.25 M LiCl, 1% NP-40, 1% deoxycholate, 1 mM EDTA, 10 mM Tris-HCl pH 8.0), and twice with TE buffer, rotating for 5 minutes at 4°C for each wash. After each wash, beads were pelleted as above and the supernatant discarded. Chromatin was then eluted from the beads twice by rotating 15 minutes in 250 μl ChIP elution buffer (1% SDS, 0.1 M NaHCO$_3$, freshly mixed). In each elution beads were pelleted as above and eluates combined in a new tube. NaCl was added to the eluates to a concentration of 0.2 M and samples were incubated between 4 hours and overnight to reverse crosslinks. 20 μg proteinase K, EDTA pH 8.0 to 10 mM and Tris-HCl pH 6.5 to 20 mM were added, and the samples were incubated 1 hour at 45°C. ChIP DNA was then purified with a QiaQuick PCR Purification Kit (Qiagen). 2-4 μl ChIP DNA was used per qPCR reaction.

cDNA reverse transcription

RNA was quantified on a NanoDrop or Pharmacia Biotech GeneQuant II spectrophotometer, and 1 μg total RNA was used as input for the reverse-transcription reaction. If any samples were too dilute to reach 1 μg within the standard reaction volume, input RNA for all samples in the experiment was scaled down to the maximum allowed by the most dilute sample. cDNA was synthesized with the High Capacity cDNA Reverse Transcription kit with RNase inhibitor (Applied Biosystems) according to the manufacturer's recommendations. cDNA products were diluted 1:20, and 2 μl diluted cDNA was used per subsequent PCR well.

Quantitative PCR

Quantitative PCR (qPCR) was performed on an AB7500 thermal cycler (Applied Biosystems) using ABsolute Blue qPCR SYBR Green Rox mix (Thermo Scientific) according to the manufacturer's instructions, with reactions scaled down to 20 μl. The optional melt curve was used to ensure a single, consistent melting temperature (T_m) among all samples for each primer pair. Samples with low T_m (indicating predominantly primer-primer PCR products), or samples with multiple or divergent T_m (indicating non-specific amplification) were repeated.

Relative gene expression was calculated using the 2^{-ddCt} method. Briefly, dC_t was obtained by normalizing each biological sample's threshold cycle (C_t) value for each gene of interest to a housekeeping gene that was amplified on the same plate (*ACTB* or *GAPDH*). Then ddC_t values were obtained by normalizing to the reference sample or group dCt. The 2^{-ddCt} transformation gave expression of each sample relative to the reference. Mean expression and standard error (SEM) were then calculated and plotted for experimental replicates.

ChIP enrichment was calculated as "% Input" in a manner analogous to the 2^{-ddCt} method used for expression. However, for each sample and target sequence, the C_t value for each antibody was first subtracted from the C_t of the Input for that sample. The "2^{dCt}" transformation gave enrichment of each antibody relative to the Input, and this value was converted to a percentage to plot as "% input". As with expression, mean and SEM were calculated for experimental replicates. All primer sequences are listed in Table 3.2.

Table 3.1: Human prostate cell line characteristics

Cell Line	Source	AR	PTEN	ETS
RWPE-1	normal prostate epithelium (immortalized)	null	+	moderate ETV1 expression (fusion-negative)
MDA-PCa-2b	PCa (bone metastasis)	L701H;T877A	+	ETV1 overexpression (gene fusion)
LNCaP	PCa (lymph node metastasis)	T877A	-	ETV1 overexpression (locus insertion)

Table 3.2: Real-time PCR primer sequences
(all sequences 5'-3')

<ins>qRT-PCR</ins>

ACTB F	CAAAGACCTGTACGCCAACA
ACTB R	TCAGGAGGAGCAATGATC
AQP3 F	TTGGCTTTGCTGTCACTCTG
AQP3 R	GTAGATGGGCAGCTTGATCC
AR F	CAGTGGATGGGCTGAAAAAT
AR R	GGAGCTTGGTGAGCTGGTAG
ERG F	CGCAGAGTTATCGTGCCAGCAGAT
ERG R	CCATATTCTTTCACCGCCCACTCC
ETV1 F	CTACCCCATGGACCACAGATTT
ETV1 R	CTTAAAGCCTTGTGGTGGGAAG
FKBP5 F	CGCAGGATATACGCCAACAT
FKBP5 R	CTTGCCCATTGCTTTATTGG
GAPDH F	TGCACCACCAACTGCTTAGC
GAPDH R	GGCATGGACTGTGGTCATGAG
KLK3 F	CACCTGCTCGGGTGATTCTG
KLK3 R	CCACTTCCGGTAATGCACCA
MME F	CCGAACCTACAAGGAGTCCA
MME R	GCAAATGCTGCTTCCACATA
NKX3-1 F	GAGACGCTGGCAGAGACC
NKX3-1 R	CGCCTGAAGTGTTTTCAGAG
NT5E F	CTGGGAGCTTACGATTTTGC
NT5E R	GCTGAACCTTGGTGAAGAGC
TMPRSS2 (eRNA) F	GAAAGGAATGGGGGTTTGAGG
TMPRSS2 (eRNA) R	TGCCTGGAAGACGTGGTTTTT
TMPRSS2 (mRNA) F	TACTCTGGAAGTTCATGGGC
TMPRSS2 (mRNA) R	GTCATCCACTATTCCTTGGCT

<ins>ChIP</ins>

KLK3 (enhancer) F	GCCTGGATCTGAGAGAGATATCATC
KLK3 (enhancer) R	ACACCTTTTTTTTTCTGGATTGTTG
TMPRSS2 (enhancer) F	TGGAGCTAGTGCTGCATGTC
TMPRSS2 (enhancer) R	CTGCCTTGCTGTGTGAAAAA
GAPDH (TSS) F	TACTAGCGGTTTTACGGGCG
GAPDH (TSS) R	TCGAACAGGAGGAGCAGAGAGCGA
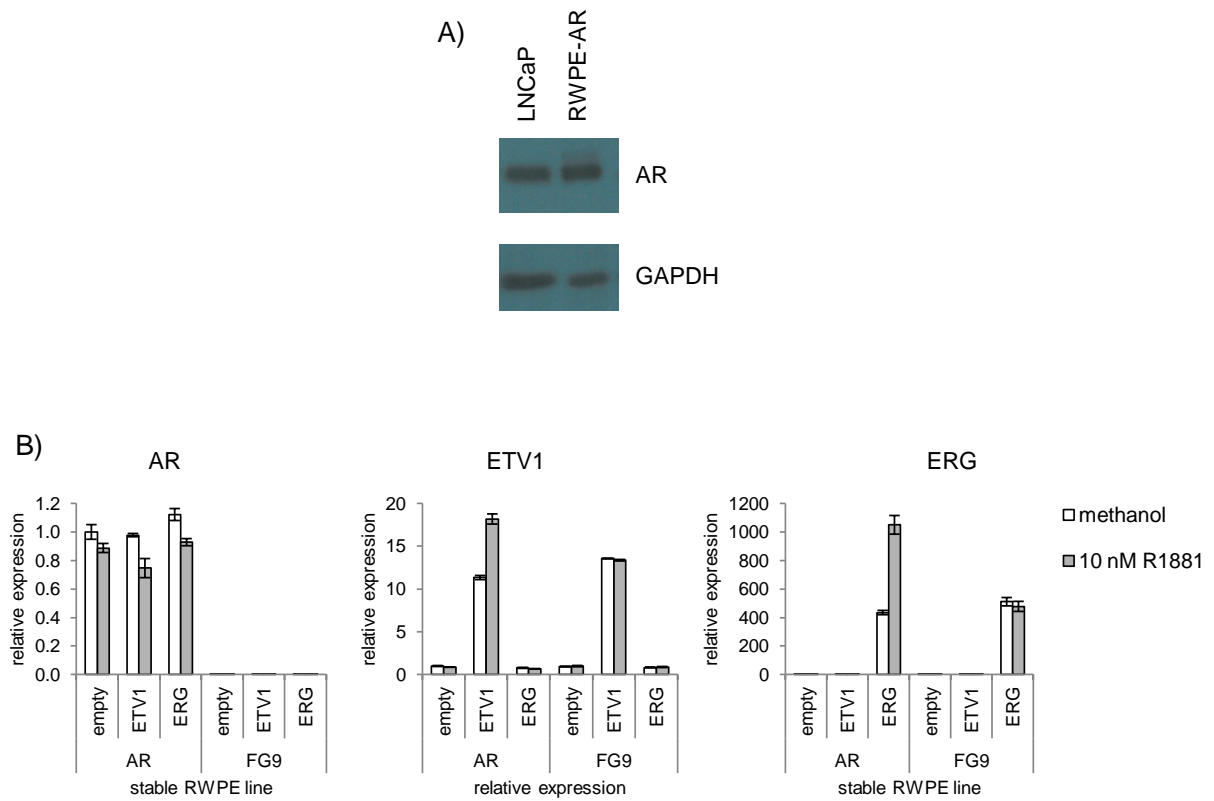
Figure 3.1: Stable AR, ETV1 and ERG expression in RWPE-1 cells

Benign RWPE-1 prostate cells were transduced with lentiviral constructs to stably express AR, or with empty vector (FG9), and then with additional lentiviral vectors expressing ETV1, ERG or empty vector. A) A Western blot shows AR protein levels in stable RWPE-AR cells compared to endogenous AR in LNCaP cells, with similar amounts of protein loaded. B) qRT-PCR shows robust, specific expression of *AR*, *ETV1* or *ERG*, with no expression in the empty vector-transduced controls. Expression was normalized to *ACTB*, with mean and SEM plotted for biological triplicate samples. Grey bars represent androgen-induced expression and white bars represent vehicle control.
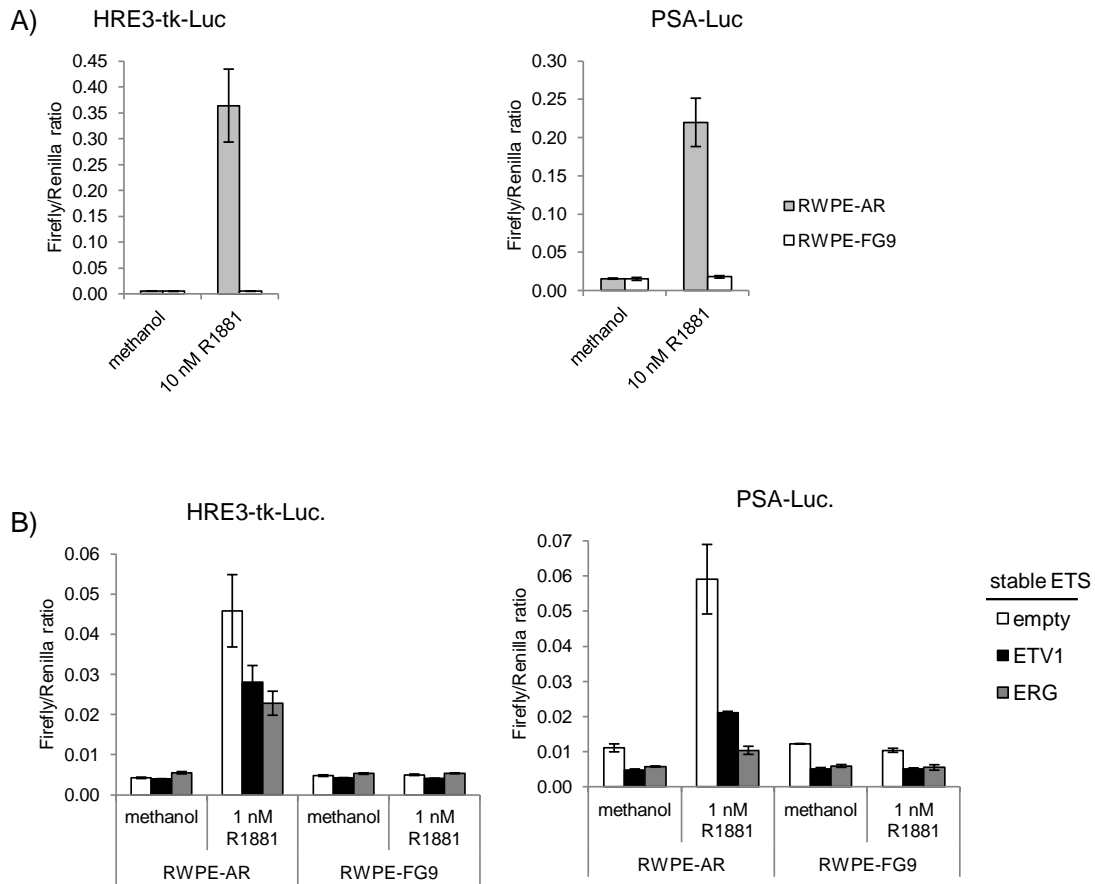
Figure 3.2: ETV1 and ERG inhibit AR activation of luciferase reporters in RWPE-1 cells

Luciferase reporters driven by hormone response elements were transfected into stable RWPE-AR cells to verify AR function. A) Both HRE3-tk-Luc and PSA-Luc are activated by R1881 stimulation in RWPE-AR cells, but not in the RWPE-FG9 empty vector control. B) Stable overexpression of ETV1 or ERG inhibits R1881 induction of both luciferase reporters, as well as baseline activity of PSA-Luc. Data are plotted as the ratio of AR-responsive Firefly luciferase activity to activity of the co-transfected Renilla luciferase reporter. Mean and SEM are plotted for biological triplicate samples. White, black and grey bars represent stable empty vector control, ETV1 or ERG expression, respectively.
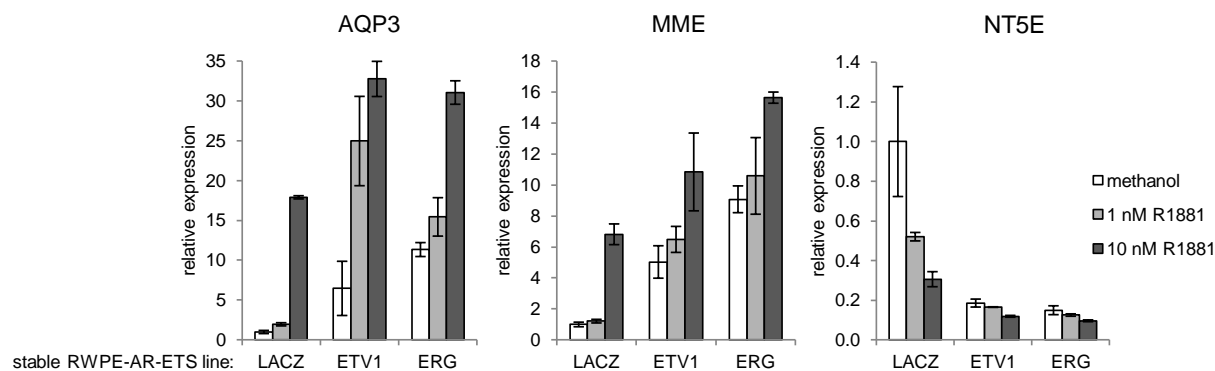
Figure 3.3: ETV1 and ERG enhance AR regulation of endogenous targets in RWPE-1 cells

To ask how ETS overexpression affects AR activity at endogenous targets in benign prostate cells, stable RWPE-AR-ETV1, RWPE-AR-ERG and RWPE-AR-LACZ control cells were stimulated with 1 or 10 nM R1881 (light or dark grey bars, respectively) or methanol vehicle (white bars). Expression of the androgen-induced genes *AQP3* and *MME* and the AR-repressed gene *NT5E* was measured by qRT-PCR. Expression was normalized to *ACTB,* with mean and SEM plotted for biological triplicate samples. Both ETV1 and ERG enhanced androgen induction or repression, as well as baseline induction or repression, of the target genes.
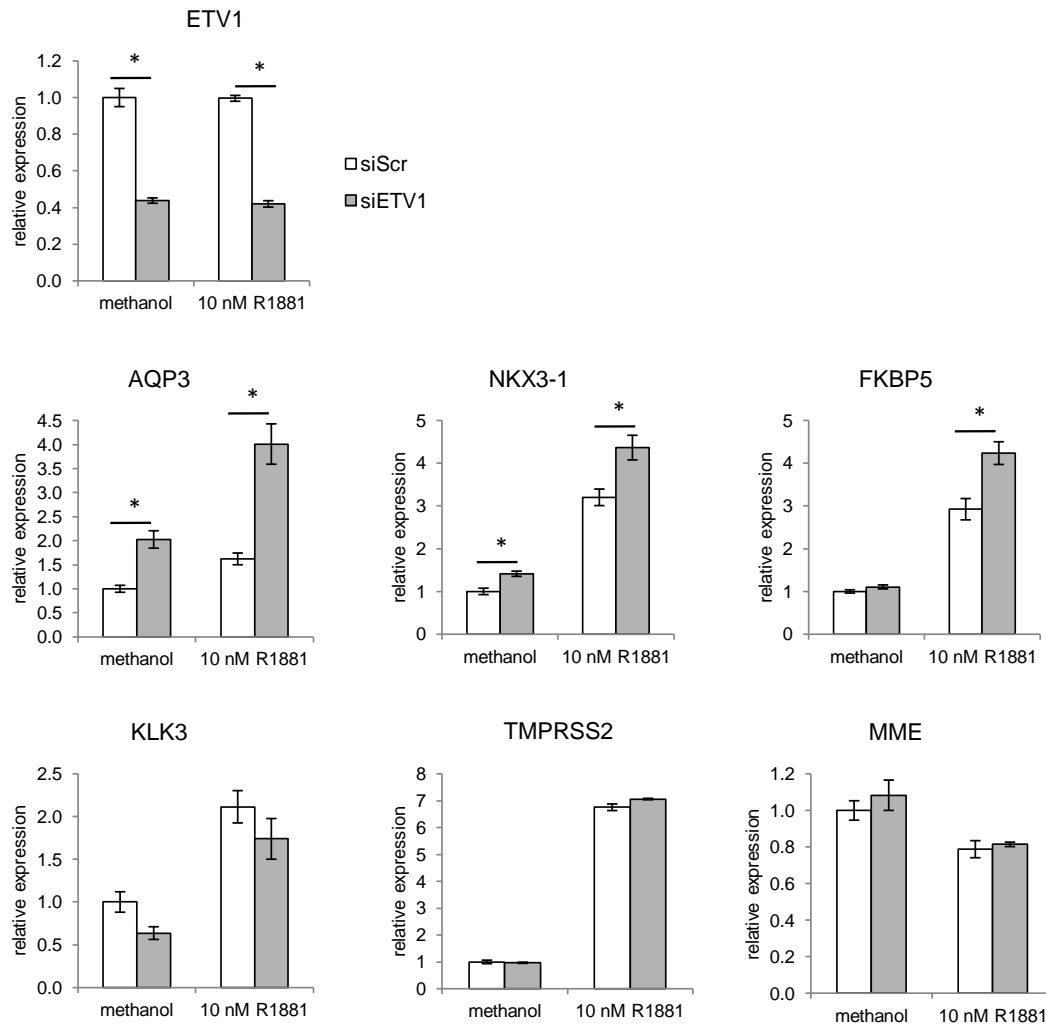
Figure 3.4: ETV1 antagonizes AR at a subset of targets in MDA-PCa-2b cells

To address ETV1 effects on AR activity in PCa cells, MDA-PCa-2b cells were transfected with siETV1 or siScr and stimulated with 10 nM R1881 or methanol vehicle. ETV1 knockdown was quantified with qRT-PCR. Expression of the AR target genes *AQP3*, *NKX3-1*, *FKBP5*, *KLK3, TMPRSS2* and *MME* was quantified with qRT-PCR as well. Expression was normalized to *GAPDH*, with mean and SEM plotted for biological triplicate samples. ETV1 knockdown increased androgen induction of *AQP3*, *NKX3-1* and *FKBP5*, with a trend toward decreased hormone-independent expression of *KLK3* and no effect on *TMPRSS2* or *MME*.
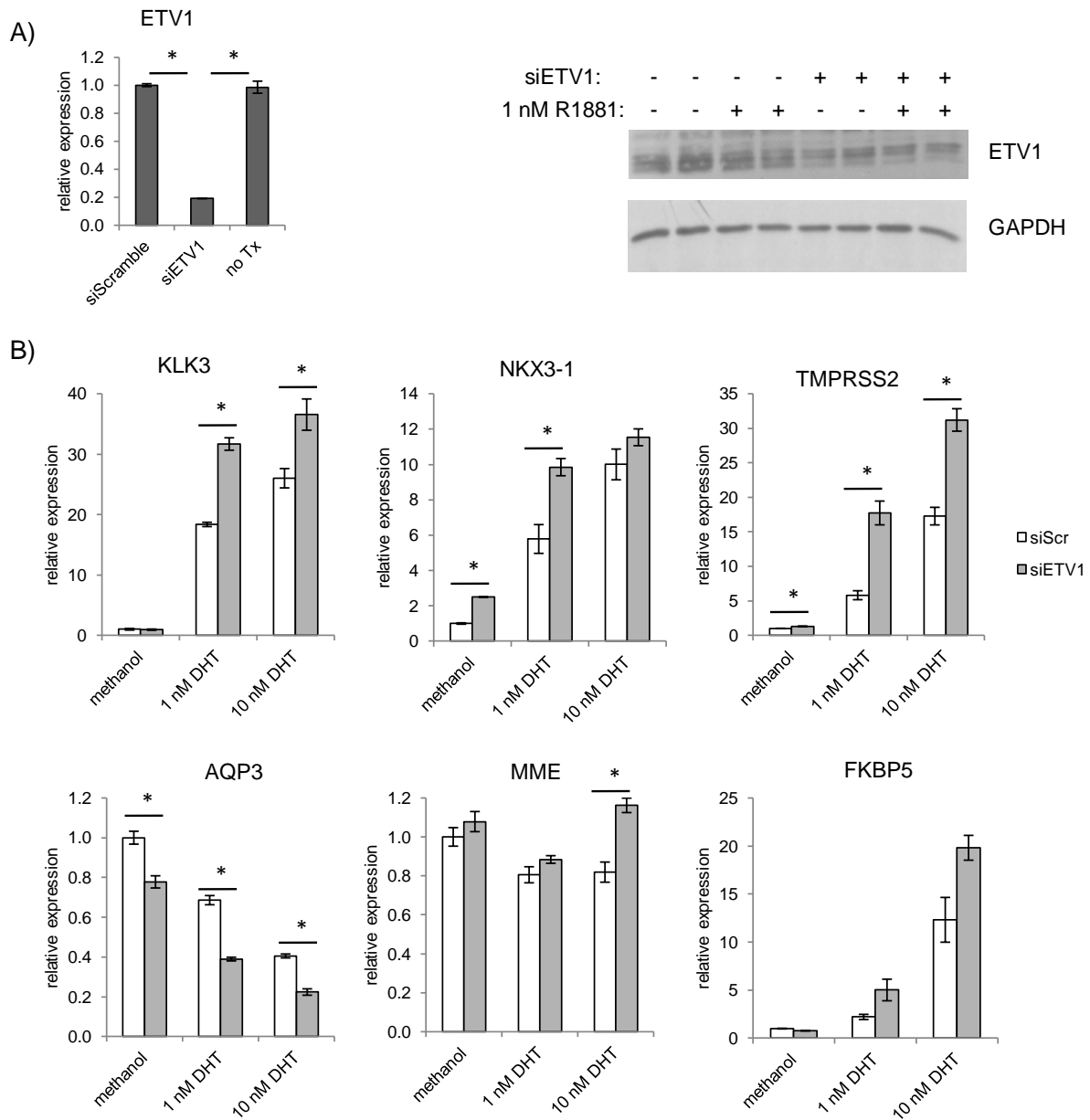
Figure 3.5: ETV1 antagonizes AR in LNCaP cells

The effect of ETV1 knockdown on AR target gene expression was assessed in LNCaP cells. A) *ETV1* transcript expression in LNCaP cells was measured by qRT-PCR in cells transfected with siScr or siETV1, and in untransfected cells. An ETV1 antibody was used to measure protein levels, with GAPDH as a loading control. B) LNCaP cells were transfected with siETV1 or siScr and stimulated with 1 or 10 nM DHT or methanol vehicle. Expression of the AR target genes *KLK3*, *TMPRSS2*, *AQP3*, *NKX3-1* and *MME* was quantified by qRT-PCR. In all qRT-PCR, expression was normalized to *ACTB*. Mean and SEM are plotted for biological triplicate samples. ETV1 knockdown increases induction or repression of AR targets, suggesting ETV1 inhibition of AR activity.
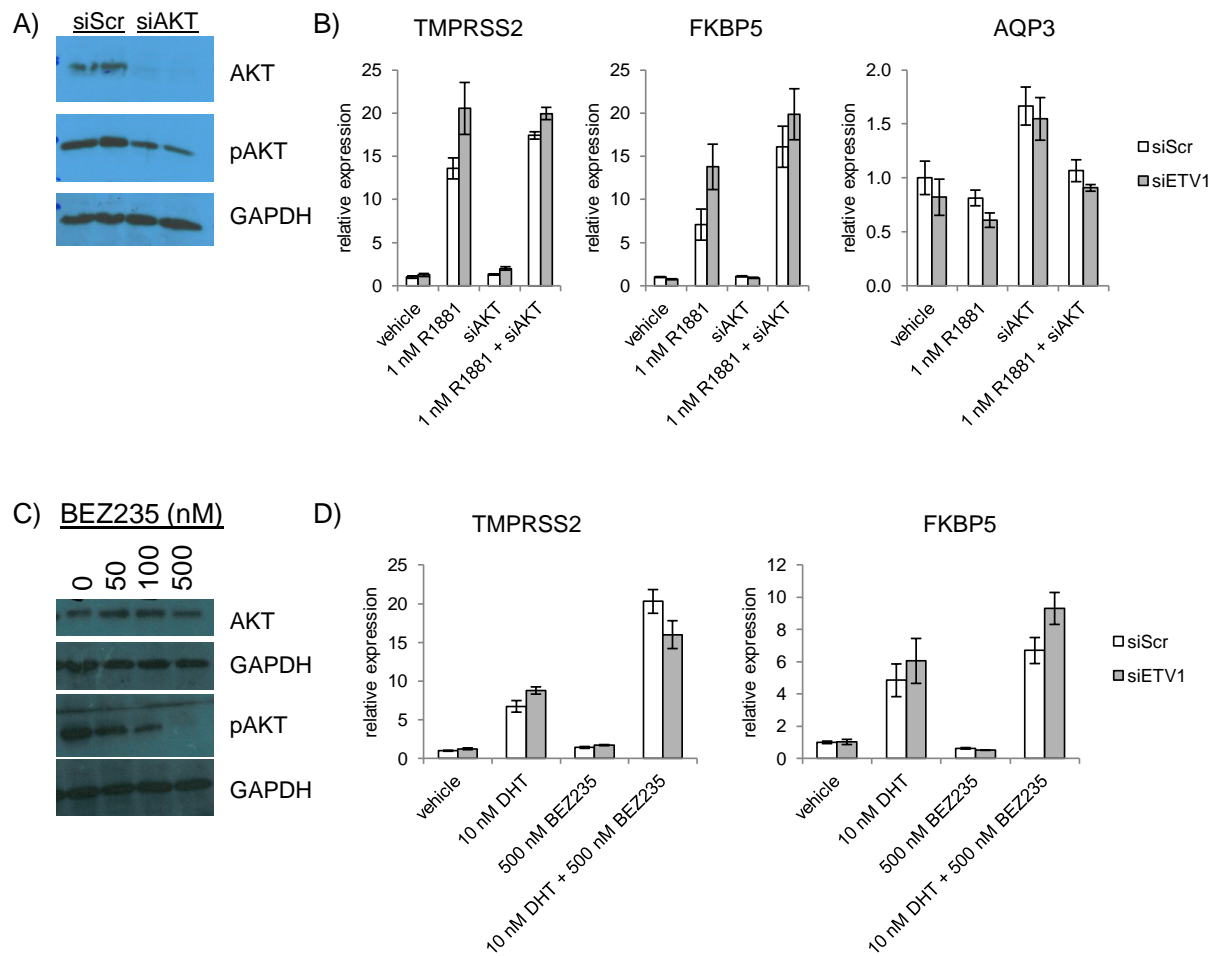
Figure 3.6: AKT and PI3K signaling do not alter the ETV1-AR interaction in LNCaP cells

To ask whether ETV1 repression of AR was affected by the PTEN signaling pathway, AKT or PI3K were inhibited as a proxy for restoring PTEN function. A) Effective AKT knockdown by siRNA (siAKT) was validated by Western blot for total AKT and pAKT in duplicate samples. B) siAKT and/or siETV1 were transfected vs. siScr, and cells were treated with 1 nM R1881 or vehicle. The AR target genes *TMPRSS2*, *FKBP5* and *AQP3* were tested by qRT-PCR. Mean and SEM are plotted for biological triplicate samples. C) Dose-dependent inhibition of pAKT, but not total AKT, by BEZ235 is verified by Western blot. D) Cells were transfected with siETV1 or siScr and treated with 10 nM DHT and/or 500 nM BEZ235. Expression of the AR target genes *TMPRSS2* and *FKBP5* was tested by qRT-PCR. Mean and SEM are plotted for biological triplicate samples. In BEZ235-treated cells, ETV1 knockdown reduces DHT induction of *TMPRSS2* vs. siScr. Otherwise, the effects of ETV1 knockdown or PI3K/pAKT inhibition appear independent or additive.

A)

chr21:

41,805,000

41,810,000

41,815,000

AR_LNCaP-ethanol_Yu_2010

AR_LNCaP-R1881_Yu_2010

AR_LNCaP-shETV1_2_Chen_2013

AR_LNCaP-shScr_Chen_2013

ETV1_LNCaP_Baena_2013

ETV1_LNCaP_Chen_2013

ETV1_RWPE_Hollenhorst_2011

RefSeq Genes

TMPRSS2

TMPRSS2

B)

TMPRSS2 (enhancer)

PSA (enhancer)

C)

TMPRSS2 (enhancer)

TMPRSS2 (enhancer)

GAPDH (TSS)

GAPDH (TSS)

D)

TMPRSS2 (mRNA)

TMPRSS2 (eRNA)

114
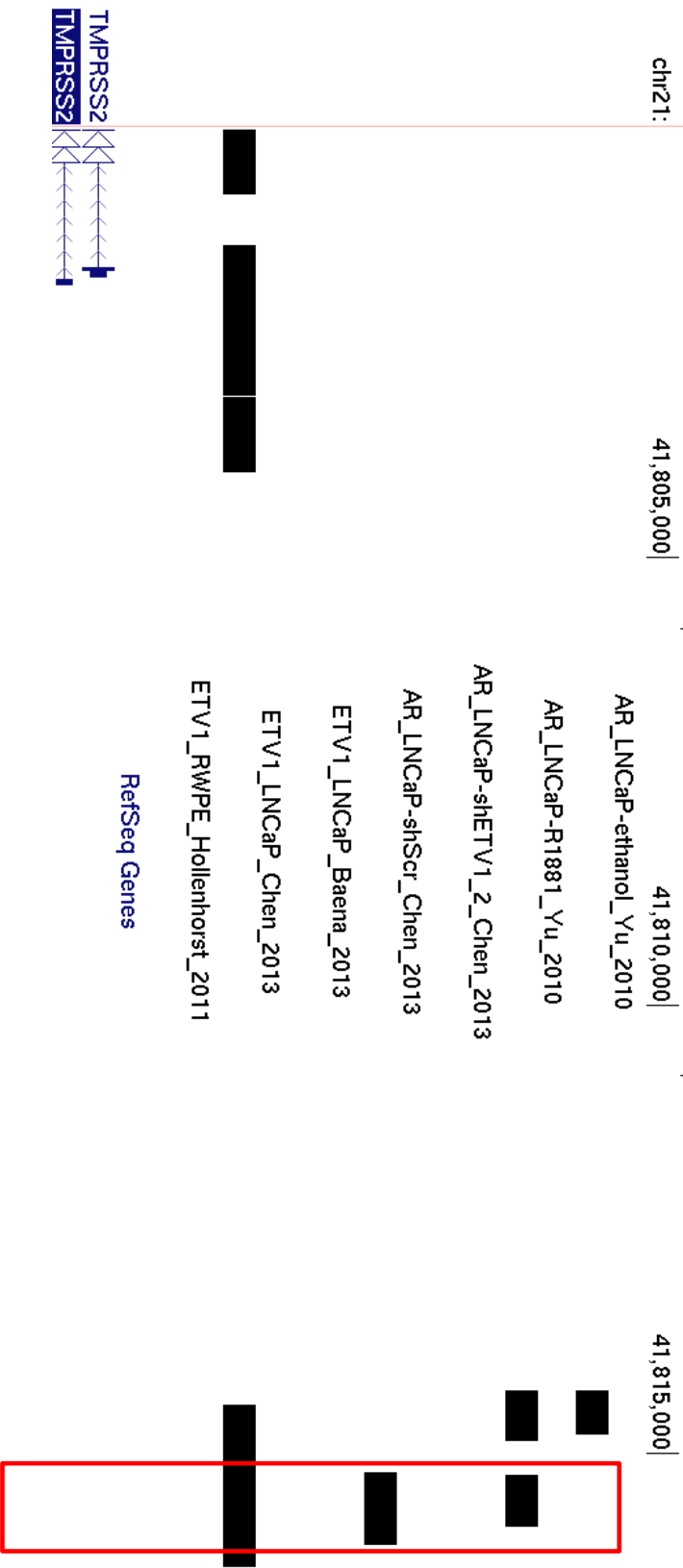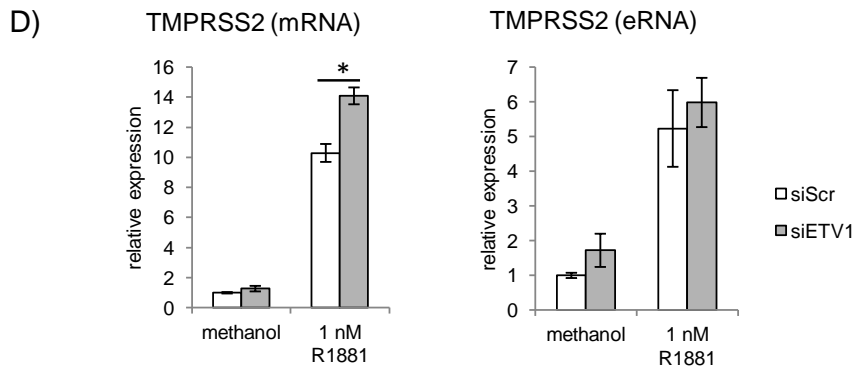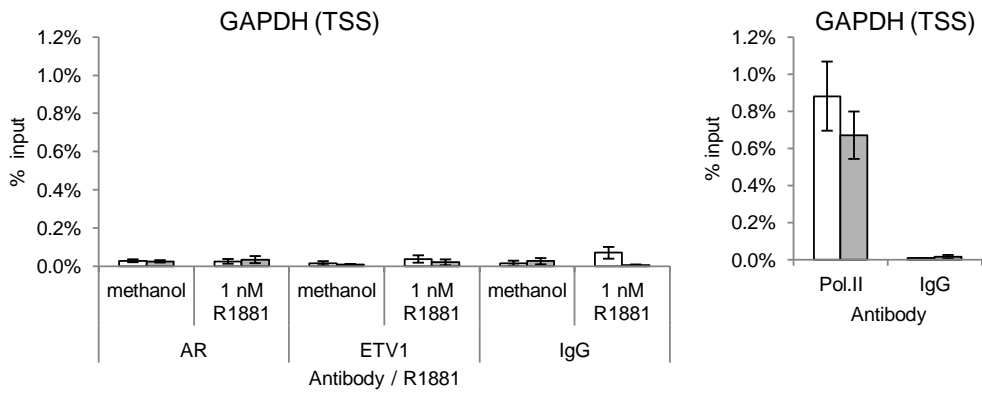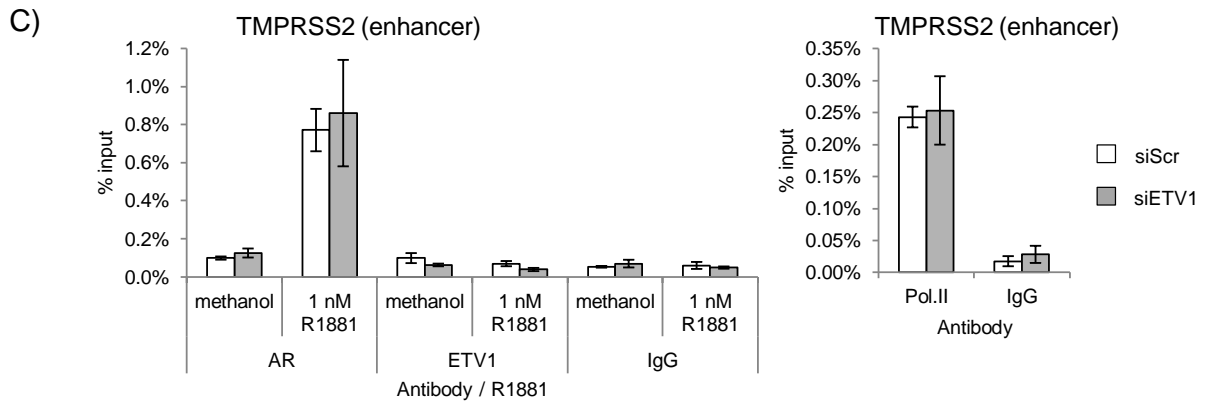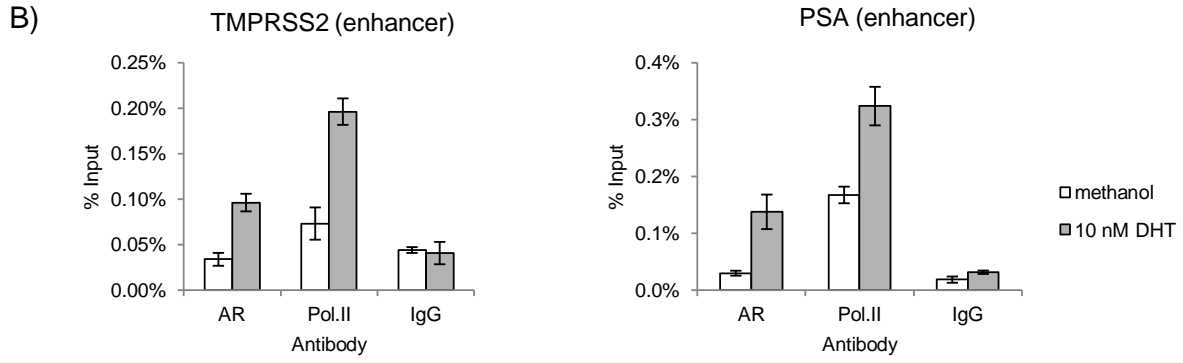
Figure 3.7: ETV1 does not alter AR genomic binding or eRNA expression at *TMPRSS2* in LNCaP cells

       The effect of ETV1 on AR and PolII genomic binding was tested by ChIP. A) A screenshot from the UCSC Genome Browser shows AR and ETV1 ChIP-seq peaks as custom tracks. Overlapping ETV1 and AR binding sites in the *TMPRSS2* -13 kb enhancer, where the qPCR primers were targeted, are highlighted in the red box. B) LNCaP cells transfected with siScr were stimulated with 10 nM DHT or methanol vehicle to confirm androgen induction. Chromatin was immunoprecipitated with antibodies to AR or PolII, or with IgG control. qPCR determined enrichment of immunoprecipitated DNA at the *TMPRSS2* and PSA (*KLK3*) enhancers relative to the Input. C) As in B, but cells were transfected with siETV1 or siScr and stimulated with 1 nM R1881. Chromatin was immunoprecipitated with antibodies to AR, PolII or ETV1, or with IgG control. qPCR determined enrichment of immunoprecipitated DNA at the *TMPRSS2* enhancer and *GAPDH* TSS relative to the Input. D) qRT-PCR quantified relative expression of the *TMPRSS2* gene and eRNA transcripts. Expression was normalized to *ACTB*. For all plots, mean and SEM are shown for biological triplicate samples. Neither binding of AR or RNA PolII, nor eRNA expression, is significantly affected by ETV1 knockdown.

Chapter 4

Conclusion

This thesis has used *in vivo* and *in vitro* models to examine the context-dependent interactions of prominent signaling pathways in PCa: AR signaling (genetic variation), ETS gene fusions (oncogene activation) and PTEN (tumor suppressor loss). In mice, the interaction of strong or weak *AR* alleles with oncogenic ETV1 was examined alone or in the context of reduced expression of *Pten*, modeling disease course in humans (Figure 1.2). A similar progression was modeled *in vitro*, first examining interactions in benign human prostate cells, then in ETV1$^+$ PCa cells with or without functional PTEN. Our results suggest that the prognostic value of ETS rearrangements or other potential biomarkers may be improved by considering the impact of multiple key signaling pathways together. Furthermore, comparison of mouse tumors with patient expression data suggests novel roles in PCa of genes associated with other cancers, as well as potential ETV1 regulation of known PCa genes.

Varying AR strength via Q-tract length does not significantly affect the early neoplasia phenotype induced by prostatic ETV1 overexpression in mice. In fact, the overall rate of PIN was lower than expected based on a previous study with the same founder *ETV1^{Tg}* mice (Tomlins et al., 2007). It is possible that *hAR* partially suppresses the ETV1-induced neoplasia, or perhaps the mixed C57BL/6-FVB transgenic offspring here were protected relative to the original inbred

116

FVB transgenics. In any case, ETV1 strongly antagonizes AR transcriptional activity in benign and early neoplastic prostate tissue. Direct AR targets such as *Tmprss2* and *Nkx3-1* are significantly repressed by ETV1, as are the tumor suppressor *Pten* and other prostate differentiation genes. Despite this strong AR antagonism, prostates of the *ETV1^{Tg}* mice appear grossly normal, while total androgen ablation by castration causes substantial regression of the prostate. These results suggest that selective AR antagonism by ETV1, along with a broader deprogramming of prostate differentiation genes, can favor proliferation and early neoplasia in epithelial cells rather than apoptosis and atrophy.

On the *Pten$^{+/-}$* background, the striking ETV1 antagonism of AR is largely abrogated and fewer genes are differentially expressed in prostates of *ETV1^{Tg}* mice overall. This may be due to greater variance among biological replicate RNA pools than in the first series of mice, perhaps reflecting heterogeneity and stochastic variation between individuals, especially as disease initiated. There is a general repression of the AR expression program associated with PTEN reduction, suggesting that factors downstream of PTEN affect the ETV1-AR interaction as well as overall AR activity. A set of 15 genes are significantly upregulated in prostates of *ETV1^{Tg}* mice on both backgrounds, suggesting a core set of ETV1-targeted genes. Progression to adenocarcinoma occurs in *ETV1^{Tg};Pten$^{+/-}$* mice, signifying that the concurrent oncogene activation and tumor suppressor loss cooperate in tumorigenesis. Because human patients frequently harbor both lesions, clinical studies should determine whether the specific combination of ETV1 fusion and PTEN loss is associated with worse prognosis than either single alteration. Significant repression of AR-induced genes occurs in the tumors of these mice, suggesting that selective AR antagonism by ETV1 is important in early as well as later stages of oncogenesis, with repression by PTEN perhaps playing a greater role in intermediate stages.

Additional insights into the relevance of expression changes in $ETV1^{Tg}$ mice to human PCa can be attained via the cBioPortal database (www.cbioportal.org). cBioPortal facilitates analysis of expression, copy number and mutation data from studies across a variety of cancers, including provisional data from The Cancer Genome Atlas (TCGA) (Cerami et al., 2012; Gao et al., 2013). Gene sets or individual genes can be queried against the database. *KCNN4*, *SOX4*, *HPN* and *PSCA*, which are upregulated in $ETV1^{Tg}$ mice (Figures 2.7, 2.9), show consistent amplification or overexpression across several PCa data sets, including TCGA, as well as across a variety of tumor types (Baca et al., 2013; Barbieri et al., 2012; Grasso et al., 2012; Hieronymus et al., 2014; Taylor et al., 2010). This suggests that while ETV1 may promote expression of these factors, at least in mouse prostate, they may be more generally associated with PCa and other cancers as well. *LRP8* (Figure 2.9) shows substantial upregulation in one PCa data set (Taylor et al., 2010), but a comparable rate of deletion/underexpression vs. amplification/overexpression in the provisional TCGA data. This suggests that *LRP8* expression may be more sensitive to ETV1 or other factors, or could potentially have tumor suppressive function in some contexts. Nearly 500 PCa patient tumors were profiled in TCGA, more than twice the number in the next-largest study in cBioPortal, so perhaps a greater breadth of tumor subtypes was represented in the TCGA data set.

SEMA4G, *REC8* and *SDF2L1* are among the genes downregulated in prostates and tumors of $ETV1^{Tg}$ mice as well as in ETS$^+$ PCa patients, and are downregulated in additional cancers (Figure 2.9). *SEMA4G* and *REC8* show primarily deletion/downregulation in several PCa data sets on cBioPortal (Baca et al., 2013; Grasso et al., 2012; Taylor et al., 2010), yet substantial amplification/upregulation in TCGA. *SDF2L1* shows consistent amplification/upregulation in multiple PCa data sets as well as across several cancer types. This

suggests that, as with the ETV1-induced genes, perhaps the expression patterns of *SEMA4G* and *REC8* are more broadly represented in the large TCGA set, yet there are distinct PCa subtypes where downregulation plays a greater role. Furthermore, perhaps *SDF2L1* repression in PCa is exquisitely restricted to ETS$^+$ tumors. It was identified as such in the Taylor et al. data set (Figure 2.9) (Taylor et al., 2010), yet the same study shows an overall upregulation of *SDF2L1* in PCa vs. normal tissue. Functional analysis of these genes in ETS$^+$ vs. ETS$^-$ PCa cells, or stratification of additional patient data sets by ETS and PTEN status, may be able to shed light on these apparent discrepancies.

Baena, et al. reported that concurrent ETV1 overexpression was insufficient to promote progression to adenocarcinoma in *Pten$^{+/-}$* mice, instead promoting only a higher rate of PIN (Baena et al., 2013). However, in our *hAR;ETV1^{Tg};Pten$^{+/-}$* mice we observed progression to adenocarcinoma which was more frequent in *hAR^{12Q}*, including among castrated mice. This finding again highlights the interaction between the androgen axis, oncogene activation and tumor suppressor loss in mice. In the *hAR;TRAMP* study, prostate oncogenesis in the *hAR^{21Q}* mice was most similar to that in the *mAr* controls, with *hAR^{12Q}* and *hAR^{48Q}* showing the most divergent progression (Albertelli et al., 2008). Here, it is possible that a lifetime of increased androgen signaling in the *hAR^{12Q}* mice predisposed them to tumorigenesis following oncogene activation (ETV1) combined with tumor suppressor loss (PTEN). Alternatively, given that AR and ETV1 can physically interact (Shin et al., 2009), acute dysregulation of shared target genes may promote greater oncogenesis with *hAR^{12Q}* in the *Pten*-hemizygous background.

In vitro, antagonism of AR by ETV1 is observed in benign and malignant cell lines. This includes significant repression of the tumor suppressor gene *NKX3-1* in MDA-PCa-2b as well as LNCaP cells, similar to the repression seen in *hAR;ETV1^{Tg}* mice and DLP tumors. ETV1 also

significantly represses androgen induction of *FKBP5* in MDA-PCa-2b cells, with the same trend in LNCaP. Decreased FKBP5 would be predicted to increase oncogenic PI3K/AKT activity even with intact PTEN signaling (Mulholland et al., 2011). Except for very focal reduction, the *Pten*$^{+/-}$ mice in this study retain PTEN protein expression even in tumors, yet also show intense pAKT staining. It is possible that reduction of FKBP5 by ETV1 contributes to the increase in pAKT levels. The MDA-PCa-2b and LNCaP cell lines both overexpress ETV1 due to genomic rearrangement, but the former retains PTEN expression while the latter lacks it. While the specific subset of significantly altered AR targets varies slightly between the cell lines, the general pattern of ETV1 antagonism of AR regulation is consistent, including antagonism of AR activated as well as repressed targets. Furthermore, these results suggest that *NKX3-1* and *FKBP5* are core ETV1-repressed targets across *in vivo* and *in vitro* systems.

The fact that we saw consistent ETV1 repression of AR in LNCaP cells proved to take up a substantial amount of time and resources. The initial goal had been to quickly confirm that ETV1 enhanced AR genomic binding and target gene activation (Baena et al., 2013; Chen et al., 2013; Shin et al., 2009), and then move on to experiments involving additional cofactors. Despite knocking down ETV1 in a variety of experimental conditions and with fresh LNCaP cells from ATCC, ETV1 was never observed to enhance AR genomic binding or target gene activation (see Chapter 3 Discussion). These results highlight the problem of reproducibility between labs, even when mirroring experimental samples and protocols as closely as possible.

ETV1 and ERG promote similar physiological outcomes, e.g. invasion *in vitro* and early neoplasia *in vivo* (Hollenhorst et al., 2011a; Tomlins et al., 2007; Tomlins et al., 2008a). However, it has been suggested that they do so through divergent gene expression programs, with ERG repressing AR and ETV1 cooperating with AR (Baena et al., 2013). In this thesis

work, ETV1 repressed key AR target genes in prostates of *ETV1*[Tg] mice as well as in tumors. ETV1 similarly repressed AR at a number of the same targets in LNCaP and MDA-PCa-2b cells, in contrast to reports describing ETV1-AR cooperation in LNCaP (Baena et al., 2013; Shin et al., 2009). ERG represses AR in LNCaP and additional PCa cell lines (Tomlins et al., 2008a; Yu et al., 2010), in line with the behavior observed here for ETV1. In benign prostate cells, both ETV1 and ERG repressed AR-induced luciferase reporters yet enhanced either activation or repression of endogenous AR targets. In a mouse model with ERG overexpression, ERG alone had little effect on AR target genes. However, following prostatic deletion of *Pten*, ERG enhanced expression of a panel of AR targets (Chen et al., 2013). Here, antagonism of AR was observed in prostates of *ETV1*[Tg] mice and in tumors of *ETV1*[Tg]*;Pten*^{+/-} mice, but not pre-tumor prostate tissue of *ETV1*[Tg]*;Pten*^{+/-} mice. However, we did not compare ETV1-negative tumors, and the tumors retained at least partial PTEN protein expression, so direct comparison to results with ERG is difficult (Chen et al., 2013). The emerging picture from this work and other recent studies is that, while by no means identical, molecular actions of ETV1 and ERG may actually be more similar than different. It may largely be the cellular context or disease stage that influences their differential activity, rather than inherently divergent function, including sensitivity to PTEN alterations *in vivo*.

As stated above, overexpression of either ETV1 or ERG repressed AR activation of luciferase reporters in benign prostate cells, as expected. However, both ETV1 and ERG enhanced activation or repression of endogenous AR targets, even in the absence of androgen. RWPE-1 cells lack endogenous AR expression (Altintas et al., 2011). Thus, it is possible that they have developed an aberrant epigenetic signature that prevents AR activation of some canonical target genes while leaving other genes open to activation (or repression) by a wider

variety of transcription factors. AQP3 and MME are expressed in normal tissues, but upregulation is associated with several cancers (Chen et al., 2015; Lee et al., 2015). MME was initially thought to be a tumor suppressor in PCa based on *in vitro* behavior and overall reduced expression in tumors. However, the subset of patients that retained high MME expression had significantly worse survival (Fleischmann et al., 2011; Sumitomo et al., 2005). Similarly, in the Prostate Cancer Prevention Trial finasteride lowered the overall rate of PCa yet increased the proportion of aggressive tumors and provided no net survival benefit (Thompson et al., 2013). It is important to consider molecular subgroups and multiple endpoints when gauging the benefit of therapy or the prognostic value of biomarkers. Here, the inappropriate activation of MME and AQP3 by ETV1 and ERG in benign prostate cells suggests a potential early role in ETS[+] PCa.

It remains an open question as to whether repression of PSA-Luc or HRE3-tk-Luc by ETV1 and ERG in the benign RWPE-1 cells is mediated by inhibition of AR or PolII binding. ChIP was attempted with antibodies to these proteins and with qPCR primers spanning known AREs represented on the PSA-Luc plasmid (Perez-Stable et al., 2000; Shin et al., 2009). Unfortunately, even in hormone-stimulated cells with robust AR activation of the reporter, the ChIP signal was not sufficiently above background to be informative. PolII binding at the GAPDH transcription start site (TSS), which served as a positive control, confirmed that the overall ChIP protocol was successful (data not shown). The PSA-Luc plasmid sequence was robustly detected in the Input samples by qPCR, meaning that the plasmid, which is not incorporated into the chromosomes, was neither being excessively sonicated nor lost in the lysis or wash steps. No-template qPCR reactions showed absence of plasmid contamination. Comparison of raw C_t values among targets in the Inputs revealed that the transfected PSA-Luc plasmid was present in cells at roughly 1000 times the copy number of genomic loci (data not

shown). It is possible that this high copy number could ironically make binding more difficult to detect above background, if a minority of copies were bound by AR. Reducing the quantity of transfected PSA-Luc plasmid in additional experiments could aid detection of AR and PolII binding.

It remains controversial whether ETV1 or ERG fusion status alone is a prognostic indicator of PCa aggressiveness (Rubin et al., 2011; Taris et al., 2014a). However, ERG staining in prostate biopsies is useful in distinguishing HG-PIN and PCa from other histological abnormalities. Our mice provide evidence that ETV1 overexpression alone is insufficient for aggressive disease, yet cooperation with additional somatic alterations can enhance tumorigenesis. Even if ETS$^+$ patients do not have worse prognosis, ETS overexpression is still likely to be driving prostate tumorigenesis. Among possible PCa drivers, ETS fusions need not be significantly worse than other oncogenic pathways to be bona-fide oncogenes. Therefore it is still likely to be worthwhile to stratify PCa patients according to ETS fusion status for targeted management and treatment.

Overall, these experiments highlight the capacity for ETV1 to selectively repress AR signaling *in vivo* as well as in benign and malignant human prostate cells. Consistent ETV1 inhibition of androgen-induced tumor suppressors and prostate differentiation genes was seen in multiple PCa cell lines as well as in mouse prostates and tumors (Higgins et al., 2015). These findings support a model in which ETV1 gene fusions, which occur early in PCa, act by initially antagonizing tumor suppressor gene expression and maintaining cells in a dedifferentiated state, similar to ERG. During disease progression ETV1 cooperates with further tumor suppressor loss as well as the androgen axis to promote oncogenesis.

Future Directions

Resistance to therapy continues to be an issue in PCa, even with newer treatment strategies. Despite recent improvements in survival, novel therapeutic approaches are still needed. This thesis work identified a number of the ETV1-upregulated genes in mice that are associated with PCa or other cancers, and can be targeted with small molecules or antibodies *in vitro* or in mouse models. *KCNN4*, upregulated in BPH and intermediate Gleason grade PCa as well as in *ETV1^{Tg}* mice here, can be targeted with a potassium channel inhibitor (Ohya et al., 2011). *HPN* and *PSCA* are upregulated in *ETV1^{Tg}* mice and overexpressed in human tumors, and have been targeted in model systems as well (Tang et al., 2014; Yu et al., 2013). These targets should be tested in xenografts using PCa cell lines overexpressing ETV1. Additionally, recent reports have described YK-4-279 as a small molecule inhibitor of ETS oncoprotein activity. Initially identified as an inhibitor of the EWS-FLI1 fusion protein in Ewing's sarcoma cells (Rahim et al., 2011), YK-4-279 inhibits ETV1 or ERG-driven invasion *in vitro* along with tumor growth in LNCaP (ETV1^{+}) xenografts (Rahim et al., 2014). For YK-4-279 as well as the previously mentioned compounds, patient-derived tumor xenografts (PDTX) from ETV1^{+} PCa patients would be a valuable next step in screening (Malaney et al., 2014). PDTXs from a panel of patients would provide greater heterogeneity than the handful of fusion-positive PCa cell lines in terms of individual variation, as well as the cellular diversity within a tumor compared to relatively homogeneous cell lines.

While siRNA knockdown consistently showed that ETV1 represses AR transcriptional activity in LNCaP and MDA-PCa-2b cells (Figures 3.4, 3.5, 3.7), neither AR nor PolII genomic binding was significantly affected by ETV1 knockdown in LNCaP (Figure 3.7). A remaining

hypothesis is that recruitment of additional AR cofactors is inhibited by ETV1. Further ChIP

experiments to determine whether binding of SRC1, SRC3 or other AR coactivators is affected

by ETV1 would be informative. Additionally, given that ERG is known to repress AR by

recruitment of the polycomb repressive complex (PRC) and the placement of repressive

H3K27me3 histone marks (Yu et al., 2010), ETV1 may act by a similar mechanism. ChIP for

these proteins and histone marks would reveal whether ETV1 recruits PRC as well. Another

hypothesis is that while PolII binding at the promoter and enhancer is unaffected by ETV1

knockdown, ETV1 may inhibit transcription initiation or elongation. ChIP for the histone

modification H3K36me3, which marks transcriptional elongation (Hon et al., 2009), or for PolII

further into the gene body, would address this possibility.

In some clinical studies, patients positive for the androgen-activated *TMPRSS2-ERG*

gene fusion showed more favorable response to abiraterone acetate or orchiectomy (Attard et al.,

2009; Graff et al., 2015). Both treatments target AR signaling and therefore presumably inhibit

oncogenic ERG expression. However, other studies report no association. In future studies of this

nature, the patient's AR allele may prove informative as a clinical variable that should be

considered. Tumors with a *TMPRSS2-ERG* fusion driven by a stronger AR may be more

exclusively dependent on androgen signaling and therefore may be more sensitive to abiraterone

acetate or other inhibitors. Alternatively, TMPRSS2-ERG activation via the stronger AR may be

better able to persist in spite of hormone therapy. Finally, although ETV1 fusion-positive

patients are less common than ERG, they still account for 5-10% of PCa, which is equivalent to

approximately 10,000-20,000 patients per year in the U.S. alone. Prospective studies should

address the effectiveness of abiraterone acetate and other hormonal therapies against tumors

harboring an androgen-induced ETV1 fusion, as well as the wider collection of ETS fusions, while considering AR and PTEN status.

Table 4.1
cBioPortal gene summary

	ETV1^Tg Mice	ETS⁺ Local PCa	PCa Broad/Cornell Nat Gen 2012 CNA = 109 mRNA = 31	PCa Broad/Cornell Cell 2013 CNA = 56	PCa, Metastatic Michigan Nat 2012 CNA = 61	PCa MSKCC Can Cell 2010 CNA = 157 local, 37 met mRNA = 131 local, 19 met	PCa, CNA Study MSKCC PNAS 2014 CNA = 104	PCa TCGA Provisional CNA = 492 mRNA = 487
KCNN4	Up	Up	x	Del: 1	Amp: 1	mRNA (local) up: 20 mRNA (local) down: 5 mRNA (met) up: 4 mRNA (met) down: 3	x	Del: 5 Amp: 1 mRNA up: 20
SOX4	Up	Up	mRNA up: 1	Del: 1	Del: 1	Amp (met): 1 mRNA (local) up: 49 mRNA (met) up: 14	x	Del: 6 Amp: 2 mRNA up: 14
HPN	Up	Up	mRNA down: 1	x	x	mRNA (local) up: 87 mRNA (met) up: 13 mRNA (local) down: 2	x	Del: 3 Amp: 2 mRNA up: 9
PSCA	Up	Up	Amp: 1 mRNA up: 1	Amp: 1 Del: 1	Amp: 10	Amp (local): 1 Amp (met): 5 mRNA (local) up: 2 mRNA (met) up: 2	Amp: 2	Amp: 26 Del: 3 mRNA up: 8 (1 w/Amp)
LRP8	Up	Up	mRNA up: 2	x	Del: 1	mRNA (local) up: 13 mRNA (met) up: 7	x	Del: 9 Amp: 2 mRNA up: 7
SEMA4G	Down	Down	mRNA up: 1	Del: 1	Del: 4	mRNA (local) up: 2 mRNA (local) down: 4 mRNA (met) down: 2	x	Del: 14 Amp: 1 mRNA up: 11
REC8	Down	Down	mRNA up: 1	x	x	mRNA (local) up: 6 mRNA (local) down: 10 mRNA (met) up: 1 mRNA (met) down: 4	x	Del: 1 mRNA up: 9
SDF2L1	Down	Down	mRNA up: 1	x	Del: 1	mRNA (local) up: 10 mRNA (met) up: 3	x	Del: 4 Amp: 1 mRNA up: 20

Bibliography

Abate-Shen, C., Banach-Petrosky, W.A., Sun, X., Economides, K.D., Desai, N., Gregg, J.P., Borowsky, A.D., Cardiff, R.D., and Shen, M.M. (2003). Nkx3.1; Pten mutant mice develop invasive prostate adenocarcinoma and lymph node metastases. Cancer Res *63*, 3886-3890.

Abate-Shen, C., and Shen, M.M. (2000). Molecular genetics of prostate cancer. Genes Dev *14*, 2410-2434.

Abate-Shen, C., and Shen, M.M. (2002). Mouse models of prostate carcinogenesis. Trends Genet *18*, S1-5.

Albertelli, M.A., O'Mahony, O.A., Brogley, M., Tosoian, J., Steinkamp, M., Daignault, S., Wojno, K., and Robins, D.M. (2008). Glutamine tract length of human androgen receptors affects hormone-dependent and -independent prostate cancer in mice. Hum Mol Genet *17*, 98-110.

Albertelli, M.A., Scheller, A., Brogley, M., and Robins, D.M. (2006). Replacing the mouse androgen receptor with human alleles demonstrates glutamine tract length-dependent effects on physiology and tumorigenesis in mice. Mol Endocrinol *20*, 1248-1260.

Alimonti, A., Carracedo, A., Clohessy, J.G., Trotman, L.C., Nardella, C., Egia, A., Salmena, L., Sampieri, K., Haveman, W.J., Brogi, E.*, et al.* (2010). Subtle variations in Pten dose determine cancer susceptibility. Nat Genet *42*, 454-458.

Altintas, D.M., Vlaeminck, V., Angelov, D., Dimitrov, S., and Samarut, J. (2011). Cell cycle regulated expression of NCoR might control cyclic expression of androgen responsive genes in an immortalized prostate cell line. Mol Cell Endocrinol *332*, 149-162.

Alvarado, C., Beitel, L.K., Sircar, K., Aprikian, A., Trifiro, M., and Gottlieb, B. (2005). Somatic mosaicism and cancer: a micro-genetic examination into the role of the androgen receptor gene in prostate cancer. Cancer Res *65*, 8514-8518.

Anders, S., McCarthy, D.J., Chen, Y., Okoniewski, M., Smyth, G.K., Huber, W., and Robinson, M.D. (2013). Count-based differential expression analysis of RNA sequencing data using R and Bioconductor. Nat Protoc *8*, 1765-1786.

Antonarakis, E.S., Lu, C., Wang, H., Luber, B., Nakazawa, M., Roeser, J.C., Chen, Y., Mohammad, T.A., Fedor, H.L., Lotan, T.L.*, et al.* (2014). AR-V7 and Resistance to Enzalutamide and Abiraterone in Prostate Cancer. N Engl J Med.

Attard, G., Reid, A.H., Olmos, D., and de Bono, J.S. (2009). Antitumor activity with CYP17 blockade indicates that castration-resistant prostate cancer frequently remains hormone driven. Cancer Res *69*, 4937-4940.

Baca, S.C., Prandi, D., Lawrence, M.S., Mosquera, J.M., Romanel, A., Drier, Y., Park, K., Kitabayashi, N., MacDonald, T.Y., Ghandi, M.*, et al.* (2013). Punctuated evolution of prostate cancer genomes. Cell *153*, 666-677.

Baena, E., Shao, Z., Linn, D.E., Glass, K., Hamblen, M.J., Fujiwara, Y., Kim, J., Nguyen, M., Zhang, X., Godinho, F.J.*, et al.* (2013). ETV1 directs androgen metabolism and confers aggressive prostate cancer in targeted mice and patients. Genes Dev *27*, 683-698.

Barbieri, C.E., Baca, S.C., Lawrence, M.S., Demichelis, F., Blattner, M., Theurillat, J.P., White, T.A., Stojanov, P., Van Allen, E., Stransky, N.*, et al.* (2012). Exome sequencing identifies recurrent SPOP, FOXA1 and MED12 mutations in prostate cancer. Nat Genet.

Barbieri, C.E., Bangma, C.H., Bjartell, A., Catto, J.W., Culig, Z., Gronberg, H., Luo, J., Visakorpi, T., and Rubin, M.A. (2013). The Mutational Landscape of Prostate Cancer. Eur Urol.

Barbieri, C.E., and Tomlins, S.A. (2014). The prostate cancer genome: perspectives and potential. Urol Oncol *32*, 53 e15-22.

Bastus, N.C., Boyd, L.K., Mao, X., Stankiewicz, E., Kudahetti, S.C., Oliver, R.T., Berney, D.M., and Lu, Y.J. (2010). Androgen-induced TMPRSS2:ERG fusion in nonmalignant prostate epithelial cells. Cancer Res *70*, 9544-9548.

Beato, M. (1989). Gene regulation by steroid hormones. Cell *56*, 335-344.

Begley, L.A., Kasina, S., Mehra, R., Adsule, S., Admon, A.J., Lonigro, R.J., Chinnaiyan, A.M., and Macoska, J.A. (2008). CXCL5 promotes prostate cancer progression. Neoplasia *10*, 244-254.

Bello, D., Webber, M.M., Kleinman, H.K., Wartinger, D.D., and Rhim, J.S. (1997). Androgen responsive adult human prostatic epithelial cell lines immortalized by human papillomavirus 18. Carcinogenesis *18*, 1215-1223.

Berquin, I.M., Min, Y., Wu, R., Wu, H., and Chen, Y.Q. (2005). Expression signature of the mouse prostate. J Biol Chem *280*, 36442-36451.

Bertram, J., Peacock, J.W., Fazli, L., Mui, A.L., Chung, S.W., Cox, M.E., Monia, B., Gleave, M.E., and Ong, C.J. (2006). Loss of PTEN is associated with progression to androgen independence. Prostate *66*, 895-902.

Bhalla, R., Kunju, L.P., Tomlins, S.A., Christopherson, K., Cortez, C., Carskadon, S., Siddiqui, J., Park, K., Miguel Mosquera, J., Pestano, G.A.*, et al.* (2013). Novel dual-color immunohistochemical methods for detecting ERG-PTEN and ERG-SPINK1 status in prostate carcinoma. Mod Pathol.

Bismar, T.A., Yoshimoto, M., Vollmer, R.T., Duan, Q., Firszt, M., Corcos, J., and Squire, J.A. (2011). PTEN genomic deletion is an early event associated with ERG gene rearrangements in prostate cancer. BJU Int *107*, 477-485.

Bowen, C., Bubendorf, L., Voeller, H.J., Slack, R., Willi, N., Sauter, G., Gasser, T.C., Koivisto, P., Lack, E.E., Kononen, J.*, et al.* (2000). Loss of NKX3.1 expression in human prostate cancers correlates with tumor progression. Cancer Res *60*, 6111-6115.

Brawer, M.K. (2005). Prostatic intraepithelial neoplasia: an overview. Rev Urol *7 Suppl 3*, S11-18.

Bryce, A., and Ryan, C.J. (2011). Development and Clinical Utility of Abiraterone Acetate as an Androgen Synthesis Inhibitor. Clin Pharmacol Ther.

Buchanan, G., Yang, M., Cheong, A., Harris, J.M., Irvine, R.A., Lambert, P.F., Moore, N.L., Raynor, M., Neufing, P.J., Coetzee, G.A.*, et al.* (2004). Structural and functional consequences of glutamine tract variation in the androgen receptor. Hum Mol Genet *13*, 1677-1692.

Carver, B.S., Chapinski, C., Wongvipat, J., Hieronymus, H., Chen, Y., Chandarlapaty, S., Arora, V.K., Le, C., Koutcher, J., Scher, H.*, et al.* (2011). Reciprocal Feedback Regulation of PI3K and Androgen Receptor Signaling in PTEN-Deficient Prostate Cancer. Cancer Cell *19*, 575-586.

Carver, B.S., Tran, J., Gopalan, A., Chen, Z., Shaikh, S., Carracedo, A., Alimonti, A., Nardella, C., Varmeh, S., Scardino, P.T.*, et al.* (2009). Aberrant ERG expression cooperates with loss of PTEN to promote cancer progression in the prostate. Nat Genet *41*, 619-624.

Ceraline, J., Cruchant, M.D., Erdmann, E., Erbs, P., Kurtz, J.E., Duclos, B., Jacqmin, D., Chopin, D., and Bergerat, J.P. (2004). Constitutive activation of the androgen receptor by a point mutation in the hinge region: a new mechanism for androgen-independent growth in prostate cancer. Int J Cancer *108*, 152-157.

Cerami, E., Gao, J., Dogrusoz, U., Gross, B.E., Sumer, S.O., Aksoy, B.A., Jacobsen, A., Byrne, C.J., Heuer, M.L., Larsson, E.*, et al.* (2012). The cBio cancer genomics portal: an open platform for exploring multidimensional cancer genomics data. Cancer Discov *2*, 401-404.

Chamberlain, N.L., Driver, E.D., and Miesfeld, R.L. (1994). The length and location of CAG trinucleotide repeats in the androgen receptor N-terminal domain affect transactivation function. Nucleic Acids Res *22*, 3181-3186.

Chen, C.D., Welsbie, D.S., Tran, C., Baek, S.H., Chen, R., Vessella, R., Rosenfeld, M.G., and Sawyers, C.L. (2004). Molecular determinants of resistance to antiandrogen therapy. Nat Med *10*, 33-39.

Chen, J., Wang, Z., Xu, D., Liu, Y., and Gao, Y. (2015). Aquaporin 3 promotes prostate cancer cell motility and invasion via extracellular signal-regulated kinase 1/2-mediated matrix metalloproteinase-3 secretion. Mol Med Rep *11*, 2882-2888.

Chen, Y., Chi, P., Rockowitz, S., Iaquinta, P.J., Shamu, T., Shukla, S., Gao, D., Sirota, I., Carver, B.S., Wongvipat, J.*, et al.* (2013). ETS factors reprogram the androgen receptor cistrome and prime prostate tumorigenesis in response to PTEN loss. Nat Med.

Chen, Z., Lan, X., Thomas-Ahner, J.M., Wu, D., Liu, X., Ye, Z., Wang, L., Sunkel, B., Grenade, C., Chen, J.*, et al.* (2014). Agonist and antagonist switch DNA motifs recognized by human androgen receptor in prostate cancer. EMBO J.

Chevalier-Larsen, E.S., O'Brien, C.J., Wang, H., Jenkins, S.C., Holder, L., Lieberman, A.P., and Merry, D.E. (2004). Castration restores function and neurofilament alterations of aged symptomatic males in a transgenic mouse model of spinal and bulbar muscular atrophy. J Neurosci *24*, 4778-4786.

Choucair, K., Ejdelman, J., Brimo, F., Aprikian, A., Chevalier, S., and Lapointe, J. (2012). PTEN genomic deletion predicts prostate cancer recurrence and is associated with low AR expression and transcriptional activity. BMC Cancer *12*, 543.

Chua, J.P., and Lieberman, A.P. (2013). Pathogenic mechanisms and therapeutic strategies in spinobulbar muscular atrophy. CNS Neurol Disord Drug Targets *12*, 1146-1156.

Coetzee, G.A., and Ross, R.K. (1994). Re: Prostate cancer and the androgen receptor. J Natl Cancer Inst *86*, 872-873.

Core, L.J., Waterfall, J.J., and Lis, J.T. (2008). Nascent RNA sequencing reveals widespread pausing and divergent initiation at human promoters. Science *322*, 1845-1848.

Culig, Z., Hobisch, A., Cronauer, M.V., Cato, A.C., Hittmair, A., Radmayr, C., Eberle, J., Bartsch, G., and Klocker, H. (1993). Mutant androgen receptor detected in an advanced-stage prostatic carcinoma is activated by adrenal androgens and progesterone. Mol Endocrinol *7*, 1541-1550.

Culig, Z., Hobisch, A., Cronauer, M.V., Radmayr, C., Trapman, J., Hittmair, A., Bartsch, G., and Klocker, H. (1994). Androgen receptor activation in prostatic tumor cell lines by insulin-like growth factor-I, keratinocyte growth factor, and epidermal growth factor. Cancer Res *54*, 5474-5478.

Culig, Z., Hobisch, A., Hittmair, A., Peterziel, H., Cato, A.C., Bartsch, G., and Klocker, H. (1998). Expression, structure, and function of androgen receptor in advanced prostatic carcinoma. Prostate *35*, 63-70.

Cunha, G.R., Donjacour, A.A., Cooke, P.S., Mee, S., Bigsby, R.M., Higgins, S.J., and Sugimura, Y. (1987). The endocrinology and developmental biology of the prostate. Endocr Rev *8*, 338-362.

Dehm, S., and Tindall, D.J. (2011). Alternatively spliced androgen receptor variants. Endocr Relat Cancer.

Dehm, S.M., Schmidt, L.J., Heemers, H.V., Vessella, R.L., and Tindall, D.J. (2008). Splicing of a novel androgen receptor exon generates a constitutively active androgen receptor that mediates prostate cancer therapy resistance. Cancer Res *68*, 5469-5477.

DePrimo, S.E., Diehn, M., Nelson, J.B., Reiter, R.E., Matese, J., Fero, M., Tibshirani, R., Brown, P.O., and Brooks, J.D. (2002). Transcriptional programs activated by exposure of human prostate cancer cells to androgen. Genome Biol *3*, RESEARCH0032.

Ding, D., Xu, L., Menon, M., Reddy, G.P., and Barrack, E.R. (2004). Effect of a short CAG (glutamine) repeat on human androgen receptor function. Prostate *58*, 23-32.

Dun, B., Sharma, A., Teng, Y., Liu, H., Purohit, S., Xu, H., Zeng, L., and She, J.X. (2013). Mycophenolic acid inhibits migration and invasion of gastric cancer cells via multiple molecular pathways. PLoS One *8*, e81702.

Ellwood-Yen, K., Graeber, T.G., Wongvipat, J., Iruela-Arispe, M.L., Zhang, J., Matusik, R., Thomas, G.V., and Sawyers, C.L. (2003). Myc-driven murine prostate cancer shares molecular features with human prostate tumors. Cancer Cell *4*, 223-238.

Etzioni, R., Penson, D.F., Legler, J.M., di Tommaso, D., Boer, R., Gann, P.H., and Feuer, E.J. (2002). Overdiagnosis due to prostate-specific antigen screening: lessons from U.S. prostate cancer incidence trends. J Natl Cancer Inst *94*, 981-990.

Etzioni, R.D., and Thompson, I.M. (2014). What do the screening trials really tell us and where do we go from here? Urol Clin North Am *41*, 223-228.

Fang, Y., Fliss, A.E., Robins, D.M., and Caplan, A.J. (1996). Hsp90 regulates androgen receptor hormone binding affinity in vivo. J Biol Chem *271*, 28697-28702.

Feldman, B.J., and Feldman, D. (2001). The development of androgen-independent prostate cancer. Nat Rev Cancer *1*, 34-45.

Fleischmann, A., Rocha, C., Saxer-Sekulic, N., Zlobec, I., Sauter, G., and Thalmann, G.N. (2011). High CD10 expression in lymph node metastases from surgically treated prostate cancer independently predicts early death. Virchows Arch *458*, 741-748.

Furuya, Y., Krajewski, S., Epstein, J.I., Reed, J.C., and Isaacs, J.T. (1996). Expression of bcl-2 and the progression of human and rodent prostatic cancers. Clin Cancer Res *2*, 389-398.

Gao, J., Aksoy, B.A., Dogrusoz, U., Dresdner, G., Gross, B., Sumer, S.O., Sun, Y., Jacobsen, A., Sinha, R., Larsson, E.*, et al.* (2013). Integrative analysis of complex cancer genomics and clinical profiles using the cBioPortal. Sci Signal *6*, pl1.

Gao, J., Arnold, J.T., and Isaacs, J.T. (2001). Conversion from a paracrine to an autocrine mechanism of androgen-stimulated growth during malignant transformation of prostatic epithelial cells. Cancer Res *61*, 5038-5044.

Gao, N., Zhang, J., Rao, M.A., Case, T.C., Mirosevich, J., Wang, Y., Jin, R., Gupta, A., Rennie, P.S., and Matusik, R.J. (2003). The role of hepatocyte nuclear factor-3 alpha (Forkhead Box A1) and androgen receptor in transcriptional regulation of prostatic genes. Mol Endocrinol *17*, 1484-1507.

Garnis, C., Campbell, J., Davies, J.J., Macaulay, C., Lam, S., and Lam, W.L. (2005). Involvement of multiple developmental genes on chromosome 1p in lung tumorigenesis. Hum Mol Genet *14*, 475-482.

Gingrich, J.R., Barrios, R.J., Morton, R.A., Boyce, B.F., DeMayo, F.J., Finegold, M.J., Angelopoulou, R., Rosen, J.M., and Greenberg, N.M. (1996). Metastatic prostate cancer in a transgenic mouse. Cancer Res *56*, 4096-4102.

Graff, R.E., Pettersson, A., Lis, R.T., DuPre, N., Jordahl, K.M., Nuttall, E., Rider, J.R., Fiorentino, M., Sesso, H.D., Kenfield, S.A.*, et al.* (2015). The TMPRSS2:ERG fusion and response to androgen deprivation therapy for prostate cancer. Prostate.

Grasso, C.S., Wu, Y.M., Robinson, D.R., Cao, X., Dhanasekaran, S.M., Khan, A.P., Quist, M.J., Jing, X., Lonigro, R.J., Brenner, J.C.*, et al.* (2012). The mutational landscape of lethal castration-resistant prostate cancer. Nature.

Greenberg, N.M., DeMayo, F., Finegold, M.J., Medina, D., Tilley, W.D., Aspinall, J.O., Cunha, G.R., Donjacour, A.A., Matusik, R.J., and Rosen, J.M. (1995). Prostate cancer in a transgenic mouse. Proc Natl Acad Sci U S A *92*, 3439-3443.

Grino, P.B., Griffin, J.E., and Wilson, J.D. (1990). Testosterone at high concentrations interacts with the human androgen receptor similarly to dihydrotestosterone. Endocrinology *126*, 1165-1172.

Gumuskaya, B., Gurel, B., Fedor, H., Tan, H.L., Weier, C.A., Hicks, J.L., Haffner, M.C., Lotan, T.L., and De Marzo, A.M. (2013). Assessing the order of critical alterations in prostate cancer development and progression by IHC: further evidence that PTEN loss occurs subsequent to ERG gene fusion. Prostate Cancer Prostatic Dis.

Guo, X., Wang, W., Hu, J., Feng, K., Pan, Y., Zhang, L., and Feng, Y. (2012). Lentivirus-Mediated RNAi Knockdown of NUPR1 Inhibits Human Nonsmall Cell Lung Cancer Growth In Vitro and In Vivo. Anat Rec (Hoboken) *295*, 2114-2121.

Haffner, M., De Marzo, A.M., Meeker, A.K., Nelson, W.G., and Yegnasubramanian, S. (2011). Transcription-induced DNA double strand breaks: both an oncogenic force and potential therapeutic target? Clin Cancer Res.

Hamidi, T., Algul, H., Cano, C.E., Sandi, M.J., Molejon, M.I., Riemann, M., Calvo, E.L., Lomberk, G., Dagorn, J.C., Weih, F.*, et al.* (2012). Nuclear protein 1 promotes pancreatic cancer development and protects cells from stress by inhibiting apoptosis. J Clin Invest *122*, 2092-2103.

Han, B., Mehra, R., Dhanasekaran, S.M., Yu, J., Menon, A., Lonigro, R.J., Wang, X., Gong, Y., Wang, L., Shankar, S.*, et al.* (2008). A fluorescence in situ hybridization screen for E26

transformation-specific aberrations: identification of DDX5-ETV4 fusion protein in prostate cancer. Cancer Res *68*, 7629-7637.

Han, G., Buchanan, G., Ittmann, M., Harris, J.M., Yu, X., Demayo, F.J., Tilley, W., and Greenberg, N.M. (2005). Mutation of the androgen receptor causes oncogenic transformation of the prostate. Proc Natl Acad Sci U S A *102*, 1151-1156.

He, B., Kemppainen, J.A., Voegel, J.J., Gronemeyer, H., and Wilson, E.M. (1999). Activation function 2 in the human androgen receptor ligand binding domain mediates interdomain communication with the NH(2)-terminal domain. J Biol Chem *274*, 37219-37225.

He, B., Kemppainen, J.A., and Wilson, E.M. (2000). FXXLF and WXXLF sequences mediate the NH2-terminal interaction with the ligand binding domain of the androgen receptor. J Biol Chem *275*, 22986-22994.

Heinlein, C.A., and Chang, C. (2004). Androgen receptor in prostate cancer. Endocr Rev *25*, 276-308.

Hieronymus, H., Schultz, N., Gopalan, A., Carver, B.S., Chang, M.T., Xiao, Y., Heguy, A., Huberman, K., Bernstein, M., Assel, M.*, et al.* (2014). Copy number alteration burden predicts prostate cancer relapse. Proc Natl Acad Sci U S A *111*, 11139-11144.

Higgins, J., Brogley, M., Palanisamy, N., Mehra, R., Ittmann, M.M., Li, J.Z., Tomlins, S.A., and Robins, D.M. (2015). Interaction of the Androgen Receptor, ETV1, and PTEN Pathways in Mouse Prostate Varies with Pathological Stage and Predicts Cancer Progression. Horm Cancer.

Hollenhorst, P.C., Ferris, M.W., Hull, M.A., Chae, H., Kim, S., and Graves, B.J. (2011a). Oncogenic ETS proteins mimic activated RAS/MAPK signaling in prostate cells. Genes Dev *25*, 2147-2157.

Hollenhorst, P.C., Paul, L., Ferris, M.W., and Graves, B.J. (2011b). The ETS gene ETV4 is required for anchorage-independent growth and a cell proliferation gene expression program in PC3 prostate cells. Genes Cancer *1*, 1044-1052.

Holzbeierlein, J., Lal, P., LaTulippe, E., Smith, A., Satagopan, J., Zhang, L., Ryan, C., Smith, S., Scher, H., Scardino, P.*, et al.* (2004). Gene expression analysis of human prostate carcinoma during hormonal therapy identifies androgen-responsive genes and mechanisms of therapy resistance. Am J Pathol *164*, 217-227.

Hon, G.C., Hawkins, R.D., and Ren, B. (2009). Predictive chromatin signatures in the mammalian genome. Hum Mol Genet *18*, R195-201.

Horoszewicz, J.S., Leong, S.S., Kawinski, E., Karr, J.P., Rosenthal, H., Chu, T.M., Mirand, E.A., and Murphy, G.P. (1983). LNCaP model of human prostatic carcinoma. Cancer Res *43*, 1809-1818.

Huang Da, W., Sherman, B.T., and Lempicki, R.A. (2009). Systematic and integrative analysis of large gene lists using DAVID bioinformatics resources. Nat Protoc *4*, 44-57.

Huggins, C., and Hodges, C.V. (2002). Studies on prostatic cancer: I. The effect of castration, of estrogen and of androgen injection on serum phosphatases in metastatic carcinoma of the prostate. 1941. J Urol *168*, 9-12.

Irvine, R.A., Ma, H., Yu, M.C., Ross, R.K., Stallcup, M.R., and Coetzee, G.A. (2000). Inhibition of p160-mediated coactivation with increasing androgen receptor polyglutamine length. Hum Mol Genet *9*, 267-274.

Ittmann, M., Huang, J., Radaelli, E., Martin, P., Signoretti, S., Sullivan, R., Simons, B.W., Ward, J.M., Robinson, B.D., Chu, G.C.*, et al.* (2013). Animal models of human prostate cancer: the consensus report of the New York meeting of the Mouse Models of Human Cancers Consortium Prostate Pathology Committee. Cancer Res *73*, 2718-2736.

Jabbour, E., and Kantarjian, H. (2014). Chronic myeloid leukemia: 2014 update on diagnosis, monitoring, and management. Am J Hematol *89*, 547-556.

Jenster, G., Trapman, J., and Brinkmann, A.O. (1993). Nuclear import of the human androgen receptor. Biochem J *293 (Pt 3)*, 761-768.

Jeon, I.S., Davis, J.N., Braun, B.S., Sublett, J.E., Roussel, M.F., Denny, C.T., and Shapiro, D.N. (1995). A variant Ewing's sarcoma translocation (7;22) fuses the EWS gene to the ETS gene ETV1. Oncogene *10*, 1229-1234.

Johnson, M.A., Iversen, P., Schwier, P., Corn, A.L., Sandusky, G., Graff, J., and Neubauer, B.L. (2005). Castration triggers growth of previously static androgen-independent lesions in the transgenic adenocarcinoma of the mouse prostate (TRAMP) model. Prostate *62*, 322-338.

Jones, S.B., DePrimo, S.E., Whitfield, M.L., and Brooks, J.D. (2005). Resveratrol-induced gene expression profiles in human prostate cancer cells. Cancer Epidemiol Biomarkers Prev *14*, 596-604.

Jung, S.H., Lee, A., Yim, S.H., Hu, H.J., Choe, C., and Chung, Y.J. (2012). Simultaneous copy number gains of NUPR1 and ERBB2 predicting poor prognosis in early-stage breast cancer. BMC Cancer *12*, 382.

Jung, Y., Kim, J.K., Shiozawa, Y., Wang, J., Mishra, A., Joseph, J., Berry, J.E., McGee, S., Lee, E., Sun, H.*, et al.* (2013). Recruitment of mesenchymal stem cells into prostate tumours promotes metastasis. Nat Commun *4*, 1795.

Kang, H., Escudero-Esparza, A., Douglas-Jones, A., Mansel, R.E., and Jiang, W.G. (2009). Transcript analyses of stromal cell derived factors (SDFs): SDF-2, SDF-4 and SDF-5 reveal a different pattern of expression and prognostic association in human breast cancer. Int J Oncol *35*, 205-211.

Kaplan-Lefko, P.J., Chen, T.M., Ittmann, M.M., Barrios, R.J., Ayala, G.E., Huss, W.J., Maddison, L.A., Foster, B.A., and Greenberg, N.M. (2003). Pathobiology of autochthonous prostate cancer in a pre-clinical transgenic mouse model. Prostate *55*, 219-237.

Kim, D., Pertea, G., Trapnell, C., Pimentel, H., Kelley, R., and Salzberg, S.L. (2013). TopHat2: accurate alignment of transcriptomes in the presence of insertions, deletions and gene fusions. Genome Biol *14*, R36.

Kim, M.J., Bhatia-Gaur, R., Banach-Petrosky, W.A., Desai, N., Wang, Y., Hayward, S.W., Cunha, G.R., Cardiff, R.D., Shen, M.M., and Abate-Shen, C. (2002a). Nkx3.1 mutant mice recapitulate early stages of prostate carcinogenesis. Cancer Res *62*, 2999-3004.

Kim, M.J., Cardiff, R.D., Desai, N., Banach-Petrosky, W.A., Parsons, R., Shen, M.M., and Abate-Shen, C. (2002b). Cooperativity of Nkx3.1 and Pten loss of function in a mouse model of prostate carcinogenesis. Proc Natl Acad Sci U S A *99*, 2884-2889.

King, J.C., Xu, J., Wongvipat, J., Hieronymus, H., Carver, B.S., Leung, D.H., Taylor, B.S., Sander, C., Cardiff, R.D., Couto, S.S.*, et al.* (2009). Cooperativity of TMPRSS2-ERG with PI3-kinase pathway activation in prostate oncogenesis. Nat Genet *41*, 524-526.

Klezovitch, O., Risk, M., Coleman, I., Lucas, J.M., Null, M., True, L.D., Nelson, P.S., and Vasioukhin, V. (2008). A causal role for ERG in neoplastic transformation of prostate epithelium. Proc Natl Acad Sci U S A *105*, 2105-2110.

Kluth, L.A., Shariat, S.F., Kratzik, C., Tagawa, S., Sonpavde, G., Rieken, M., Scherr, D.S., and Pummer, K. (2014). The hypothalamic-pituitary-gonadal axis and prostate cancer: implications for androgen deprivation therapy. World J Urol *32*, 669-676.

Knudsen, K.E., and Kelly, W.K. (2011). Outsmarting androgen receptor: creative approaches for targeting aberrant androgen signaling in advances prostate cancer.

Krohn, A., Diedler, T., Burkhardt, L., Mayer, P.S., De Silva, C., Meyer-Kornblum, M., Kotschau, D., Tennstedt, P., Huang, J., Gerhauser, C.*, et al.* (2012). Genomic Deletion of PTEN Is Associated with Tumor Progression and Early PSA Recurrence in ERG Fusion-Positive and Fusion-Negative Prostate Cancer. Am J Pathol.

Kunju, L.P., Carskadon, S., Siddiqui, J., Tomlins, S.A., Chinnaiyan, A.M., and Palanisamy, N. (2014). Novel RNA Hybridization Method for the In Situ Detection of ETV1, ETV4, and ETV5 Gene Fusions in Prostate Cancer. Appl Immunohistochem Mol Morphol *22*, e32-e40.

La Spada, A.R., Wilson, E.M., Lubahn, D.B., Harding, A.E., and Fischbeck, K.H. (1991). Androgen receptor gene mutations in X-linked spinal and bulbar muscular atrophy. Nature *352*, 77-79.

Labrie, F. (2011). Blockade of testicular and adrenal androgens in prostate cancer treatment. Nat Rev Urol.

Lapointe, J., Li, C., Higgins, J.P., van de Rijn, M., Bair, E., Montgomery, K., Ferrari, M., Egevad, L., Rayford, W., Bergerheim, U.*, et al.* (2004). Gene expression profiling identifies clinically relevant subtypes of prostate cancer. Proc Natl Acad Sci U S A *101*, 811-816.

Lee, K.W., Sung, C.O., Kim, J.H., Kang, M., Yoo, H.Y., Kim, H.H., Um, S.H., and Kim, S.H. (2015). CD10 expression is enhanced by Twist1 and associated with poor prognosis in esophageal squamous cell carcinoma with facilitating tumorigenicity in vitro and in vivo. Int J Cancer *136*, 310-321.

Lesche, R., Groszer, M., Gao, J., Wang, Y., Messing, A., Sun, H., Liu, X., and Wu, H. (2002). Cre/loxP-mediated inactivation of the murine Pten tumor suppressor gene. Genesis *32*, 148-149.

Li, W., Notani, D., Ma, Q., Tanasa, B., Nunez, E., Chen, A.Y., Merkurjev, D., Zhang, J., Ohgi, K., Song, X.*, et al.* (2013). Functional roles of enhancer RNAs for oestrogen-dependent transcriptional activation. Nature *498*, 516-520.

Liao, Y., and Hung, M.C. (2010). Physiological regulation of Akt activity and stability. Am J Transl Res *2*, 19-42.

Lin, C., Yang, L., Tanasa, B., Hutt, K., Ju, B.G., Ohgi, K., Zhang, J., Rose, D.W., Fu, X.D., Glass, C.K.*, et al.* (2009). Nuclear receptor-induced chromosomal proximity and DNA breaks underlie specific translocations in cancer. Cell *139*, 1069-1083.

Lindstrom, S., Ma, J., Altshuler, D., Giovannucci, E., Riboli, E., Albanes, D., Allen, N.E., Berndt, S.I., Boeing, H., Bueno-de-Mesquita, H.B.*, et al.* (2010). A Large Study of Androgen Receptor Germline Variants and Their Relation to Sex Hormone Levels and Prostate Cancer Risk. Results from the National Cancer Institute Breast and Prostate Cancer Cohort Consortium. J Clin Endocrinol Metab.

Lindstrom, S., Wiklund, F., Adami, H.O., Balter, K.A., Adolfsson, J., and Gronberg, H. (2006a). Germ-line genetic variation in the key androgen-regulating genes androgen receptor, cytochrome P450, and steroid-5-alpha-reductase type 2 is important for prostate cancer development. Cancer Res *66*, 11077-11083.

Lindstrom, S., Zheng, S.L., Wiklund, F., Jonsson, B.A., Adami, H.O., Balter, K.A., Brookes, A.J., Sun, J., Chang, B.L., Liu, W.*, et al.* (2006b). Systematic replication study of reported genetic associations in prostate cancer: Strong support for genetic variation in the androgen pathway. Prostate *66*, 1729-1743.

Lois, C., Hong, E.J., Pease, S., Brown, E.J., and Baltimore, D. (2002). Germline transmission and tissue-specific expression of transgenes delivered by lentiviral vectors. Science *295*, 868-872.

Lupien, M., and Brown, M. (2009). Cistromics of hormone-dependent cancer. Endocr Relat Cancer *16*, 381-389.

Ma, X., Ziel-van der Made, A.C., Autar, B., van der Korput, H.A., Vermeij, M., van Duijn, P., Cleutjens, K.B., de Krijger, R., Krimpenfort, P., Berns, A.*, et al.* (2005). Targeted biallelic inactivation of Pten in the mouse prostate leads to prostate cancer accompanied by increased epithelial cell proliferation but not by reduced apoptosis. Cancer Res *65*, 5730-5739.

Malaney, P., Nicosia, S.V., and Dave, V. (2014). One mouse, one patient paradigm: New avatars of personalized cancer therapy. Cancer Lett *344*, 1-12.

Mani, R.S., Tomlins, S.A., Callahan, K., Ghosh, A., Nyati, M.K., Varambally, S., Palanisamy, N., and Chinnaiyan, A.M. (2009). Induced chromosomal proximity and gene fusions in prostate cancer. Science *326*, 1230.

May, W.A., Lessnick, S.L., Braun, B.S., Klemsz, M., Lewis, B.C., Lunsford, L.B., Hromas, R., and Denny, C.T. (1993). The Ewing's sarcoma EWS/FLI-1 fusion gene encodes a more potent transcriptional activator and is a more powerful transforming gene than FLI-1. Mol Cell Biol *13*, 7393-7398.

Mehra, R., Han, B., Tomlins, S.A., Wang, L., Menon, A., Wasco, M.J., Shen, R., Montie, J.E., Chinnaiyan, A.M., and Shah, R.B. (2007). Heterogeneity of TMPRSS2 gene rearrangements in multifocal prostate adenocarcinoma: molecular evidence for an independent group of diseases. Cancer Res *67*, 7991-7995.

Mesquita, D., Barros-Silva, J.D., Santos, J., Skotheim, R.I., Lothe, R.A., Paulo, P., and Teixeira, M.R. (2014). Specific and redundant activities of ETV1 and ETV4 in prostate cancer aggressiveness revealed by co-overexpression cellular contexts. Oncotarget.

Mirochnik, Y., Veliceasa, D., Williams, L., Maxwell, K., Yemelyanov, A., Budunova, I., and Volpert, O.V. (2012). Androgen receptor drives cellular senescence. PLoS One *7*, e31052.

Moras, D., and Gronemeyer, H. (1998). The nuclear receptor ligand-binding domain: structure and function. Curr Opin Cell Biol *10*, 384-391.

Mounir, Z., Lin, F., Lin, V.G., Korn, J.M., Yu, Y., Valdez, R., Aina, O.H., Buchwalter, G., Jaffe, A.B., Korpal, M.*, et al.* (2014). TMPRSS2:ERG blocks neuroendocrine and luminal cell differentiation to maintain prostate cancer proliferation. Oncogene.

Mukherji, D., Pezaro, C.J., and De-Bono, J.S. (2012). MDV3100 for the treatment of prostate cancer. Expert Opin Investig Drugs.

Mulholland, D.J., Tran, L.M., Li, Y., Cai, H., Morim, A., Wang, S., Plaisier, S., Garraway, I.P., Huang, J., Graeber, T.G.*, et al.* (2011). Cell Autonomous Role of PTEN in Regulating Castration-Resistant Prostate Cancer Growth. Cancer Cell.

Nakagawa, T., Kollmeyer, T.M., Morlan, B.W., Anderson, S.K., Bergstralh, E.J., Davis, B.J., Asmann, Y.W., Klee, G.G., Ballman, K.V., and Jenkins, R.B. (2008). A tissue biomarker panel predicting systemic progression after PSA recurrence post-definitive prostate cancer therapy. PLoS One *3*, e2318.

O'Mahony, O.A., Steinkamp, M.P., Albertelli, M.A., Brogley, M., Rehman, H., and Robins, D.M. (2008). Profiling human androgen receptor mutations reveals treatment effects in a mouse model of prostate cancer. Mol Cancer Res *6*, 1691-1701.

Ohya, S., Kimura, K., Niwa, S., Ohno, A., Kojima, Y., Sasaki, S., Kohri, K., and Imaizumi, Y. (2009). Malignancy grade-dependent expression of K+-channel subtypes in human prostate cancer. J Pharmacol Sci *109*, 148-151.

Ohya, S., Niwa, S., Kojima, Y., Sasaki, S., Sakuragi, M., Kohri, K., and Imaizumi, Y. (2011). Intermediate-conductance Ca2+-activated K+ channel, KCa3.1, as a novel therapeutic target for benign prostatic hyperplasia. J Pharmacol Exp Ther *338*, 528-536.

Okamoto, Y., Sawaki, A., Ito, S., Nishida, T., Takahashi, T., Toyota, M., Suzuki, H., Shinomura, Y., Takeuchi, I., Shinjo, K.*, et al.* (2012). Aberrant DNA methylation associated with aggressiveness of gastrointestinal stromal tumour. Gut *61*, 392-401.

Park, J.H., Walls, J.E., Galvez, J.J., Kim, M., Abate-Shen, C., Shen, M.M., and Cardiff, R.D. (2002). Prostatic intraepithelial neoplasia in genetically engineered mice. Am J Pathol *161*, 727-735.

Paulsen, M.T., Veloso, A., Prasad, J., Bedi, K., Ljungman, E.A., Magnuson, B., Wilson, T.E., and Ljungman, M. (2014). Use of Bru-Seq and BruChase-Seq for genome-wide assessment of the synthesis and stability of RNA. Methods *67*, 45-54.

Pellecchia, A., Pescucci, C., De Lorenzo, E., Luceri, C., Passaro, N., Sica, M., Notaro, R., and De Angioletti, M. (2012). Overexpression of ETV4 is oncogenic in prostate cells through promotion of both cell proliferation and epithelial to mesenchymal transition. Oncogenesis *1*, e20.

Pencheva, N., Tran, H., Buss, C., Huh, D., Drobnjak, M., Busam, K., and Tavazoie, S.F. (2012). Convergent multi-miRNA targeting of ApoE drives LRP1/LRP8-dependent melanoma metastasis and angiogenesis. Cell *151*, 1068-1082.

Perez-Stable, C.M., Pozas, A., and Roos, B.A. (2000). A role for GATA transcription factors in the androgen regulation of the prostate-specific antigen gene enhancer. Mol Cell Endocrinol *167*, 43-53.

Pettersson, A., Graff, R.E., Bauer, S.R., Pitt, M.J., Lis, R.T., Stack, E.C., Martin, N.E., Kunz, L., Penney, K.L., Ligon, A.H.*, et al.* (2012). The TMPRSS2:ERG rearrangement, ERG expression, and prostate cancer outcomes: a cohort study and meta-analysis. Cancer Epidemiol Biomarkers Prev *21*, 1497-1509.

Price, D.K., Chau, C.H., Till, C., Goodman, P.J., Baum, C.E., Ockers, S.B., English, B.C., Minasian, L., Parnes, H.L., Hsing, A.W.*, et al.* (2010). Androgen receptor CAG repeat length and association with prostate cancer risk: results from the prostate cancer prevention trial. J Urol *184*, 2297-2302.

Puc, J., Kozbial, P., Li, W., Tan, Y., Liu, Z., Suter, T., Ohgi, K.A., Zhang, J., Aggarwal, A.K., and Rosenfeld, M.G. (2015). Ligand-dependent enhancer activation regulated by topoisomerase-I activity. Cell *160*, 367-380.

Qin, X.F., An, D.S., Chen, I.S., and Baltimore, D. (2003). Inhibiting HIV-1 infection in human T cells by lentiviral-mediated delivery of small interfering RNA against CCR5. Proc Natl Acad Sci U S A *100*, 183-188.

Rahim, S., Beauchamp, E.M., Kong, Y., Brown, M.L., Toretsky, J.A., and Uren, A. (2011). YK-4-279 inhibits ERG and ETV1 mediated prostate cancer cell invasion. PLoS One *6*, e19343.

Rahim, S., Minas, T., Hong, S.H., Justvig, S., Celik, H., Kont, Y.S., Han, J., Kallarakal, A.T., Kong, Y., Rudek, M.A.*, et al.* (2014). A Small Molecule Inhibitor of ETV1, YK-4-279, Prevents Prostate Cancer Growth and Metastasis in a Mouse Xenograft Model. PLoS One *9*, e114260.

Ran, L., Sirota, I., Cao, Z., Murphy, D., Chen, Y., Shukla, S., Xie, Y., Kaufmann, M.C., Gao, D., Zhu, S.*, et al.* (2015). Combined Inhibition of MAP Kinase and KIT Signaling Synergistically Destabilizes ETV1 and Suppresses GIST Tumor Growth. Cancer Discov *5*, 304-315.

Rhodes, D.R., Kalyana-Sundaram, S., Tomlins, S.A., Mahavisno, V., Kasper, N., Varambally, R., Barrette, T.R., Ghosh, D., Varambally, S., and Chinnaiyan, A.M. (2007). Molecular concepts analysis links tumors, pathways, mechanisms, and drugs. Neoplasia *9*, 443-454.

Rhodes, D.R., Yu, J., Shanker, K., Deshpande, N., Varambally, R., Ghosh, D., Barrette, T., Pandey, A., and Chinnaiyan, A.M. (2004). ONCOMINE: a cancer microarray database and integrated data-mining platform. Neoplasia *6*, 1-6.

Robins, D.M. (2005). Androgen receptor and molecular mechanisms of male-specific gene expression. Novartis Found Symp *268*, 42-52; discussion 53-46, 96-49.

Robins, D.M. (2011). Androgen receptor gene polymorphisms and alterations in prostate cancer: Of humanized mice and men. Mol Cell Endocrinol.

Robins, D.M., Albertelli, M.A., and O'Mahony, O.A. (2008). Androgen receptor variants and prostate cancer in humanized AR mice. J Steroid Biochem Mol Biol *108*, 230-236.

Roche, P.J., Hoare, S.A., and Parker, M.G. (1992). A consensus DNA-binding site for the androgen receptor. Mol Endocrinol *6*, 2229-2235.

Rubin, M.A., Maher, C.A., and Chinnaiyan, A.M. (2011). Common gene rearrangements in prostate cancer. J Clin Oncol *29*, 3659-3668.

Sahu, B., Pihlajamaa, P., Dubois, V., Kerkhofs, S., Claessens, F., and Janne, O.A. (2014). Androgen receptor uses relaxed response element stringency for selective chromatin binding and transcriptional regulation in vivo. Nucleic Acids Res.

Saporita, A.J., Zhang, Q., Navai, N., Dincer, Z., Hahn, J., Cai, X., and Wang, Z. (2003). Identification and characterization of a ligand-regulated nuclear export signal in androgen receptor. J Biol Chem *278*, 41998-42005.

Sathyanarayana, U.G., Birch, C., Nagle, R.B., Tomlins, S.A., Palanisamy, N., Zhang, W., Hubbard, A., Brunhoeber, P., Wang, Y., and Tang, L. (2014). Determination of Optimum

Formalin Fixation Duration for Prostate Needle Biopsies for Immunohistochemistry and Quantum Dot FISH Analysis. Appl Immunohistochem Mol Morphol.

Serra, V., Markman, B., Scaltriti, M., Eichhorn, P.J., Valero, V., Guzman, M., Botero, M.L., Llonch, E., Atzori, F., Di Cosimo, S.*, et al.* (2008). NVP-BEZ235, a dual PI3K/mTOR inhibitor, prevents PI3K signaling and inhibits the growth of cancer cells with activating PI3K mutations. Cancer Res *68*, 8022-8030.

Shappell, S.B., Thomas, G.V., Roberts, R.L., Herbert, R., Ittmann, M.M., Rubin, M.A., Humphrey, P.A., Sundberg, J.P., Rozengurt, N., Barrios, R.*, et al.* (2004). Prostate pathology of genetically engineered mice: definitions and classification. The consensus report from the Bar Harbor meeting of the Mouse Models of Human Cancer Consortium Prostate Pathology Committee. Cancer Res *64*, 2270-2305.

Sharma, N.L., Massie, C.E., Ramos-Montoya, A., Zecchini, V., Scott, H.E., Lamb, A.D., Macarthur, S., Stark, R., Warren, A.Y., Mills, I.G.*, et al.* (2012). The Androgen Receptor Induces a Distinct Transcriptional Program in Castration-Resistant Prostate Cancer in Man. Cancer Cell.

Shen, H.C., and Coetzee, G.A. (2005). The androgen receptor: unlocking the secrets of its unique transactivation domain. Vitam Horm *71*, 301-319.

Shen, M.M., and Abate-Shen, C. (2010). Molecular genetics of prostate cancer: new prospects for old challenges. Genes Dev *24*, 1967-2000.

Shin, S., Kim, T.D., Jin, F., van Deursen, J.M., Dehm, S.M., Tindall, D.J., Grande, J.P., Munz, J.M., Vasmatzis, G., and Janknecht, R. (2009). Induction of prostatic intraepithelial neoplasia and modulation of androgen receptor by ETS variant 1/ETS-related protein 81. Cancer Res *69*, 8102-8110.

Shin, S., Oh, S., An, S., and Janknecht, R. (2012). ETS variant 1 regulates matrix metalloproteinase-7 transcription in LNCaP prostate cancer cells. Oncol Rep.

Siegel, R.L., Miller, K.D., and Jemal, A. (2015). Cancer statistics, 2015. CA Cancer J Clin *65*, 5-29.

Simanainen, U., Brogley, M., Gao, Y.R., Jimenez, M., Harwood, D.T., Handelsman, D.J., and Robins, D.M. (2011). Length of the human androgen receptor glutamine tract determines androgen sensitivity in vivo. Mol Cell Endocrinol *342*, 81-86.

Singh, M., Jha, R., Melamed, J., Shapiro, E., Hayward, S.W., and Lee, P. (2014). Stromal Androgen Receptor in Prostate Development and Cancer. Am J Pathol.

Sobel, R.E., and Sadar, M.D. (2005a). Cell lines used in prostate cancer research: a compendium of old and new lines--part 1. J Urol *173*, 342-359.

Sobel, R.E., and Sadar, M.D. (2005b). Cell lines used in prostate cancer research: a compendium of old and new lines--part 2. J Urol *173*, 360-372.

Sorensen, P.H., Lessnick, S.L., Lopez-Terrada, D., Liu, X.F., Triche, T.J., and Denny, C.T. (1994). A second Ewing's sarcoma translocation, t(21;22), fuses the EWS gene to another ETS-family transcription factor, ERG. Nat Genet *6*, 146-151.

Stambolic, V., Suzuki, A., de la Pompa, J.L., Brothers, G.M., Mirtsos, C., Sasaki, T., Ruland, J., Penninger, J.M., Siderovski, D.P., and Mak, T.W. (1998). Negative regulation of PKB/Akt-dependent cell survival by the tumor suppressor PTEN. Cell *95*, 29-39.

Steinkamp, M.P., O'Mahony, O.A., Brogley, M., Rehman, H., Lapensee, E.W., Dhanasekaran, S., Hofer, M.D., Kuefer, R., Chinnaiyan, A., Rubin, M.A.*, et al.* (2009). Treatment-dependent androgen receptor mutations in prostate cancer exploit multiple mechanisms to evade therapy. Cancer Res *69*, 4434-4442.

Stiles, B., Groszer, M., Wang, S., Jiao, J., and Wu, H. (2004). PTENless means more. Dev Biol *273*, 175-184.

Sumitomo, M., Shen, R., and Nanus, D.M. (2005). Involvement of neutral endopeptidase in neoplastic progression. Biochim Biophys Acta *1751*, 52-59.

Sun, F., Chen, H.G., Li, W., Yang, X., Wang, X., Jiang, R., Guo, Z., Chen, H., Huang, J., Borowsky, A.D.*, et al.* (2014). Androgen receptor splice variant AR3 promotes prostate cancer via modulating expression of autocrine/paracrine factors. J Biol Chem *289*, 1529-1539.

Svensson, M.A., LaFargue, C.J., MacDonald, T.Y., Pflueger, D., Kitabayashi, N., Santa-Cruz, A.M., Garsha, K.E., Sathyanarayana, U.G., Riley, J.P., Yun, C.S.*, et al.* (2011). Testing mutual exclusivity of ETS rearranged prostate cancer. Lab Invest *91*, 404-412.

Tan, J., Sharief, Y., Hamil, K.G., Gregory, C.W., Zang, D.Y., Sar, M., Gumerlock, P.H., deVere White, R.W., Pretlow, T.G., Harris, S.E.*, et al.* (1997). Dehydroepiandrosterone activates mutant androgen receptors expressed in the androgen-dependent human prostate cancer xenograft CWR22 and LNCaP cells. Mol Endocrinol *11*, 450-459.

Tang, X., Mahajan, S.S., Nguyen, L.T., Beliveau, F., Leduc, R., Simon, J.A., and Vasioukhin, V. (2014). Targeted inhibition of cell-surface serine protease Hepsin blocks prostate cancer bone metastasis. Oncotarget *5*, 1352-1362.

Taris, M., Irani, J., Blanchet, P., Multigner, L., Cathelineau, X., and Fromont, G. (2014a). ERG expression in prostate cancer: the prognostic paradox. Prostate *74*, 1481-1487.

Taris, M., Irani, J., Blanchet, P., Multigner, L., Cathelineau, X., and Fromont, G. (2014b). ERG expression in prostate cancer: The prognostic paradox. Prostate.

Taylor, B.S., Schultz, N., Hieronymus, H., Gopalan, A., Xiao, Y., Carver, B.S., Arora, V.K., Kaushik, P., Cerami, E., Reva, B.*, et al.* (2010). Integrative genomic profiling of human prostate cancer. Cancer Cell *18*, 11-22.

Tewari, A.K., Yardimci, G.G., Shibata, Y., Sheffield, N.C., Song, L., Taylor, B.S., Georgiev, S.G., Coetzee, G.A., Ohler, U., Furey, T.S., *et al.* (2012). Chromatin accessibility reveals insights into androgen receptor activation and transcriptional specificity. Genome Biol *13*, R88.

Thomas, C., Lamoureux, F., Crafter, C., Davies, B.R., Beralidi, E., Fazli, L., Kim, S., Thaper, D., Gleave, M.E., and Zoubeidi, A. (2013). Synergistic targeting of PI3K/AKT-pathway and androgen-receptor axis significantly delays castration-resistant prostate cancer progression in vivo. Mol Cancer Ther.

Thompson, I.M., Jr., Goodman, P.J., Tangen, C.M., Parnes, H.L., Minasian, L.M., Godley, P.A., Lucia, M.S., and Ford, L.G. (2013). Long-term survival of participants in the prostate cancer prevention trial. N Engl J Med *369*, 603-610.

Thompson, V.C., Day, T.K., Bianco-Miotto, T., Selth, L.A., Han, G., Thomas, M., Buchanan, G., Scher, H.I., Nelson, C.C., Greenberg, N.M., *et al.* (2011). A gene signature identified using a mouse model of androgen receptor-dependent prostate cancer predicts biochemical relapse in human disease. Int J Cancer.

Tian, T.V., Tomavo, N., Huot, L., Flourens, A., Bonnelye, E., Flajollet, S., Hot, D., Leroy, X., de Launoit, Y., and Duterque-Coquillaud, M. (2013). Identification of novel TMPRSS2:ERG mechanisms in prostate cancer metastasis: involvement of MMP9 and PLXNA2. Oncogene.

Tomlins, S.A., Laxman, B., Dhanasekaran, S.M., Helgeson, B.E., Cao, X., Morris, D.S., Menon, A., Jing, X., Cao, Q., Han, B., *et al.* (2007). Distinct classes of chromosomal rearrangements create oncogenic ETS gene fusions in prostate cancer. Nature *448*, 595-599.

Tomlins, S.A., Laxman, B., Varambally, S., Cao, X., Yu, J., Helgeson, B.E., Cao, Q., Prensner, J.R., Rubin, M.A., Shah, R.B., *et al.* (2008a). Role of the TMPRSS2-ERG gene fusion in prostate cancer. Neoplasia *10*, 177-188.

Tomlins, S.A., Rhodes, D.R., Perner, S., Dhanasekaran, S.M., Mehra, R., Sun, X.W., Varambally, S., Cao, X., Tchinda, J., Kuefer, R., *et al.* (2005). Recurrent fusion of TMPRSS2 and ETS transcription factor genes in prostate cancer. Science *310*, 644-648.

Tomlins, S.A., Rhodes, D.R., Yu, J., Varambally, S., Mehra, R., Perner, S., Demichelis, F., Helgeson, B.E., Laxman, B., Morris, D.S., *et al.* (2008b). The role of SPINK1 in ETS rearrangement-negative prostate cancers. Cancer Cell *13*, 519-528.

Trotman, L.C., Niki, M., Dotan, Z.A., Koutcher, J.A., Di Cristofano, A., Xiao, A., Khoo, A.S., Roy-Burman, P., Greenberg, N.M., Van Dyke, T., *et al.* (2003). Pten dose dictates cancer progression in the prostate. PLoS Biol *1*, E59.

Vander Griend, D.J., Litvinov, I.V., and Isaacs, J.T. (2014). Conversion of Androgen Receptor Signaling From a Growth Suppressor in Normal Prostate Epithelial Cells to an Oncogene in Prostate Cancer Cells Involves a Gain of Function in c-Myc Regulation. Int J Biol Sci *10*, 627-642.

Wang, L., Li, Y., Yang, X., Yuan, H., Li, X., Qi, M., Chang, Y.W., Wang, C., Fu, W., Yang, M., *et al.* (2014). ERG-SOX4 interaction promotes epithelial-mesenchymal transition in prostate cancer cells. Prostate.

Wang, Q., Udayakumar, T.S., Vasaitis, T.S., Brodie, A.M., and Fondell, J.D. (2004). Mechanistic relationship between androgen receptor polyglutamine tract truncation and androgen-dependent transcriptional hyperactivity in prostate cancer cells. J Biol Chem *279*, 17319-17328.

Wang, S., Gao, J., Lei, Q., Rozengurt, N., Pritchard, C., Jiao, J., Thomas, G.V., Li, G., Roy-Burman, P., Nelson, P.S., *et al.* (2003). Prostate-specific deletion of the murine Pten tumor suppressor gene leads to metastatic prostate cancer. Cancer Cell *4*, 209-221.

Wang, X., Kruithof-de Julio, M., Economides, K.D., Walker, D., Yu, H., Halili, M.V., Hu, Y.P., Price, S.M., Abate-Shen, C., and Shen, M.M. (2009). A luminal epithelial stem cell that is a cell of origin for prostate cancer. Nature *461*, 495-500.

Wang, X., Zbou, C., Qiu, G., Fan, J., Tang, H., and Peng, Z. (2008). Screening of new tumor suppressor genes in sporadic colorectal cancer patients. Hepatogastroenterology *55*, 2039-2044.

Waterbor, J.W., and Bueschen, A.J. (1995). Prostate cancer screening (United States). Cancer Causes Control *6*, 267-274.

Whang, Y.E., Wu, X., Suzuki, H., Reiter, R.E., Tran, C., Vessella, R.L., Said, J.W., Isaacs, W.B., and Sawyers, C.L. (1998). Inactivation of the tumor suppressor PTEN/MMAC1 in advanced human prostate cancer through loss of expression. Proc Natl Acad Sci U S A *95*, 5246-5250.

Wu, X.J., Zhi, Y., Zheng, J., He, P., Zhou, X.Z., Li, W.B., and Zhou, Z.S. (2014). Dutasteride on benign prostatic hyperplasia: a meta-analysis on randomized clinical trials in 6460 patients. Urology *83*, 539-543.

Wu, Y.T., Ouyang, W., Lazorchak, A.S., Liu, D., Shen, H.M., and Su, B. (2011). mTOR complex 2 targets Akt for proteasomal degradation via phosphorylation at the hydrophobic motif. J Biol Chem *286*, 14190-14198.

Yoo, S., Pettersson, A., Jordahl, K.M., Lis, R.T., Lindstrom, S., Meisner, A., Nuttall, E.J., Stack, E.C., Stampfer, M.J., Kraft, P., *et al.* (2014). Androgen receptor CAG repeat polymorphism and risk of TMPRSS2:ERG positive prostate cancer. Cancer Epidemiol Biomarkers Prev.

Yu, J., Mani, R.S., Cao, Q., Brenner, C.J., Cao, X., Wang, X., Wu, L., Li, J., Hu, M., Gong, Y., *et al.* (2010). An integrated network of androgen receptor, polycomb, and TMPRSS2-ERG gene fusions in prostate cancer progression. Cancer Cell *17*, 443-454.

Yu, S., Feng, F., Wang, K., Men, C., Lin, C., Liu, Q., Yang, D., and Gao, Z. (2013). The therapeutic efficacy of I131-PSCA-mAb in orthotopic mouse models of prostate cancer. Eur J Med Res *18*, 56.

Yu, Y.P., Landsittel, D., Jing, L., Nelson, J., Ren, B., Liu, L., McDonald, C., Thomas, R., Dhir, R., Finkelstein, S*., et al.* (2004). Gene expression alterations in prostate cancer predicting tumor aggression and preceding development of malignancy. J Clin Oncol *22*, 2790-2799.

Zhu, M., Chen, Q., Liu, X., Sun, Q., Zhao, X., Deng, R., Wang, Y., Huang, J., Xu, M., Yan, J*., et al.* (2014). lncRNA H19/miR-675 axis represses prostate cancer metastasis by targeting TGFBI. FEBS J *281*, 3766-3775.

Zitzmann, M., and Nieschlag, E. (2003). The CAG repeat polymorphism within the androgen receptor gene and maleness. Int J Androl *26*, 76-83.

Zoghbi, H.Y., and Orr, H.T. (2000). Glutamine repeats and neurodegeneration. Annu Rev Neurosci *23*, 217-247.

Zong, Y., Xin, L., Goldstein, A.S., Lawson, D.A., Teitell, M.A., and Witte, O.N. (2009). ETS family transcription factors collaborate with alternative signaling pathways to induce carcinoma from adult murine prostate cells. Proc Natl Acad Sci U S A *106*, 12465-12470.